OPTIMAL OPERATION CONTROL OF HYBRID RENEWABLE ENERGY SYSTEMS

By

KANZUMBA KUSAKANA

DOCTOR TECHNOLOGIAE: Electrical Engineering

In the Department of Electrical, Electronic and Computer Engineering

Faculty of Engineering and Information Technology

Central University of Technology, Free State

Promoter: Prof. H.J. Vermaak (PhD)

October 2014

Declaration

I, KANZUMBA KUSAKANA, student number 213098709, do hereby declare that this research project which has been submitted to the Central University of Technology Free State, for the degree DOCTOR TECHNOLOGIAE: ENGINEERING: ELECTRICAL, is my own independent work and complies with the Code of Academic Integrity, as well as other relevant policies, procedures, rules and regulations of the Central University of Technology, Free State, and has not been submitted before by any person in fulfilment (or partial fulfilment) of the requirements for the attainment of any qualification.

K. KUSAKANA Date

Dedication

TO MY LORD AND SAVIOUR JESUS CHRIST FOR THE MANY BLESSING UNDESERVINGLY BESTOWED UPON ME.

Acknowledgments

The realization of this work was only possible due to the collaboration of several people, to whom I desire to express my gratefulness.

To Professor Herman Jacobus Vermaak, my promoter, I am grateful for the trust placed in my work and for the motivation demonstrated during this arduous course. His support was without a doubt crucial in my dedication in this research work.

I would like to acknowledge the inspirational instruction, guidance and the initial impetus to study optimal operation control from Mr. Bubele Papy Numbi, who has given me a deep appreciation and love for the beauty and detail of this subject.

I would also like to acknowledge the support and assistance given to me by the Central University of Technology, Free State (CUT), and by my colleagues from the Research Group in Evolvable Manufacturing Systems (RGEMS). CUT has been very generous in supporting my academic pursuits and many of my colleagues have contributed with ideas, feedback and advice.

I would like to thank my Parents, Mr. Christophe Kusakana and Mrs. Charlotte Djo, my brothers and sister, Erick, Christian and Gracia Kusakana, for their support and encouragement.

Finally, I would like to thank in a special way, my wife and daughter, Nanousha Kamala and Elani Kusakana, for their support, prayers and good wishes. I could not have completed this effort without their assistance, tolerance and enthusiasm. Thank you.

Abstract

For a sustainable and clean electricity production in isolated rural areas, renewable energies appear to be the most suitable and usable supply options. Apart from all being renewable and sustainable, each of the renewable energy sources has its specific characteristics and advantages that make it well suited for specific applications and locations. Solar photovoltaic and wind turbines are well established and are currently the mostly used renewable energy sources for electricity generation in small-scale rural applications. However, for areas in which adequate water resources are available, micro-hydro is the best supply option compared to other renewable resources in terms of cost of energy produced.

Apart from being capital-cost-intensive, the other main disadvantages of the renewable energy technologies are their resource-dependent output powers and their strong reliance on weather and climatic conditions. Therefore, they cannot continuously match the fluctuating load energy requirements each and every time.

Standalone diesel generators, on the other hand, have low initial capital costs and can generate electricity on demand, but their operation and maintenance costs are very high, especially when they run at partial loads. In order for the renewable sources to respond reliably to the load energy requirements, they can be combined in a hybrid energy system with back-up diesel generator and energy storage systems. The most important feature of such a hybrid system is to generate energy at any time by optimally using all available energy sources. The fact that the renewable resources available at a given site are a function of the season of the year implies that the fraction of the energy provided to the load is not constant. This means that for hybrid systems comprising diesel generator, renewable sources and battery storage in their architecture, the renewable energy fraction and the energy storage capacity are projected to have a significant impact on the diesel generator fuel consumption, depending on the complex interaction between the daily variation of renewable resources and the non-linear load demand.

This was the context on which this research was based, aiming to develop a tool to minimize the daily operation costs of standalone hybrid systems. However, the complexity of this problem is of an extremely high mathematical degree due to the non-linearity of the load demand as well as the non-linearity of the renewable resources profiles. Unlike the algorithms already developed, the objective was to develop a tool that could minimize the diesel generator control variables while maximizing the hydro, wind, solar and battery control variables resulting in saving fuel and operation costs.

An innovative and powerful optimization model was then developed capable of efficiently dealing with these types of problems.

The hybrid system optimal operation control model has been simulated using fmincon interior-point in MATLAB. Using realistic and actual data for several case studies, the developed model has been successfully used to analyse the complex interaction between the daily non-linear load, the non-linear renewable resources as well as the battery dynamic, and their impact on the hybrid system's daily operation cost minimization.

The model developed, as well as the solver and algorithm used in this work, have low computational requirements for achieving results within a reasonable time, therefore this can be seen as a faster and more accurate optimization tool.

Keywords:

Hybrid system, optimal operation control, cost minimization, renewable energy, optimization algorithm.

Content

List of figures

List of Tables

Chapter I: Introduction

1.1. Hybrid energy systems

Currently, fossil fuels constitute the bulk of the world's main energy sources. One of the advantages of fossil fuels is that huge amounts of electricity can be produced at a single location. However, the dependence on fossil fuels has created energy security risks because these resources are not sustainable and will eventually be exhausted. Even if the costs of electricity produced from fossil fuels are low compared to other options, the conversion of these resources into electricity induces major pollution problems, such as the emission of greenhouse gases in the environment which contribute to the global warming the earth is currently experiencing (Goedeckeb et al., 2007). Because this electricity is generated at a single location, transmission lines are required to transport it to isolated and remote areas. However, there are still a huge number of rural communities throughout the world which are not electrified through the grid due to the uneconomical cost of extension lines or difficult terrain, especially in rural areas. These remote areas are generally electrified by means of standalone diesel generators (DGs) which also emit pollutants in the environment (Kusakana and Vermaak, 2013a). On the other hand, the worldwide rise in fuel prices as well as the high transport and delivery costs to these isolated areas makes the cost of energy produced by diesel generators very expensive (Mahmoud and Ibrik, 2006). A need exists for more sustainable energy sources which can be cheaper, more reliable and have very low or zero negative impacts on the environment. For a sustainable energy production, renewable energies are the most established and usable supply options (Kusakana and Vermaak, 2013b). Apart from all being renewable and sustainable, each of the renewable energy sources has its specific characteristics and advantages that make it well suited for specific applications and locations (Hepbasli, 2008).

The solar photovoltaic (PV) systems and wind turbines (WT) are well established and are currently the most used renewable energy sources for electricity generation in small scale

rural applications. However, for areas in which adequate water resources are available, micro-hydro is the best supply option when compared to other renewable energy sources in terms of cost of energy produced (Paish, 2002). Unlike conventional hydropower technology, hydrokinetic (HKT) is a relatively recent type of hydropower system that generates electricity by extracting the kinetic energy of flowing water instead of the potential energy of falling water. This makes hydrokinetic less site-specific and more competitive than to traditional micro hydropower even though they can extract almost the same amount of energy (Vermaak et al., 2014).

It has to be noted that apart from being capital-cost-intensive, the other main disadvantages of renewable energy technologies are their resource-dependent output powers and their strong reliance on weather and climatic conditions (Chen et al., 2007). Therefore, they cannot always match the fluctuating load energy requirements each and every time.

Standalone diesel generators, on the other hand, have very low initial capital costs and can generate electricity on demand, but their operation and maintenance costs are very high, especially when they run at partial loads (Kusakana and Vermaak, 2013b). Renewable energy sources and DG have complementary characteristics in terms of costs and resource availability. In order for the renewable sources to respond successfully to the load energy requirements, it can be combined in a hybrid energy system with back-up DG and battery storage systems. The most important feature of such a hybrid system is to generate energy at any time by optimally using all available energy sources (Tazvinga et al., 2013). Furthermore, the size of the storage system can be reduced slightly as there is less reliance on one unique energy source (Supriya and Siddarthan, 2011).

1.2. Problem Statement

The sum of the power generated by the different components of the hybrid system must always match the fluctuating load demand. The implementation of such a dynamic operating system is not straightforward due to the following prominent problems:

1.2.1. Sub-Problem 1: The non-linearity of the renewable energy sources.

The fact that the available renewable resources at a given site are varying in function of hours and seasons implies that the fractions of the energy provided to the load by these sources are not constant. This means that, for any hybrid system, the energy fractions from the different renewable sources are projected to have a significant impact on the DG fuel consumption, depending on the interaction between the intermittent resources and on the continuous fluctuation of load demand.

Previous works have mostly used average monthly renewable resources to calculate approximate operation costs, as the interaction between the non-linear renewable powers produced and the load on a smaller time scale is not investigated in most cases. Therefore detailed time series data reflecting the real non-linearity renewable resource profiles will be used in this work.

1.2.2. Sub-Problem 2: The non-linearity of the DG fuel consumption curve.

Diesel generators achieve high fuel efficiency when operating at 80% and above of their rated capacities and their fuel efficiency become very low when operating below 30% of their ratings. Therefore the DG operation fuel consumption or operation cost depends on its instantaneous output power level and on the running time. Several developed fuel consumption models, such as the one used in HOMER software, assume linear characteristics between the fuel consumption and the DG output power level, using the following equation:

$$f_C = F_0.Y_{gen} + F_1.P_{gen} \tag{1.1}$$

Where F_0 is the fuel curve intercept coefficient (L/hr/kW),

F_1 is the fuel curve slope (L/hr/kW),

Y_{gen} is the rated capacity of the generator (kW),

P_{gen} is the electrical output of the generator (kW).

The fuel consumption relation presented above becomes more non-linear when the actual generator response is being taken into account. Therefore in the present work an alternative non-linear quadratic model of the DG fuel consumption as function of its generated power is proposed. This relation accurately models the actual response of conventional diesel generators.

1.2.3. Sub-Problem 3: The dissimilarity of the load demand pattern.

Previous works have assumed a fixed load demand and constant daily operational cost, which can be extrapolated to obtain monthly or yearly operation costs. However, the assumption is not precise because different consumer's behaviour with days or seasons; therefore a more practical and realistic daily operational cost model is considered in this work.

1.2.4. Sub-Problem 4: Battery operation limits

The battery system stores the excess energy from the renewable sources when the load demand is entirely satisfied. This battery system has a set maximum state of charge and can be discharge to a minimum allowable limit when there is a deficit of energy from the renewable sources before the DG can be switched on. There is a conflict between the following battery operation settings:

- A battery with longer depth of discharge certainly reduces the DG running time and fuel consumption but, on the other hand, decreases the battery life span leading to premature replacement.
- A battery with shorter depth of discharge will have a long operating life, but the DG start and stop numbers, running time and the resultant fuel consumption cost, will be increased.

The impact of the battery operation limits or battery control settings on the hybrid system operation cost has to be investigated.

1.3. Objectives

The optimal operation control of any hybrid system's power sources is an essential and challenging step to achieve a low system's life cycle costs (Kusakana et al., 2012; Zhang, 2011). The hybrid system's optimal operation control problem is non-linear due to the non-linearity of the load demand; the non-linearity of the renewable resources, the non-linearity of the DG fuel consumption curve as well as the complexity of the optimization problem itself. According to Jansen et al. (1993), the complexity in resolving an optimal operation control problem generally lies in the dimension of the problem.

The present study focuses on minimizing the operation cost of a hybrid renewable energy system with DG and battery during a 24 hours period, considering the interactions between system sizing and operational control settings; yielding an optimal system configuration for given energy needs, as well as an optimal operation strategy in the form of control settings.
The specific objectives of this research are listed below:

- Knowing that the energy from the renewable resources is varying depending on the time of the day, on the geographic locations as well as on the seasons, analysis of the renewable resources on selected sites will be conducted first, in order to efficiently design the different hybrid system's renewable energy sources.
- The model development of the PV, WT, HKT, DG and battery system which are the components of the considered hybrid system, will be the basic work in the hybrid system mathematical modelling.
- The hybrid system's optimal operation control simulation model, including technical and economical characteristics, is to be developed. This model will be based on the description of the power flowing from the different energy sources, converters as well as storage systems, taking into account the losses and the impact of the operating decisions (starting and stopping of the DG) along the way up to the loads.

- Very few feasibility studies have been conducted to develop standalone HKT power systems (Kusakana and Vermaak, 2012; Kusakana and Vermaak, 2013c). In addition, currently there is no literature available showing the use of this technology operating in combination with other power generation systems. Therefore, in this study, the techno-economic impacts of the hydrokinetic module on the whole hybrid energy system's operation will be analysed.

1.4. Research methodology

The creation of an effective tool requires several methodological steps:

- Reviewing the literature related to HKT, PV, WT and DG conversion systems as well as to existing methods for operation control of hybrid renewable systems, in order to ascertain the validity of the simulation model developed as well as of the positive impact of the hydrokinetic module on the hybrid system's performance.
- After studying the different power modules as standalone as well as in hybrid system operation modes, the mathematical model of the proposed hybrid system's optimal operation control will be developed. The objective function will be derived, and the constraints and variables will be identified in order to arrive at the main structure of this research.
- After getting the necessary daily renewable resources data for a selected location, the technical and economical data from the hybrid system's components as well as the daily load data, the hybrid system will be optimally sized using HOMER and the results will be used as input for the optimal operation control simulation.
- Referring to the optimization equations obtained above, different optimization algorithms will be studied, in order to justify the choice wisely. MATLAB software will then be used for the optimization computation.

- Using realistic and actual data, the developed model will be used through simulations to minimize the operation cost of the hybrid operating under variable non-linear load and non-linear renewable resources.

1.5. Hypothesis

The system operation costs are all the running expenses incurring after installation. These expenses are usually calculated on an annual basis and then discounted for the project's duration. The hybrid system's long-term operation costs take maintenance, fuel, component repair and replacement costs into account. These costs are generally estimated and therefore are more difficult to establish than the initial investment costs. Considering a short time horizon (24 hours), the operation costs of the battery and of the renewable systems are negligible, therefore only the fuel cost of the DG can be considered.

- The first hypothesis is that the proposed hybrid system's optimization model will reduce the fuel consumption (daily operation cost) compared to the diesel only scenario.
- The second hypothesis is that the seasonal load and renewable energy resource variations will have a significant impact on the hybrid system's daily operation cost.
- The third hypothesis is that the hydrokinetic module will have a high impact on the hybrid system's daily operation cost minimization.
- The forth hypothesis is that the battery operation limits (control settings) will have a high impact on the hybrid system's daily operation cost minimization.
- The fifth hypothesis is that for the same kilowatt rating, different DGs from different manufacturers will have different impacts on the hybrid system's daily operation cost minimization.

1.6. Delimitation

This research work did not consider the following:

- The hybrid system's optimal sizing.
- The hybrid system's life cycle cost.
- The grid connected hybrid system.

1.7. Contributions to Knowledge

- The author firstly presents a general overview of hybrid systems. The different energy sources and other components that can be used in hybrid system configurations are presented and discussed in detail. Finally, the author introduces the hydrokinetic system as one of the main components which can potentially have a huge impact on the performance and on the cost of energy produced via the hybrid energy system.
- The development of a model to assist in the optimal operation control of energy flow in a hybrid configuration is presented. The effectiveness of the developed model is then outlined by means of case studies using more practical and realistic daily and seasonal fluctuations in the load energy demand, as well as renewable resources.
- The developed model combined with the solver and the algorithm used in this work have low computational requirements achieving results in reasonable time, therefore this can be seen as a faster and more accurate optimization tool.

1.8. Publications during the study

Journal papers published:

- KUSAKANA K. 2014. Techno-economic analysis of off-grid hydrokinetic-based hybrid energy systems for onshore/ remote area in South Africa. Energy, 68:947-

957.

- KUSAKANA K. 2014. A survey of innovative technologies increasing the viability of micro-hydropower as a cost effective rural electrification option in South Africa. Renewable and Sustainable Energy Reviews, 37:370-379.
- VERMAAK H.J., KUSAKANA K., KOKO S.P. 2014. Status of micro-hydrokinetic river technology in rural applications: A review of literature. Renewable and Sustainable Energy Reviews, 29:625-633.
- KUSAKANA K., VERMAAK H.J. 2014. Hybrid diesel generator/renewable energy system performance modelling". Renewable Energy, 67:97-102.
- VERMAAK H.J., KUSAKANA K. 2014. Design of a photovoltaic-wind charging station for small electric Tuk-tuk in D.R.Congo. Renewable Energy, 67:40-45.
- KUSAKANA K., VERMAAK H.J. 2013. Hybrid renewable power systems for mobile telephony base station in developing countries. Renewable Energy, 51:419-425.
- KUSAKANA K., VERMAAK H.J. 2013. Hydrokinetic power generation for rural electricity supply: Case of South Africa. Renewable Energy, 55:467-473.
- KUSAKANA K., VERMAAK H.J., YUMA G.P. 2013. Optimization of Hybrid Standalone Renewable Energy Systems by Linear Programming. Advanced Science Letters, 19:2501-2504.
- KUSAKANA K., VERMAAK H.J. 2013. A Survey of Particle Swarm Optimization Applications for Sizing Hybrid Renewable Power Systems. Advanced Science Letters, 19:2463-2467.

Journal papers submitted:

- KUSAKANA K., VERMAAK H.J., NUMBI B.P. Optimal operation control of hydrokinetic based hybrid systems. Submitted to Renewable Energy (Under review).

- KUSAKANA K. Optimal operation control of hybrid renewable energy systems: Overview of different approaches. Submitted to Renewable Energy (Under review).

Conferences papers:

- KUSAKANA K., VERMAAK H.J. 2014. Cost and performance evaluation of hydrokinetic-diesel hybrid system. 6th International Conference on Applied Energy (ICAE2014), Taipei, Taiwan, China, 30 May-2 June, Energy Procedia 61, 2439-2442.
- KUSAKANA K., VERMAAK H.J. 2013. Hybrid Diesel Generator-battery systems for off-grid rural applications". IEEE International Conference on Industrial Technology (ICIT 2013), Cape Town, 25-28 February, 839-844.
- KUSAKANA K., VERMAAK H.J., NUMBI B.P. 2012. Optimal sizing of a hybrid renewable energy plant using linear programming. IEEE PES Conference and Exposition Johannesburg, (PowerAfrica 2012) South Africa, 09-13 July.
- KUSAKANA K., VERMAAK H. 2012. Feasibility Study of Hydrokinetic Power for Energy Access in Rural South Africa. Proceedings of the IASTED Asian Conference, Power and Energy Systems, Phuket, Thailand, 2-4 April, 433-438.
- KUSAKANA K., VERMAAK H.J. 2011. Small scale photovoltaic-wind hybrid systems in D.R. Congo: Status and sustainability". IASTED International Conference on Power and Energy systems (EuroPES 2011) Crete, Greece, June 22 - 24.
- KUSAKANA K., VERMAAK H.J. 2011. Hybrid Photovoltaic-Wind system as power solution for network operators in the D.R. Congo. The International Conference on Clean Electrical Power (ICCEP 2011) Italy, June 14-16.

1.9. Thesis structure

This thesis has been organized into 6 Chapters, with the main research results being presented in Chapter IV and Chapter V.

Chapter I presents the background of the work, underlines the problems and gives the objectives and methodology.

Chapter II reports the thorough review presenting the state-of-the-art hybrid renewable energy systems' optimal operation control. This Chapter also identifies different challenges encountered as well as future developments that can help in improving the optimal operation control of hybrid renewable energy systems.

Chapter III describes the different components that can be incorporated in the architecture of a hybrid system. The emphasis will be on component designs, their standalone operation principle and issues, as well as on their operation in a hybrid system configuration.

Chapter IV gives a general overview of the optimization problem. The mathematical model of the problem to be solved in this work is formulated. The choice of a suitable optimization algorithm is discussed.

Chapter V presents and discusses all the optimization results obtained from simulation.

Finally, Chapter VI concludes the work of this thesis and sets the stage for future studies.

Chapter II: Literature review

2.1. Introduction

A hybrid energy system is a combination of renewable energy sources with back-up as well as storage systems used to respond to given load energy requirements. Given that the electrical output of each renewable source is fluctuating with the change in weather conditions, and since the load demand also varies with time, one of the main challenges of hybrid systems is to respond to the load demand at any time by optimally controlling each energy source, storage and back-up system. The induced optimization problem is to compute the optimal operation control of the system with the aim of minimizing operation costs while efficiently and reliably responding to the load energy requirement. Current optimization research and development on hybrid systems are mainly focusing on the sizing aspect. Thus the aim of this Chapter is to report the thorough review presenting the state-of-the-art of hybrid renewable energy systems' optimal operation control. This Chapter also identifies different challenges encountered as well as future developments that can help in improving the optimal operation control of hybrid renewable energy systems. A summary of available approaches for hybrid systems' optimal operation control is also presented.

2.2. Review on approaches for hybrid systems' optimal operation control

Many practical hybrid systems' design and control often use conventional approaches such as "Rule of thumb methods" (Seeling-Hochmuth, 1996) and "Paper-based methods" (Sandia National Laboratories, 1995). These methods are based on progressive experience and trials, including errors. However, they do have their limitations as they can merely give broad intuitive guidelines that might still be open to improvement.

Several research works have been done using numerical methods for the hybrid systems' component sizing and cost optimization, according to the load demand and the energy resources available from the sites (Diaf S. et al, 2006; Kusakana and Vermaak, 2011; Tina et al.,2006). These methodologies are time-consuming and their level of complexity increases exponentially with the number of energy sources or variables considered in the architecture of hybrid systems. Moreover, only the sizing linked to the optimization of the initial investment cost can be achieved using these methods, not the running cost by the mean of optimal operation control.

Other approaches such as the "Graphic method" (Borowy and Salameh, 1996), "Probabilistic techniques" (Yang et al., 2007) and "Iterative method" (Wang, 2008) are derivative-based and have confirmed their efficacy in handling many types of optimization problems, but they are not applicable to certain advanced optimization problems such as combined optimal sizing and operation control.

Several approaches, such as linear programming, gradient method, Newton method, nonlinear programming method, success linear programming method, mixed integer programming method, dynamic programming method, interior point method, network flows, etc., are available to solve optimization problems (Bakare et al., 2007; Zhigang and Liye, 2008; Yu et al., 2009; Zhu, 2009). These methods are typically pure in mathematical analysis but are not suited to solve problems with high non-linearity (such as hybrid systems' combined sizing and operation control); they oftentimes even suffer from the "curse of dimensionality" (Zhou et al., 2009). The drawback of gradient and Newton methods resides in the difficulty in handling inequality constraints. The linear programming method suffers from oscillation and slow convergence problems when the iterative step is not selected properly during the linearization process of both objective functions and constraints. The nonlinear programming method suffers from computational complexity, poor convergence and instability, while the mixed integer programming method suffers from computational time (Numbi, 2012).

Different software packages to size and optimize given "pre-designed" hybrid systems are available. They are based on a mathematical description of the components' operational

characteristics and system energy resources (Ibrahim et al., 2011; Seeling-Hochmuth, 1998). These software tools use simplified and linear models or a complex model but vary the design randomly within a preset interval on component sizes. However, the results might not be near optimum due to the complexities involved in an actual system.

Due to high complexity and high nonlinearity of hybrid systems' optimal operation control problems, new techniques based on Artificial or Computational Intelligence have been proposed as an alternative to traditional analytical approaches (Singiresu, 2009). These techniques include artificial neural networks (ANNs), tabu search (TS), simulated annealing (SA), expert systems (ES), genetic algorithms (GAs), differential evolution (DE), evolutionary programming (EP) and particle swarm optimization (PSO). To get the best of these modern optimization approaches, detailed and accurate models describing the non-linear hybrid systems' performance and the complex relationship between the components' optimal sizing and operation control, must be developed.

2.3. Review papers on hybrid systems' optimal operation control

Few reviews regarding the optimal operation control of hybrid renewable energy systems have been conducted. Some of the relevant review publications related to the topic of this research are summarized in the following.

Nema et al. (2009) reviewed the state of the design, operation and control requirement of the standalone PV solar-wind hybrid energy systems using conventional back-up sources such as diesel generators. The application of an advanced control technique, such as artificial intelligence for the energy management and optimal operation of hybrid energy, was proposed for future work.

Nehrir et al. (2011) summarized the available approaches for different renewable energy systems' configuration, sizing and control as well as energy management. The authors also discussed the current status and future tendencies of renewable energy power generation, the challenges facing the extensive deployment and research vision for the future of renewable energy systems.

Banos et al. (2011) as well as Bernal-Agustın and Dufo-Lopez (2009a), have provided an overview of the research developments relating to the use of optimization algorithms for renewable energies' design, planning and control problems. The first conclusion of these studies is that there is an increase in the number of papers that use traditional as well as heuristic optimization methods to solve renewable energy problems. The authors have pointed out that Pareto-based multi-objective optimization and parallel processing are promising research areas in the field of renewable and sustainable energy.

Erdinc and Uzunoglu (2012) have examined different optimization methods, including those available from software tools, to potential optimization techniques. The papers reviewed in this article were mostly based on sizing and not on optimal operation control.

Deshmukh and Deshmukh (2008) reviewed the state of solar and wind hybrid renewable energy systems' modelling. Descriptions of the methodologies commonly used for modeling system components are described. This is followed by a review of work reported by several authors. It has been shown that in 69 publications reviewed on hybrid solar and wind, only 4 deal with control in general, but none of them with optimal operation control.

Bajpai and Dash (2012) presented a comprehensive review of the research in the four main areas, i.e. unit sizing, optimization, energy flow management and modelling of the hybrid renewable energy system components in the past 10 years. It has been noticed that this paper only summarizes the key parameters that influence or assist in deciding on the optimal energy management strategy. It does not give extensive information on optimal operation control.

Zhou et al. (2010) reviewed the state of the simulation, optimization and control technologies for the standalone hybrid solar-wind energy systems with battery storage. They have found that continued research into and development of this area of study is still needed for improving the systems' performance; establishing techniques for accurately predicting their output, and reliably integrating them with other renewable or conventional power generation sources.

2.4. Software and algorithms used in hybrid systems' optimal operation control

Several optimization tools have been developed and extensively used in optimization applications. A comprehensive literature survey of available software tools used for hybrid renewable systems' performance evaluation is available in the paper from Connolly (2010). The simulation results obtained using these tools often incorporate financial costing of the proposed hybrid system configuration (Kusakana and Vermaak, 2013d; Ibrahim et al., 2011). However, only the most relevant software tools, as well as algorithms used in literature dealing with optimal operation control, will be presented in this section.

Dufo-Lopez and Bernal-Agustın (2005) have developed the HOGA program (Hybrid Optimization by Genetic Algorithms) used to design a PV-Diesel system (sizing and operation control of a PV-Diesel system). The program has been developed in C++. Two algorithms are used in HOGA. The main algorithm obtains the optimal configuration of the hybrid system, minimizing its Total Net Present Cost. For each vector of the main algorithm, the optimal strategy is obtained (minimizing the non-initial costs, including operation and maintenance costs) by means of the secondary algorithm. In the paper, a PV-Diesel system optimized by HOGA is compared with a standalone PV system that has been dimensioned using a classical design method based on the available energy under worst-case conditions. HOGA is also compared with a commercial program for optimization of hybrid systems such as the Hybrid Optimization Model for Energy Renewable (HOMER) and HYBRID2. In Dufo-Lopez and Bernal-Agustın (2008a), the same authors have presented a study of the influence of mathematical models in the optimal design of PV-Diesel systems. For this purpose, HOGA has been used. The mathematical models of some hybrid system elements have been improved in comparison to those usually employed in hybrid systems' design programs. Furthermore, a more complete general control strategy has been developed, one that also takes into account more characteristics than those usually considered in this kind of design.

Razak et al. (2010) discussed the optimization of the renewable energy hybrid system based on the sizing and operational strategy of the generation system using HOMER software. The sensitivity analysis was also performed to obtain the optimal configuration of hybrid renewable energy based on different combinations of the generation system.

Souissi et al. (2010) discussed an optimization solution of a hybrid system of renewable energy sources by using the HOMER software. They emphasised the importance of the emergency generator in order to ensure the reliability and the economy of the system. Fulzele and Dutt (2012) developed a methodology for optimum planning of a hybrid PV-Wind system with some battery backup. The local solar radiation, wind data and components database from different manufacturers have been analysed and simulated in HOMER to assess the technical and economic viability of the integrated system. The performance of each component has been evaluated and finally, the sensitivity analysis has been performed to optimize the system in different conditions. Razak et al. (2009) discussed the optimization of the hybrid system in the context of minimizing the excess energy and cost of energy. The hybrid of pico-hydro, solar, wind and generator and battery as back-up is the basis of assessment. The system configuration of the hybrid is derived based on a theoretical domestic load at a remote location and local solar radiation, wind and water flow rate data. Three demand loads are used in the simulation using HOMER to find the optimum combination and sizing of components. In (Razak et al., 2008) the same authors reviewed an optimization of a renewable hybrid system in which pico-hydro is considered as a dominant component. The system focuses on maximizing the use of the renewable energy system while minimizing the usage of a diesel generator. Initial evaluation is done using HOMER. Optimization viability is based on the component sizing and the hybrid operational strategy. Final evaluation by genetics algorithm is used to evaluate both conditions in minimizing the life cycle cost for optimum configuration. Performance of each component of the hybrid was evaluated. Sensitivity analysis is also performed to optimize the system in different conditions.

Nafeh (2009) developed and applied an operational control technique, based on using the fuzzy logic controller (FLC) and the commonly used ON-OFF controller for a Photovoltaic-

Diesel-Battery hybrid energy system. This control technique aims to reliably satisfy the system's load, and at the same time to optimize the battery and diesel operation under all working atmospheric conditions. The proposed hybrid energy system is modelled and simulated using MATLAB/Simulink and FUZZY toolbox. The FLC is mainly designed to overcome the nonlinearity and the associated parameters variation of the components included in the hybrid energy system, therefore yielding better system's response in both transient and steady state conditions.

Ribeiro et al. (2011) presented the specification, design and development of a standalone micro-grid supplied by a hybrid wind-solar generating source. The goal of the project was to provide a reliable, continuous, sustainable and good-quality electricity service to users, as provided in bigger cities.

Woon et al. (2008) reviewed an optimal control approach used by Tiryono et al. (2003) to evaluate the differences in operating strategies and configurations during the design of a PV-diesel-battery model. However, Tiryono et al. (2003) did not capture all realistic aspects of the hybrid power system. In this paper, the optimal control model was analysed and compared with three different simulation and optimization programs. The authors proposed several improvements to the current model to make it more representative to real systems.

Gupta et al. (2008a) presented the flowcharts of the optimum control algorithm based on combined dispatch strategies, to achieve the optimal cost of battery incorporated hybrid energy system for electricity generation, during a period of time, by solving the mathematical model, which was developed in one of their previous papers. The main purpose of the control system proposed here was to reduce, as much as possible, the participation of the diesel generator in the electricity generation process, taking the maximum advantage of the renewable sources available. The overall load dispatch scenario was controlled by the availability of renewable power, total system load demand, diesel generator operational constraints and proper management of the battery bank.

Schmitt (2002) developed SimPhoSys (Simulation of Photovoltaic Energy Systems) to simulate the performance of photovoltaic energy systems. Detailed mathematical models of the system components have been implemented in a MATLAB/Simulink environment.

SimPhoSys provides component models only for the PV generator, battery, battery charge controller, electronic converter, diesel generator and various types of loads.

Engin (2013) developed a procedure for sizing hybrid systems using mathematical models for photovoltaic cell, wind turbine, and battery that are present in the literature. This sizing procedure can simulate the performance of different renewable source combinations achieving the lowest energy cost. The output of the program displays the annual performance of the system, the total cost of the system, and the best size for the hybrid system.

2.5. Operation control and hybrid system reliability

Several performance indicators to evaluate the reliability of hybrid renewable systems have been reported in the literature (Kaviani et al., 2008; Ghosh et al., 2003). Hence, this section will present only the research works in which the most common reliability indices are used together with operation control strategies.

Diaf et al. (2007) presented a methodology to perform the optimal sizing of an autonomous hybrid PV/wind system. The methodology aims at finding the configuration, among a set of system components, which meets the desired system's reliability requirements, with the lowest value of levelised cost of energy. Modelling a hybrid PV/wind system is considered as the first step in the optimal sizing procedure. The authors proposed more accurate mathematical models for characterizing a PV module, wind generator and a battery. The second step consists of the optimized sizing of a system according to the loss of power supply probability (LPSP) and the levelised cost of energy (LCE) concepts.

Satar et al. (2012) presented a hybrid system control algorithm and also dispatched strategy design in which wind is the primary energy resource linked with photovoltaic cells. The main task of the proposed algorithm is to take full advantage of the wind energy and solar energy when it is available and to minimize diesel fuel consumption. In this paper the system operation cost was given as a linear function of the total capacity in MW. No other mathematical model of the system's control was presented.

Ashari and Nayar (1999) presented dispatch strategies for the operation of a solar photovoltaic (PV)–diesel– battery hybrid power system using 'set points'. This includes the determination of the optimum set points values for the starting and stopping of the diesel generator in order to minimize the overall system costs. A computer program for a typical dispatch strategy has been developed to predict the long-term energy performance and the life cycle cost of the system.

Rashtchi et al. (2009) introduced hybrid Photovoltaic-Fuel Cell generation system for a typical domestic load that is not located near the electric grid. In this configuration, the combination of a battery, an electrolyser and a hydrogen storage tank, were used as the energy storage system. The aim of this design was minimization of overall cost of a generation scheme over 20 years of operation. An energy based modelling has been developed using MATLAB/Simulink to observe evolution of the system during a typical day, and the results are reported and discussed. An overall power management strategy was designed for the proposed system to manage power flows among the different energy sources and the storage unit in the system.

Dursun and Kilic (2012) presented different power management strategies of a stand-alone hybrid power system. The system consists of three power generation systems, photovoltaic (PV) panels, a wind turbine and a proton exchange membrane fuel cell (PEMFC). PV and wind turbine are the main supply for the system, and the fuel cell is used as a back-up power source. Therefore, an energy storing device is needed to ensure continuous energy supply. In this proposed hybrid system, gel batteries were used. The state of charge (SOC), charge-discharge currents are affecting the battery energy efficiency. In this study, the battery energy efficiency is evaluated via three different power management strategies. The control algorithm was made possible through the use of MATLAB/Simulink.

In the paper from Wang and Singh (2007), a standalone hybrid power generation system including different power sources such as wind turbine generators, PVs, and storage batteries, is designed by minimizing total costs and maximizing reliability simultaneously using Particle Swarm Optimization (PSO). The system operation strategies are presented in terms of power balance. In Wang and Singh (2007), the same authors have designed a grid-

connected hybrid generating system comprising wind turbine generators, photovoltaic panels and storage batteries. In this system design, three design objectives were considered, that is, costs, reliability and pollutant emissions. Considering the complexity of this problem, the authors have developed a Multi-Objective Particle Swarm Optimization (MOPSO) algorithm to derive a set of non-dominated solutions, each of which represents a candidate system design. A numerical example is discussed to illustrate the design procedure and the simulation results are analysed.

Ardakani et al. (2010a) designed a hybrid wind/photovoltaic/battery generation system. The aim of this design is to minimize the annualized cost of the standalone system over its 20 years of operation. The optimization problem was subject to economic and technical constraints. System costs entailed the investments, replacements, operation and maintenance as well as loss of load costs. The technical constraint, related to system reliability, was expressed by the equivalent loss factor. The reliability index was calculated from component failure, that includes wind turbine, PV array, battery and inverter failure. In (Ardakani et al.; 2010b) the same authors conducted a similar study with a grid-connected hybrid wind/photovoltaic/battery power system.

Razak et al. (2007) reviewed the application of genetic algorithms in optimization of a hybrid system, consisting of pico-hydro system, solar photovoltaic modules, diesel generator and battery sets. The system focused on maximizing the use of the renewable system while minimizing the usage of a diesel generator. The hybrid system configuration was derived based on the required load. Optimization viability was based on the component sizing and the hybrid operational strategy. Frugal option, state of charge of the batteries and power supplied by each component of the hybrid, were the main criteria in determining the best operational strategy.

Muralikrishna and Lakshminarayana (2008) analysed the system size and performance against the influence of the Deficiency of Power Supply Probability (DPSP); Relative Excess Power Generated (REPG); Energy to Load Ratio (ELR); fraction of PV and wind energy, and coverage of PV and wind energy. The methodology of Life Cycle Cost (LCC) for

economic evaluation of a standalone photovoltaic system, standalone wind system and PV-wind hybrid system, was developed and simulated using the model.

In this study from Barley et al. (1995), time-series models were used to determine optimal dispatch strategies, in conjunction with optimally-sized components, in remote hybrid power systems. The objective of the dispatch optimization was to minimize the costs associated with diesel fuel, diesel starts, and battery erosion, based on a thorough economic analysis of present worth life cycle cost. An ideal predictive control strategy was used as a basis of comparison. The authors used a simplified time-series model to obtain preliminary conceptual results. These results illustrate the nature of the optimal dispatch strategy and indicate that a simple State of Charge set-point strategy can be practically as effective as the ideal predictive control.

Kaviani el al. (2009) designed a hybrid wind/photovoltaic/fuel cell generation system to supply power demand. The aim of this design was minimization of annualized cost of the hybrid system over its 20 years of operation. The optimization problem was subject to reliable supply of the demand. Three major components of the system, i.e. wind turbine generators, photovoltaic arrays, and DC/AC converter, may be subject to failure. Also, solar radiation, wind speed, and load data were assumed to be entirely deterministic. System costs entail the investments, replacement, operation and maintenance as well as loss of load costs.

Yang et al. (2008) recommended an optimal sizing method to optimize the configurations of a hybrid solar-wind system employing battery banks. Based on a genetic algorithm (GA), which has the ability to attain the global optimum with relative computational simplicity, one optimal sizing method was developed to calculate the optimum system configuration that can achieve the customers' required loss of power supply probability (LPSP) with a minimum annualized cost of system (ACS). The decision variables included in the optimization process were the PV module number, wind turbine number, battery number, PV module slope angle and wind turbine installation height.

Sánchez et al. (2010) presented the optimal sizing of a generation system wind-photovoltaic-fuel cell so that demand of an isolated residential load is met. The function objective was constituted by the costs of the system, and the solution method employed was

based on PSO. The aim of this work was to minimize the total cost of the system so that demand is met. In order to compare the performance of PSO with other methods, the sizing of the renewable generation system was also done by the heuristic method called Differential Evolution.

Dehghan et al. (2009) presented a hybrid wind/photovoltaic plant, with the aim of supplying an IEEE reliability test system load pattern while the plant capital investment costs are minimized by applying a hybrid particle swarm optimization (PSO) / harmony search (HS) approach, and the system fulfils the appropriate level of reliability.

Hassanzadehfard et al. (2011) formulated the optimization problem as a nonlinear integer minimization problem which minimizes the sum of the total capital, operational and maintenance and replacement cost of Distributed Energy Resources (DERs), subject to constraints such as energy limits of each DER. The authors proposed Particle Swarm Optimization (PSO) for solving this minimization problem. In this paper some notions of reliability were considered for micro-grid, and the effect of reliability on total cost of micro-grid was evaluated.

Kirthiga and Daniel (2010) used PSO and modified GA optimization techniques to determine the sizes of hybrid renewable system for autonomous operation. The authors have developed a MATLAB code for a standard 33 bus distribution system used to demonstrate the effectiveness of the methodology.

Bashir and Sadeh (2012a) proposed a new algorithm for determining the capacity of a hybrid wind, photovoltaic and battery generation system by considering the uncertainty in wind and photovoltaic power production. The algorithm of determining capacity of wind, photovoltaic and battery for supplying a certain load was formulated as an optimization problem that the objective function was the minimization of the cost and with the constraint of having specific reliability. In (Bashir and Sadeh, 2012b) the same authors have considered the combination of wind, photovoltaic and tidal as a primary and battery as an auxiliary source for which determining the capacity was formulated as an optimization problem. The objective function was the minimization of the cost with the constrain having Equivalent Loss Factor (ELF) as specific reliability index. Particle Swarm Optimization (PSO) was used

for optimal sizing of the system. Simulation results were carried out by MATLAB software. It is shown that a hybrid system is the best configuration that has minimum cost and can satisfy all constrains.

Hakimi et al. (2011) applied a novel intelligent method to the problem of sizing in a hybrid power system so that the demand of residential area was met. The system consisted of fuel cells, some wind units, some electrolysers, a reformer, an anaerobic reactor, and some hydrogen tanks. The system was assumed to be standalone and uses the biomass as an available energy resource. System costs entailed investments, replacement, operation and maintenance as well as loss of load costs. Particle swarm optimization algorithm is used for optimal sizing of the system's components.

Jalilzadeh, Kord and Rohani (2010) introduced a method for unit sizing of a hybrid Photovoltaic/Fuel Cell generation system for a typical isolated domestic load, with the aim of finding the configuration, among a set of system components, which meets the desired system reliability requirements, with the lowest value of levelised cost of energy over 20 years of operation. The authors designed a strategy for the proposed system to manage power flows among different energy sources and storage unit.

Hu and Solana (2013) presented a general model based on a real option theory for evaluating a hybrid diesel-wind generation plant. A dynamic programming method has been used to generate the optimum operational option by maximizing the net cash flow of the plant. Results showed that operational options can provide additional value to the hybrid power system when this operational flexibility is correctly utilized. This paper also provided a framework to find the optimal operating decision at each time step based on the real option model.

Giannakoudis et al. (2010) addressed the design and optimization problem under uncertainty of power generation systems using renewable energy sources and hydrogen storage. A systematic design approach was proposed that enables the simultaneous consideration of synergies developed among numerous sub-systems within an integrated power generation system, and the uncertainty involved in the system operation. The Stochastic Annealing optimization algorithm was utilized to handle the increased

combinatorial complexity and to enable the consideration of different types of uncertainty in the performed optimization. A parallel adaptation of this algorithm was proposed to address the associated computational requirements through execution in a Grid computing environment. Numerous design and operating parameters were considered as decision variables, while uncertain parameters were associated with weather fluctuations and operating efficiency of the employed sub-systems. The obtained results indicated robust performance under realizable system designs, in response to external or internal operating variations.

2.6. Hybrid system optimal operation control modeling

Several mathematical models have been developed with different objectives such as optimizing the hybrid system operation costs, pollutant emissions, unmet load, fuel consumption, etc. Therefore, this section will present the major works done by authors who attempted to develop mathematical models for hybrid system optimal operation control.

Bernal-Agustın and Dufo-Lopez (2008b) presented a triple multi-objective design of isolated hybrid systems minimizing, simultaneously, the total cost throughout the useful life of the installation, pollutant emissions (CO_2) and unmet load. For this task, a multi-objective evolutionary algorithm (MOEA) and a genetic algorithm (GA) have been used in order to find the best combination of components of the hybrid system and control strategies. In (Bernal-Agustın and Dufo-Lopez, 2009b; Bernal-Agustın and Dufo-Lopez, 2006; Bernal-Agustın et al., 2006), the authors applied the strength Pareto evolutionary algorithm to the multi-objective design of renewable hybrid systems, with the aim of minimizing together the life cycling cost and the unmet load. For the system optimal sizing and operation control, an MOEA and GA have been used. A novel control strategy has been developed and explained in this article.

Seeling-Hochmuth (1997) developed a method to jointly determine and optimally incorporate the sizing and operation control of hybrid-PV systems. This model is based on the current flow through the system from the generators to the loads. The different

operation strategies, on which depends the current flow as well as the operation costs, can be chosen by making a search through the possible system's operation control settings. The algorithm used is divided into a main (sizing) and a sub-algorithm (operation optimization), respectively.

Dagdougui et al. (2010), presented a model for integrated hybrid system based on a mix of renewable energy technologies comprising an electrolyzer, hydroelectric plant, pumping stations, wind turbines and fuel cell. The model is developed with the aim of optimizing the control of energy storage while satisfying the hourly variable electric, hydrogen, and water demands or real time operational management.

Gupta et al. (2008b) analysed and designed a mixed integer time series linear programming model for optimal cost and operation of a hybrid energy generation system consisting of a photovoltaic array, biomass, biogas, micro hydro, a battery bank and a fossil fuel generator, based on demand and potential constraints.

Dagdougui et al. (2010) have presented the structural Decision Support System (DSS) that can be used for the optimal energy management on a local scale through the integration of different renewable energy sources. The integrated model of a grid connected hybrid energy system components is developed. The system is composed of PV and solar thermal modules, wind and a biomass plant. Furthermore, a framework is presented to optimize the different means of ensuring the micro-grid's electrical and thermal energy demand as well as the water demand, with specific reference to the presence or absence of a storage system. Finally, the optimization model has been applied to a case study.

Sopian et al. (2008) reviewed the application of genetic algorithms in the optimization of hybrid systems based on component sizing and the operational strategy. Genetic algorithms are used to find the best configuration based on the lower net present cost. Random selections of sizing and operation strategy as well as sensitivity analysis are also performed to optimize the system under different conditions.

Ashok (2007) discussed different hybrid systems' components and developed a general mathematical model to find an optimal selection of energy components minimizing the life cycle cost. The optimal dispatch strategy of hybrid energy system consists of finding the

most economical schedule for different combinations of the system components, satisfying load requirements, resource availability and equipment constraints.

Tazvinga et al. (2013) developed a hybrid system model incorporating photovoltaic cells and diesel generator in which the daily energy demand fluctuations for different seasonal periods of the year in order to evaluate the equivalent fuel costs as well as the operational efficiency of the system for a 24 hours period. The results show that the developed model can give a more realistic estimate of the fuel costs reflecting fluctuations of power consumption behaviour patterns for any given hybrid system.

2.7. Limitations and future works in hybrid systems optimal operation control

From the studied literature, it has been noticed that most previously published research works have assumed a fixed load and uniform daily operational cost which can be extrapolated to get the monthly or annual cost. The renewable resources are, in most cases, given on an average monthly basis, thus the impact of the resources' variation in short periods of time is neglected, and therefore the accuracy of operation cost obtained is diminished. It has also been noticed that complete and detailed mathematical formulations are not given in most works dealing with optimal operation control. The following shortfalls can be pointed out:

- The diesel generator fuel consumption is in most cases is represented as a linear function.
- Fixed load demand and constant daily operational cost, which can be extrapolated to obtain monthly or yearly operation costs, are considered in most of the cases.
- Some renewable energy sources (Waves, Tidal, Hydrokinetic, etc.) are not included in most developed hybrid system models as well as in current optimization software such as HOMER. In addition, not all types of energy storage systems are included (such as flywheel, etc.).

Thus for future work, renewable sources such as Waves, Tidal, and Hydrokinetic should be included in the architecture of hybrid systems to assess their impact on the systems' operation control and on the cost of energy produced.

2.8. Summary

This Chapter has provided an overview of the research developments in the area of optimal operation control applied to hybrid renewable energy systems. Several papers from major referenced journals in the area of renewable hybrid system control have been reviewed. One of the findings in this Chapter is that that there are a significant number of research articles dealing with optimal sizing of hybrid systems; however, only a few research works have been dedicated to optimal operation control of hybrid renewable energy systems. Literature dealing with the current status of different optimal control approaches, their applications as well as limitations in the area of hybrid renewable systems, have been discussed. This Chapter has also highlighted and suggested future works that can make significant contributions to hybrid systems' optimal operation control research area.

Chapter III: System components and their operation in a hybrid energy system

3.1. Introduction

This Chapter will describe the different components that can be incorporated in the architecture of a hybrid system, how they interact and how they can be controlled. The main goal is to provide an understanding of the complex interaction between the energy sources, the conversion and storage components as well as the loads in a hybrid system. A hybrid system's performance is only as good as is the precision of its components; therefore, the emphasis will be on the component design, operation principle, operation issues as well as on the component operation in a hybrid system.

3.2. Diesel generator

3.2.1. General description

Diesel generators are normal diesel engines coupled to generators. DGs are the most common way of providing AC power to isolated areas not connected to the grid and are currently available in different sizes ranging from less than one kW to over MW. The energy generated (E_{DG}) by a DG with rated power output (P_{DG}) is expressed as (Hu and Solana, 2013):

$$E_{DG} = P_{DG} \times \eta_{DG} \times t \tag{3.1}$$

Where: η_{DG} is the efficiency of the DG.

t is the time (s).

Compared to other supply options such as renewable energy sources, DGs have low initial capital costs and generate electricity on demand. Some major disadvantages of DGs are the high operation and maintenance costs, transport and storage costs, and noise as well as pollution emission in the environment (Mahmoud and Ibrik, 2006).

The overall cost of the kWh resulting from the use of the DG is very high. This includes some of the following costs:

- The operating cost which comes mainly from the direct fuel cost.
- The cost of the transportation of the fuel. This can be high depending on how the area to supply is remote or isolated.
- The maintenance and replacement costs. A typical lifetime for DG can range from 25000-30000 operating hours. In the specific case of a small generator running continuously, this lifespan can be sensibly reduced.

DGs which are being used in rural applications are often sized to be able to carry the load even during peak power demand. DGs are usually designed in such a way that they always operate between 80-100 % of their kW rating to achieve high efficiency (Dufo-Lopez and Bernal-Agustın, 2008c). This condition can be used later as an operation constraint.

The following is the typical non-linear fuel consumption curve (according to manufacturers' specifications) (Jennings, 1996):

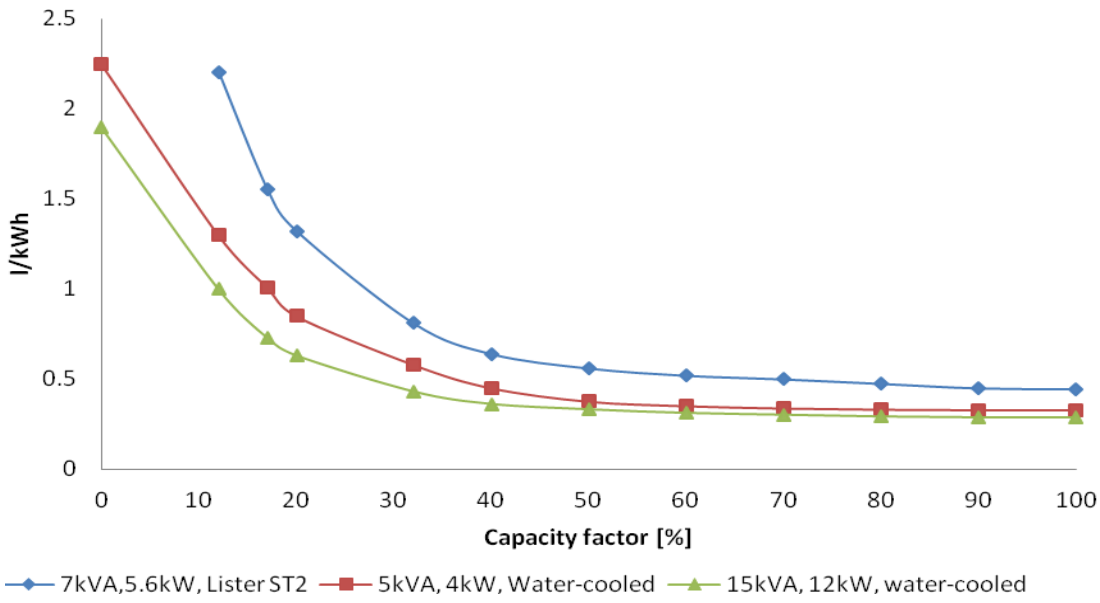

Figure 3.1: DGs specific fuel consumption curves as a function of the capacity factor

3.2.2. Diesel generator variables

The AC Diesel Generator output voltage is usually equal to the AC bus voltage, so in most cases DGs are not connected in series. They can be connected in parallel to match the system current requirements.

The instantaneous output power from the DG depends on variables such as the type or the size of the DG used (n_{DG}, *Size, Type*). It is an operation decision variable expressed as:

$$P_{DG} = P_{DG,\max/U} \times X_{DG} \tag{3.2}$$

Where: P_{DG} is the output power of the diesel generator, which is a percentage of the maximum DG power.

$P_{DG,\ max/U}$ is the maximum nominal DG power.

X_{DG} is the DG output decision variable between [0, 1]. 0 corresponds to no DG output and 1 to maximum output.

3.2.3. Operation issues

As it can be noticed from Figure 3.1 above, DGs should not be operated at low loading because this results in lowered fuel efficiency. Therefore a dump load is commonly used to dissipate energy when the load demand is low, to keep the fuel efficiency high. Some other issues in operating DGs are the start-ups (DGs should not be turned OFF for a long period; frequent start-ups result in wear and tear) and maintenance (to decrease the frequency of maintenance shorter operating times and more oil changes are recommended).

3.2.4. Operation in a hybrid system

DGs are integrated in the hybrid system as back-up and used when the renewable energy components and the battery cannot meet the demand. By using DGs in a hybrid system configuration, cost saving can be achieved due to the following factors (Xianzhang et al., 2013):

- Fuel: When turned ON, the generator will be used efficiently because it is always running at high loading. When it is OFF, there will be no fuel used, which will result in a sensible overall reduction in the fuel consumed.
- Refilling: Along with the reduction in fuel consumption, the frequency as well as the cost of the transportation of the fuel to the remote or isolated area, will also decrease.
- Maintenance and replacement: Because the DG will not be running continuously and the load is mostly supplied by the renewable sources and by the batteries, the meantime between maintenance linked to the operation hours will increase. Consequently, the DG life span will increase, resulting in a decrease in maintenance and replacement costs.

However, the integration of DGs in a hybrid system is not straightforward: problems such as high numbers of stop-start cycles or increase in the specific fuel consumption, due to the DG extended running time on low loading can occur. Therefore the cost saving

described above will largely depend on the hybrid system components' optimal sizing and on the operational control strategies adopted.

3.3. Micro-hydropower (Hydrokinetic system)

3.3.1. General description

In this study, the hydrokinetic system has been selected instead of the traditional micro-hydropower. Hydrokinetic systems extract kinetic energy from moving water without the need for a dam, barrage or penstock. Hydrokinetic can generate power from low speed flowing water with almost zero environmental impact, over a much wider range of sites than those available for conventional hydropower generation (Güney and Kaygusuz, 2010).

The hydrokinetic system operation principle is identical to that of the wind turbine. The fact that water is approximately 800 times denser than air implies that the amount of energy produced by a hydrokinetic turbine is much greater than that produced by a wind turbine of equal diameter under equal water and wind speed (Maniaci and Li, 2011). The other advantages of hydrokinetic systems are that the water resource does not fluctuate unpredictably in a very short period of time as does the wind speed, and the flow of water does not change direction as does the wind does.

The energy generated (E_{HKT}) by the hydrokinetic system is expressed as (Clark, 2007):

$$E_{HKT} = \frac{1}{2} \times \rho_W \times A_{HKT} \times C_{p,H} \times \eta_{HKT} \times \int_{t_0}^{t} v_W{}^3(t) \times f(t) \times dt \qquad (3.3)$$

Where: ρ_W is the density of water (1000kg/m^3);

$C_{p,H}$ is the coefficient of the hydrokinetic turbine performance;

η_{HKT} is the combined efficiency of the hydrokinetic turbine and the generator,

A is the turbine area (m^2);

v is the water current velocity (m/s);

t is the time (s), and

f(t) is the water probability density function.

The two main types of hydrokinetic turbines are axial-flow turbine (having their axes parallel to the water flow) and cross-flow turbine (having their axes orthogonal to the water flow but parallel to the water surface).

3.3.2. Hydrokinetic system variables

Several hydrokinetic turbines can be connected in parallel to match the current requirements of the system. The number of hydrokinetic turbines in parallel n_{HT} is a design variable.
The output power from the hydrokinetic system depends on variables such as the type or the size of the turbine used (n_{HT}, *Size, Type*). It can be express as:

$$P_{HKT,system} = P_{HKT/U} \times n_{HKT} \tag{3.4}$$

Where: P_{HKT}, system is the output power of the hydrokinetic system;

$P_{HKT/U}$ is the nominal output power of the one hydrokinetic turbine, and

n_{HKT} is the number of hydrokinetic turbines connected in parallel.

3.3.3. Operation issues

Unlike wind turbines of comparable output, the high power densities obtained with flowing water at different possible operating speeds implies that large thrust forces are applied to hydrokinetic turbines (Fraenkel, 2000). The high axial thrust necessitates the hydrokinetic turbine to be either tightly attached to the seabed via gravity based or piled platform structures, or floated underneath a vessel held by high tension moorings.

It has to be noted that water velocity from streams or rivers varies between a maximum and a minimum according to the seasons of the year; therefore, the hydrokinetic plants have to be optimally designed in such a way as to generate power all through the year.

3.3.4. Operation in a hybrid system

Kusakana (2014) have demonstrated that the hydrokinetic turbine can produce a steadier output power and much cheaper energy than that from PV or wind systems. Therefore, if the hydrokinetic turbine is combined with other energy sources, the output power and performance of the resulting hybrid system can be increased while reducing the final cost of energy produced.

3.4. Wind energy system

3.4.1. General description

Wind energy systems convert the kinetic energy of moving air into mechanical and then electrical energy. Wind turbines are available in different shapes, sizes and prices depending on manufacturers (Schallenberg-Rodriguez, 2013). Given that the wind resource is unreliable and constantly fluctuating, the corresponding output power from the wind energy system also becomes highly variable. In standalone applications, maintaining the wind system's output frequency at a constant value is a real challenge. Therefore the output current is usually rectified to DC, stored in batteries, and then converted back to AC.

As for the hydrokinetic system, the energy generated (E_{WT}) by wind system is expressed as (Ghedamsi and Aouzellag, 2013):

$$E_{WT} = \frac{1}{2} \times \rho_a \times A_{WT} \times C_{p,WT} \times \eta_{WT} \times \int_{t_0}^{t} v_a^{\,3}(t) \times f(t) \times dt \qquad (3.5)$$

Where: ϱ_a is the density of water (1.225kg/m^3);

$C_{p,W}$ is the coefficient of the hydrokinetic turbine performance;

η_{WT} is the combined efficiency of the hydrokinetic turbine and the generator;

A is the wind turbine area (m^2);

v is the wind velocity (m/s);

t is the time (s), and

$f(t)$ is the wind probability density function.

The actual output of a wind turbine is dependent on its power curve supplied by the manufacturer, as shown in Figure 3.2 (Elizondo et al., 2009).

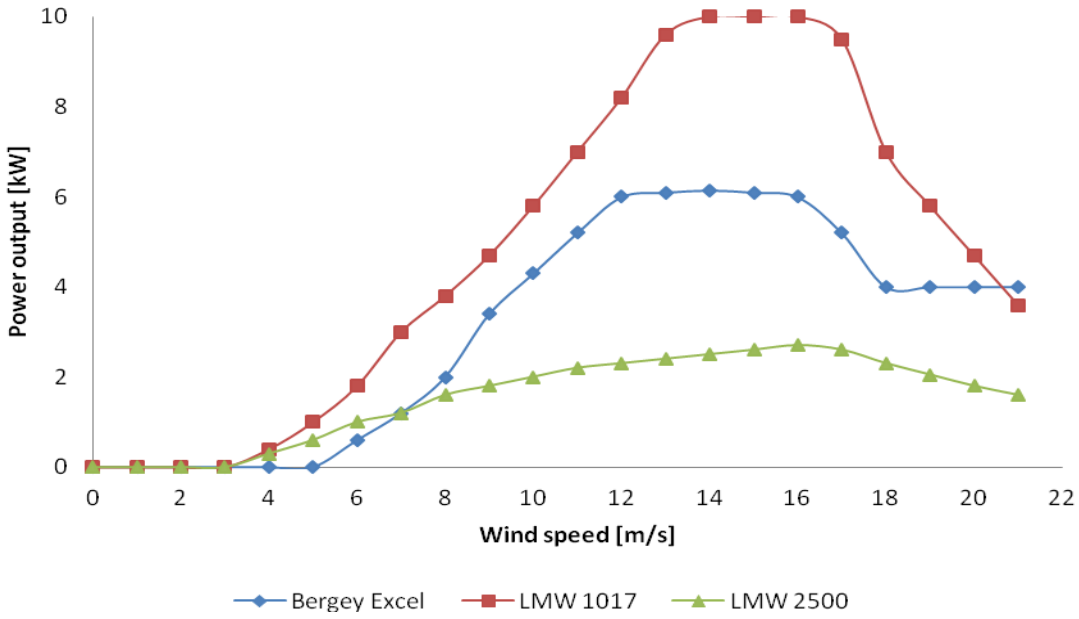

Figure 3.2: Selected wind turbines' power curve

3.4.2. Wind system variables

Several wind turbines can be connected in parallel to match the current requirements of the system. The number of wind turbines in parallel, n_{WT} is a design variable.

The output power from the wind system depends on variables such as the type or the size of the wind turbine used (n_{WT}, *Size*, *Type*). It can be express as:

$$P_{WT,system} = P_{WT/U} \times n_{WT} \quad (3.6)$$

Where: P_{WT}, System is the output power of the wind system;

$P_{WT/U}$ is the nominal output power of the one wind turbine, and

n_{WT} is the number of wind turbines connected in parallel.

3.4.3. Operation issues

As shown in Figure 3.2, the power curve can be used to illustrate the performance of a wind turbine by giving the relationship between wind speed and average output power during a given period. Generally, this output power is assumed to be proportional to the cube of the wind speed; however, different operating behaviours linked to the variation of the wind speed, need to be considered. Therefore, it is assumed that (Lydia et al., 2014):

- The turbine starts generating at the "cut-in" wind speed.
- The generated output power increases with the increases in wind speed from the "cut-in" to the "rated wind" speed.
- The turbine produces a constant or "rated power" when the wind speed varies between the rated wind and the "cut-out" wind speed, which is the maximum wind speed value at which the turbine can correctly work.
- The turbine stops generating when the wind speed goes beyond the cut-out speed for safety reasons.

The wind speed variations have a great impact on the power produced by the wind energy systems. Thus, wind turbine power ratings are usually much higher than the average electrical power demand, especially for areas with low wind resources (Tong, 2010).

3.4.4. Operation in a hybrid system

As seen in the section above, standalone wind energy systems generate highly fluctuating and therefore unreliable energy due to the constant fluctuating wind speed. If the wind turbine is used in combination with other sources in hybrid system configurations, the produced energy can become more stable, increasing the system's performance while reducing the size and the overall cost of the system.

3.5. Photovoltaic system

3.5.1. General description

When light strikes a silicon, gallium arsenide or cadmium sulphide cell, an electric current is generated through the photovoltaic effect (Skoplaki and Palyvos, 2009). The advantages of photovoltaic generation include no pollutant emitted, long operation life and low maintenance costs.

Several cells are connected together to form a PV panel. The PV panel output is DC, therefore an inverter is used to supply AC loads. The power rating of a PV panel is expressed in peak Watts (Wp) indicated at "standard test conditions" conducted at a temperature of 25°C and irradiance of 1000W/m^2.

The output energy (E_{PV}) of the solar PV system can be expressed as follows (Singh, 2013):

$$E_{PV} = A_{PV} \times \eta_{PV} \times \int_{t_0}^{t} I(t) \times f(t) \times dt \tag{3.7}$$

Where: A is the total area of the photovoltaic generator (m^2);

η_{PV} is the module efficiency;

η_{PC} is the power conditioning efficiency;

f(t) is the solar probability density function, and

I is the hourly irradiance (kWh/m^2).

The electricity generation from a PV panel is silent and there are no moving parts in the system except when a tracking system is incorporated. Maximum power point trackers (MPPT) are often used to increase the output power from PV panels. PV panels can be manufactured in different sizes and the conversion efficiency of available solar panels is around 15-19% (Wang et al., 2014).

3.5.2. PV variables

The number of PV panels in series is not a design variable, because it is dictated by the nominal voltage of the DC bus which is a constant. On the other side the number of PV panels in parallel, n_{PV} is a design variable. If n_{PV} changes, the corresponding output current of the PV array also changes.

The output power from the whole PV system depends on variables such as the type or the size of the panels used (n_{PV}, *Size, Type*). It can be expressed as:

$$P_{PV,system} = P_{PV,panel/U} \times n_{PV} \tag{3.8}$$

Where: $P_{PV,System}$ is the output power of the whole PV system;

$P_{PV,panel/U}$ is the nominal output power of the one PV panel, and

n_{PV} is the number of PV panels in parallel.

3.5.3. Operation issue

PV panels have a particular voltage-current relationship which can be represented by an IV-curve which is available from the manufacturers at different levels of solar radiation keeping other variables such as temperature and wind speed constant. The performance of a PV system strongly depends on the irradiation and temperature levels at a given time and

given location, as shown in Figure 3.3 (Duffie and Beckam, 2006). Therefore, consistent understanding and knowledge of the PV system under different operating conditions is essential for accurate module selection and precise prediction performance.

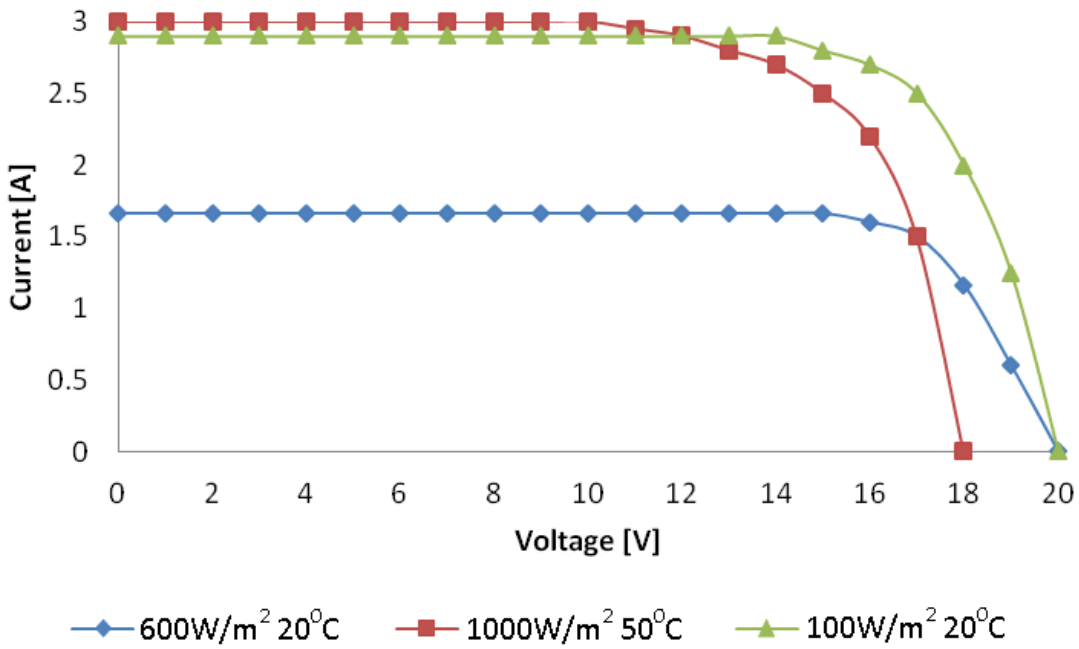

Figure 3.3: I-V curves showing the effects of solar insolation and temperature on PV panel performance.

3.5.4. Operation in a hybrid system

Better system performance may be more easily realized using a hybrid system than via a single-source system. Incorporating a PV component in a hybrid system usually reduces the size of the PV panels to realize system autonomy, in particular when complementarity of different energy sources can be used efficiently. The difference between the DC voltage of the PV panel and DC bus voltage can be minimized in hybrid systems, and maximum power point trackers are often not required, reducing the cost of the system.

3.6. Battery storage system

3.6.1. General description and operation issue

Batteries are electro-chemical devices that are used to store energy in chemical form. They are composed of one or more cells connected in series. Each cell is made of plates that are immersed in an ion-conducting medium called electrolyte. During the discharge process a chemical reaction between the plates and the electrolyte produces electricity. This chemical reaction is reversed during the battery charging process.

Batteries are available in different types, capacities and voltages. The deep-cycle lead-acid battery type is the most extensively used as a storage system or back-up in combination with renewable energy sources, because of its reliability and low cost (Krieger, 2013). However, its main constraint is that it must be used within strict limits as it is vulnerable and easily damageable under certain operating conditions such as overcharging, undercharging and remaining for a long period of time in a low state of charge (Fernández et al., 2013). The initial cost of a battery is much lower than that of other components of the system; however, under unfavourable operating conditions, its maintenance and replacement costs can grow to be a major part of the total system's life cycle costs and can prove to be very expensive in the long term. Under favourable operating conditions the battery can last up to 15 years in a standalone application.

3.6.2. Battery variables

The instantaneous output power from a battery P_{Bat} is an operation decision variable: it is a percentage of the maximum available battery power at that instant. It can be expressed as:

$$P_{Bat} = P_{Bat,\max/U} \times X_B \times n_B \tag{3.9}$$

Where: P_B is the instantaneous output power, which is a percentage of the maximum battery power at that time t.

$P_{B,max/U}$ is the maximum battery power at that time t, and

X_B is the battery output decision variable between [0, 1] as for the DG.

The number of batteries in series is dictated by the nominal voltage of the DC bus which is a constant. The instantaneous output power from the whole battery bank depends on variables such as the type and the size of the battery used (n_B, *Size, Type*) and, the number of battery strings in parallel n_B.

The dynamics of the battery state of charge (SOC) can be expressed in discrete-time domain by a first order difference equation as follows (Sechilariu et al., 2014). The battery dynamic equation can be expressed as:

$$SOC_{(j)} = SOC_{(0)} - t_s \frac{\eta_{Bat}}{E_{nom}} \sum_{i=1}^{j} P_{Bat}(i) \tag{3.10}$$

Where: *SOC* is the state of charge of the battery; η_{Bat} is the battery charging or discharging efficiency; t_s is the sampling time (interval)*;* E_{nom} is the battery system nominal energy and, P_{Bat} is the power flowing from the battery system.

3.6.3. Operation in a hybrid system

When a battery is used in conjunction with other energy sources in a hybrid system configuration, its operating life can be increased. This is because advanced control is usually incorporated in a hybrid system due to the interaction of different components. This necessitates better control of the hybrid system components operation and will also lead to better operation of the battery. Furthermore, the hybrid system does not rely on a single energy source resulting in the battery not being used to a high extent as in single-source systems, thus their size can also be optimally reduced the save costs. Reducing the battery operating cycles results in increased lifetime and reduced hybrid system overall cost.

3.7. Inverter

3.7.1. General description

Inverters are used to convert DC power, e.g. from DC power sources and batteries, to AC power, which is needed by most electrical appliances. In most of the small rural applications where renewable energies sources and batteries are used to supply low power rating household equipments, cheap single phase inverters can be selected instead of expensive ones which are mostly used for their capabilities to deal with unbalanced loads (Manchester and Swan, 2013).

The harmonic distortion of inverters gives an indication as to how close to a pure sine wave, the inverter output waves are. The following are different types of inverters available on the market according to their output waveforms:

- Square wave and quasi-square: Compared to pure sine wave inverters, these inverters will introduce harmonic distortions. However, these inverters are cheap and can be well suited to power resistive loads such as a small stove, iron, heater or incandescent lights.
- Modified sine wave: These inverters produce a better square wave with less harmonic distortion and which is close in shape to a pure sine wave. They are used to supply almost all AC electronic devices and electric motors.
- Sine wave: These expensive inverters can produce an output wave compared to that from the utility and are used to power very sensitive electronic equipments.

Normally inverters are designed to switch off when the output energy needed goes beyond its upper operating limit. However, heat-limited inverters can be used to supply in excess of their upper operating limit energy output for 30 minutes; this can be very useful in applications' such as the starting of induction motors (Mohd et al., 2010).

3.7.2. Operation issue

As shown in Figure 3.4, a typical efficiency curve can be used to illustrate the performance of an inverter at low and high power level. It can be seen that the efficiency of the inverter is directly proportional to the power level, therefore to avoid low efficiency problems, is it recommended that the inverter be operated only at preferred output levels. This can be done by designing specialized inverters with high efficiency in the low power regions or using inverters in parallel.

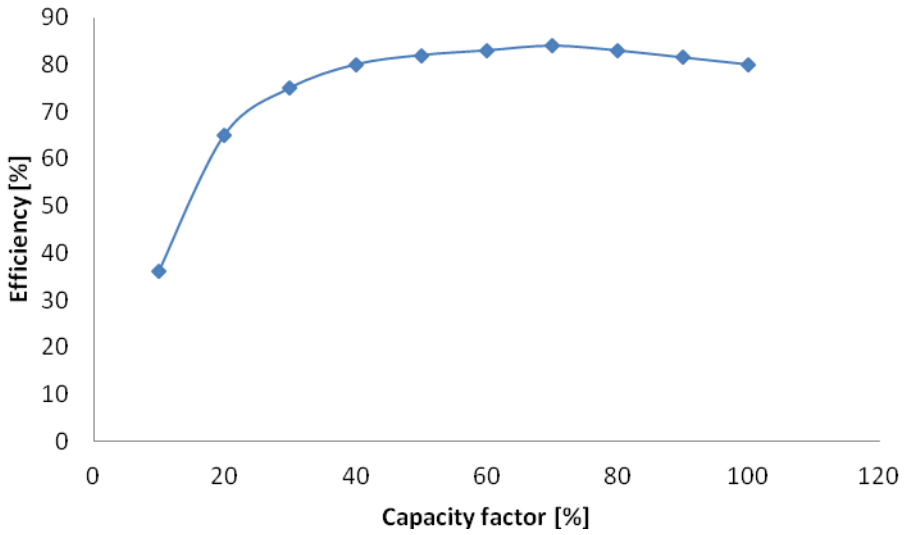

Figure 3.4: Example of inverter capacity factor versus efficiency

3.8. Rectifier

3.8.1. General description

Rectifiers are devices used to convert AC power from renewable energy sources or diesel generators to DC power, for battery charging purposes or to supply AC loads. They are usually simple in their design and inexpensive (Khaburi and Nazempour, 2012).

3.8.2. Operation issue

Battery chargers' efficiency characteristics tend to decrease due to the high charging current that is producing power losses in the transformer. The major problem with rectifiers used as battery chargers is their low power factor because current is drawn only at small parts of the AC voltage curve. This intermittent drawing of power is unwanted from the supply side as power has to be generated in short bursts, while a more constant output is recommended (Rodríguez, 2011).

3.9. Loads

The majority of available loads are 12V DC, 24V DC, 220/230V AC and 380V AC. AC appliances can be slightly cheaper than similar DC appliances.

The load power demand is not constant; it depends on the daily activities of the users which might change depending on different seasons of the year. Therefore the power sources and storage systems must be designed in such a way as to always respond to the load demands.

Dummy load (dump) can be used in cases in which a surplus of energy is produced. This dump load can be a resistive element used to convert the excess of energy into heat. Dump loads are sometimes used to control the frequency of the AC output of a system.

The output frequency of a micro-hydropower or wind turbine can be based on the dummy load principle (Kusakana et al., 2009). In this case the load presented to the turbine is more or less constant irrespective of the demand side. Thus the rotational speed of the generator is maintained approximately constant and therefore there is no need to use mechanical control devices to produce a stable frequency.

3.10. Summary

The energy sources, storage systems as well as types of load that can be incorporated in the architecture of a hybrid system have been described based on their design, their standalone operation principle and issues as well as on their operation in a hybrid system configuration. This Chapter helps one to understand the complex interaction of components in a hybrid system.

Chapter IV: Optimization model formulation and proposed algorithm

4.1. Introduction

In this Chapter a general overview of optimization problems is presented. Afterward, the mathematical expression of the hybrid system's optimal operation control problem is derived. An objective function is formulated for the operation costs minimization in a hybrid system with renewable resources and diesel generator for a 24 hours time horizon. Different constraints brought about by the system's components' design and operating limits are also formulated. Moreover, a suitable proposed optimization algorithm is presented.

4.2. Overview of optimization problems

Optimization can be defined as the process of finding the best solution that maximizes or minimizes a given objective function under given constraints. The obtained solution is called the optimal solution (Engelbrecht, 2007). The constraints which the objective function can be subject to are in most cases categorized as boundary, equality and inequality constraints. However, some objective functions are not subject to any constraints; in this case, the optimization problem is identified as an unconstrained problem.

The optimization problem can be single objective or multi-objective involving multiple objective functions. Thus, the single objective optimization problem can be seen as a particular case of a multi-objective optimization problem having only one objective function (Engelbrecht, 2007). The general mathematical formulation of a multi-objective optimization problem is given as:

$$min \text{ or } max \quad f(X) = (f_1(X), f_2(X), f_3(X), ..., f_{nobj}(X)) \tag{4.1}$$

$$\text{Subject to} \quad g_m(X) = 0, \qquad m = 1, ..., n_g \tag{4.2}$$

$$h_m(X) \leq 0, \qquad m = 1, ..., n_h \tag{4.3}$$

$$X \in [X^{\min}, X^{\max}], \qquad m = 1, ..., n_v \tag{4.4}$$

Where: $f_1, f_2, f_3, ..., f_{nobj}$ are different objective functions to be optimized;

g_m and h_m are the equality and inequality constraints respectively;

$X^{\min}$ and $X^{\max}$ are the minimal and maximal values of the bounded variable X, and

n_g, n_h n_v, are a set of equality, inequality and boundary constraints respectively.

Optimization problems can also be categorized as linear or non-linear. A linear optimization problem has linear objective function(s) and constraints while a non-linear optimization problem has at least one non-linear objective function or constraint (Singiresu, 2009).

Optimization problems can also be categorized according to the type of variables present in the objective functions or constraints. If all variables are real numbers, the optimization problem is identified as a continuous optimization problem. If all the variables are discrete numbers or binary numbers, the problem is identified as an integer programming problem. When both discrete and real numbers are contained, the optimization problem is identified as a mixed-integer programming problem (Hu and Wang, 2012).

From the description above, it can be seen that the choice of any optimization algorithm depends on the type of optimization problem.

4.3. Model formulation

The optimal operation control in a hybrid multisource system is a highly non-linear, multi-variable and multi-constraint problem where the main objective is to minimize the operation costs. These operation costs are non-linear, as they depend on the component size and type, the non-linear loads, the non-linear resources, and the dispatch strategy (Numbi et al., 2011).

The hybrid system proposed here is composed of a DG, a PV system, a wind system, a hydrokinetic system and a battery storage system, as shown in Figure 4.1. The proposed hybrid system operation model is based on a description of how the power flows from the different sources, taking into account the losses (rectifier and inverter efficiencies) and the impact of the operating decisions along the way up to the loads. The hybrid system's integrated hardware-software generic logical architecture can be found in Figure E1 from the appendix E.

In the model proposed in this work, the battery is charged by the renewable components only; this means that the DG is switched on only to supply the load. This configuration guarantees the optimum use of HKT, PV and WT outputs while no energy is wasted when the DG runs, since the total power produced matches the load demand. Therefore, the economical operation problem is to find the optimal scheduling of energy production at any given time that minimizes the DG fuel expenses, while totally responding to the load energy requirements within the system's operating limits and constraints. The system's long-term operation costs take maintenance, fuel, lubricant, components overhaul and replacement costs into account. Considering a short time horizon or optimization-time window (24 hours), the operation costs of the batteries, converters and renewable energy components are negligible, therefore only the fuel cost of the DG can be considered.

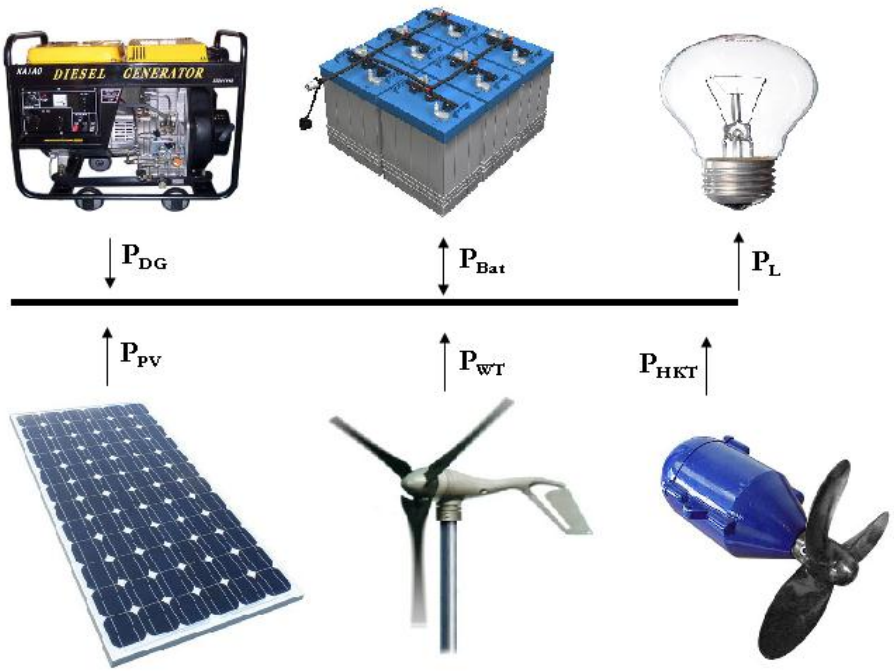

Figure 4.1: Proposed hybrid system layout

4.3.1. Objective function

The objective is to minimize the fuel consumption cost from the DG during the operation time. This can be expressed as:

$$\min \int (aP_{DG(t)} + bP_{DG(t)} + c)dt \tag{4.5}$$

Where: *a* ,*b, c* are the parameters of the DG fuel consumption curve;

$P_{DG(t)}$ is the output power or control variable from the DG at any time t.

4.3.2. Constraints

The different constraints on the operation are as follows:

- Power balance

At any time t., the sum of the supplied power for the different sources must, be equal to the demand.

$$P_{HKT(t)} + P_{PV(t)} + P_{WT(t)} + P_{DG(t)} + P_{Bat(t)} = P_{L(t)} \tag{4.6}$$

Where: $P_{HKT(t)}$ is the control variable representing power flow from the HKT to the load at any time t (kW);

$P_{PV(t)}$ is the control variable representing power flow from the PV to the load at any time t (kW);

$P_{WT(t)}$ is the control variable representing power flow from the WT to the load at any time t (kW);

$P_{DG(t)}$ is the control variable representing power flow from the DG to the load at any time t (kW);

$P_{Bat(t)}$ is the control variable representing power flow from the battery to the load at any time t (kW), and

$P_{L(t)}$ is the load demand at any time t (kW).

- Control variable limits

The HKT, PV, WT, DG and battery modules are modelled as variable power sources controllable in the range of zero to their maximum available power, or their rated power (for the DG and battery) for the 24 hours period. Therefore the variable limits are the output limits of these different power sources as well as of the battery storage system at any time t. These constraints depend on the characteristics of each power source and can be expressed as:

$$0 \le P_{HKT(t)} \le P_{HKT(t)}^{\max} \tag{4.7}$$

$$0 \le P_{PV(t)} \le P_{PV(t)}^{\max} \tag{4.8}$$

$$0 \le P_{WT(t)} \le P_{WT(t)}^{\max} \tag{4.9}$$

$$0 \le P_{DG(t)} \le P_{DG}^{\max} \tag{4.10}$$

$$-P_{Bat}^{rated} \le P_{Bat(t)} \le P_{Bat}^{rated} \tag{4.11}$$

Where: $P_{i(t)}^{\max}$ is the maximum value of a given renewable power source within at any time t,

and

$P_{DG}^{\max}$ and P_{Bat}^{rated} are the maximum and rated power of the DG and the battery system respectively.

- State variable limits: Battery state of charge

The available battery bank state of charge at any time t must not be less than the minimum allowable and must not be higher than the maximum allowable state of charge.

$$SOC^{\min} \le SOC_{(t)} \le SOC^{\max} \tag{4.12}$$

Where: $SOC^{\min}$ and $SOC^{\max}$ are respectively, the minimum and maximum of the battery state of charge.

4.4. Proposed optimization solver and algorithm

The following table is designed to help identifying and choosing a relevant solver to the optimization problem encountered.

As explained in Chapter II, most of traditional optimization methods are local minima-based methods, while the hybrid system optimal operation control is a highly non-linear problem. The non-linearity characteristic of the hybrid system's optimal operation control

makes the solution search space have several local minima and, for this reason, traditional optimization techniques may not be capable of efficiently exploring this search space in such a way to get a global minim.

Using Table 4.1, the constrained non-linear optimization problem can be solved using the "fmincon" solver in MATLAB (Rao, 2009).

Table 4.1: Solvers by Objective function and Constraint

Constraint Type	Objective types Linear	Quadratic	Least Squares	Smooth nonlinear	Nonsmooth
None	n/a (f = const, or min = -∞)	quadprog,	lsqcurvefit, lsqnonlin,	fminsearch, fminunc,	fminsearch, *
Bound	linprog,	quadprog,	lsqcurvefit, lsqlin, lsqnonlin, lsqnonneg,	fminbnd, fmincon, fseminf,	fminbnd, *
Linear	linprog,	quadprog,	lsqlin,	fmincon, fseminf,	*
General smooth	fmincon,	fmincon,	fmincon,	fmincon, fseminf,	*
Discrete	intlinprog,	*	*	*	*

* means relevant solvers are found in Global Optimization Toolbox functions (MATLAB)

Fmincon solves problems in the form:

$\min_x f(x)$ Such such that one or more of the following holds: (4.13)

$c(x) \leq 0$: Non-linear inequality constraint. (4.14)

$ceq = 0$: Non-linear equality constraint. (4.15)

$Ax \le b$: Linear equality constraint. (4.16)

$Aeqx = beq$: Linear equality constraint. (4.17)

$l \le x \le u$: Upper and lower bands. (4.18)

Where *x*, *b*, *beq*, *lb*, and *ub* are vectors, *A* and *Aeq* are matrices, *c(x)* and *ceq(x)* are functions that return vectors, and *f(x)* is a function that returns a scalar, *f(x)*, *c(x)*, and *ceq(x)* can be non-linear functions.

4.4.1. Optimization algorithm selection

There are several algorithms that can be used under the solver fmincon. These algorithms and their different attributes are summarized in the Table 4.2. It has to be noted that the "Active set" and the "Sequential Quadratic Programming (SQP)" are small and medium-scale algorithms; therefore the "Interior point" algorithm is selected to be used in "fmincon" because of its ability to solve large-scale programming problems faster, with full constraint support.

Table 4.2: Algorithm selection

Algorithm	Linear inequality constraints	Linear inequality constraints	Bounds	Non-linear constraints
Trust region reflective	No	Yes	Yes	No
Active set	Yes	Yes	Yes	Yes
Interior point	Yes	Yes	Yes	Yes
Sequential Quadratic Programming (SQP)	Yes	Yes	Yes	Yes

4.4.2. Advantages of fmincon solver with Interior-Point Algorithm

- Fmincon is state-of-the-art optimization method;
- It can solve larger-scale constrained optimization problems;
- It has the ability to supply Hessian information, and
- Interior-Point Algorithm improves the robustness of the solver.

4.5. Definition of the model in fmincon solver syntax

4.5.1. Discretization principle

In the optimal operation control problem both the objective function and constraints models and equations are time dependent which can be solved analytically. However, in the present case the energy function becomes complex and difficult to be solved using analytical methods because the load demand, the resources and DG consumption are highly non-linear and varying with time. This complex non-linear time-dependent problem can be solved through "discretization" which is the process of transferring continuous models and equations into discrete counterparts. The discretization process is usually carried out as a first step toward making them suitable for numerical evaluation and implementation on digital computers.

Therefore, the energy function to be analysed has to be subdivided into small equal intervals "*N*" with a sampling time "Δt". This discretization process induces some errors, therefore for higher accuracy the number of sampling intervals should be high with a short sampling time; this might induce longer time taken to simulate the process.

For modelling purposed, the number of sampling interval can be taken (N=2), then the derived expression of the objective function and of the different constraints can be generalized into the canonical forms required by the solver. In the MATLAB code to be developed, there will be only "*x*" as variable. Therefore the output powers from the different

sources have to be expressed in functions of the variable "*x*". The following arrangement has been made:

$$P_{HKT} = P_1 = x(1:N) = [x_1, x_2] \tag{4.19}$$

$$P_{PV} = P_2 = x(N+1:2N) = [x_3, x_4] \tag{4.20}$$

$$P_{WT} = P_3 = x(2N+1:3N) = [x_5, x_6] \tag{4.21}$$

$$P_{DG} = P_4 = x(3N+1:4N) = [x_7, x_8] \tag{4.22}$$

$$P_{Bat} = P_5 = x(4N+1:5N) = [x_9, x_{10}] \tag{4.23}$$

4.5.2. Objective function definition in fmincon syntax

From the fuel consumption curve "f_c" defined in Chapter III, and using the discretization principle developed in the above section, the objective function which is the minimization of the amount of fuel consumed "*FC*" during the DG operation time, can be expressed as follows:

$$\min FC = \Delta t(aP_{DG1}^2 + bP_{DG1} + c) + \Delta t(aP_{DG2}^2 + bP_{DG2} + c) + ... + \Delta t(aP_{DGN}^2 + bP_{DGN} + c) \tag{4.24}$$

$$\min FC = \Delta t \sum_{j=1}^{N} (aP_{DG(j)}^2 + bP_{DG(j)} + c) \tag{4.25}$$

$$\min \Delta t \sum_{j=1}^{N} (a * x(3*N+1:4*N)^2 + b * x(3*N+1:4*N) + c) \tag{4.26}$$

Where: *j* is the *j*th sampling interval.

4.5.3. Constraints definition in fmincon syntax

- Power balance

The power balance at any *j*th sampling interval can be expressed as:

$$P_{HKT(j)} + P_{PV(j)} + P_{WT(j)} + P_{DG(j)} + P_{Bat(j)} = P_{L(j)} \tag{4.27}$$

As N=2, the power balance can be developed for these two sampling intervals as:

$$\text{For } \; j = 1 \rightarrow x + x_3 + x_5 + x_7 + x_9 = P_{L1} \tag{4.28}$$

$$j = 2 \rightarrow x_2 + x_4 + x_6 + x_8 + x_{10} = P_{L2} \tag{4.29}$$

Taking the coefficient of the equations, the system can be rewritten in a matrix form as:

$$\begin{pmatrix} 1010101010 \\ 0101010101 \end{pmatrix} \begin{pmatrix} x_1 \\ x_2 \\ . \\ . \\ . \\ x_{10} \end{pmatrix} = \begin{pmatrix} P_{L1} \\ P_{L2} \end{pmatrix} \tag{4.30}$$

Using the canonical formulation of the linear equality constraints in fmincon, the power balance can be finally expressed as:

$$Aeq = [eye(N,N), eye(N,N), eye(N,N), eye(N,N), eye(N,N)] \tag{4.31}$$

$$beq = PL(1:N) \tag{4.32}$$

- Variable limits

These boundaries represent the upper and lower limits of outputs from each power sources as well as of the battery storage system for each j^{th} sampling time. These can be expressed for each j^{th} sampling interval as:

$$0 \le P_{HKT(j)} \le P_{HKT(j)}^{\max} \tag{4.33}$$

$$0 \le P_{PV(j)} \le P_{PV(j)}^{\max} \tag{4.34}$$

$$0 \le P_{WT(j)} \le P_{WT(j)}^{\max} \tag{4.35}$$

$$0 \le P_{DG(j)} \le P_{DG}^{\max} \tag{4.36}$$

$$-P_{Bat}^{rated} \le P_{Bat(j)} \le P_{Bat}^{rated} \tag{4.37}$$

$$SOC^{\min} \le SOC_{(j)} \le SOC^{\max} \tag{4.38}$$

- Lower bounds

The change of minimum values that each power source can produce in different time intervals is "zero"; however for the specific case of the battery system, this value "$-P_{Bat}^{rated}$" is the maximum power entering the battery while charging. The system's lower bounds change can be expressed in vector forms as follows:

$$lb = [zeros(N,1), zeros(N,1), zeros(N,1), zeros(N,1), -P_{5\_\max} * ones(N,1)] \tag{4.39}$$

- Upper bounds

The change of maximum values that each renewable source can produce in different time interval is " $P_{i(j)}^{\max}$ ", which depends on the availability of the renewable resources. However, for the specific case of the DG and the battery system, these values are their maximum rated values " $P_{DG}^{\max}$ " and " P_{Bat}^{rated} " respectively. The system's lower bounds change can be expressed in vector forms as follows:

$$ub = [P_{1\_\max}(1:N), P_{2\_\max}(1:N), P_{3\_\max}(1:N), P_{4\_\max} * ones(N,1), P_{5\_\max} * ones(N,1)] \quad (4.40)$$

- Battery dynamic

The battery dynamic gives the relation between the state and the control variables. This can be expressed as:

$$SOC_{(j+1)} = SOC_j - t_s \frac{\eta_{Bat}}{E_{nom}} \times P_{Bat(j)} \quad (4.41)$$

Where E_{nom} is the nominal energy from the battery system, and

η_{Bat} is the efficiency of the battery system.

This expression can be re-written as:

$$SOC_{(j+1)} = SOC_j - Z \times P_{5(j)} \ (*) \quad (4.42)$$

Proceeding by recurrence, Eq. (*) can be developed as:

$$\text{For } j = 1 \rightarrow SOC_{(2)} = SOC_1 - Z \times P_{5(1)} \quad (4.43)$$

$$j = 2 \rightarrow SOC_{(3)} = SOC_2 - Z \times P_{5(2)} = SOC_1 - Z \times P_{5(1)} - Z \times P_{5(2)} \quad (4.44)$$

$$j = j \rightarrow SOC_{(j)} = SOC_1 - Z \times \sum_{i=1}^{j} P_{5(j)} \tag{4.45}$$

Replacing Eq. (4.45) into the battery state of charge limit equation and introducing the initial battery state of charge, Eq. (4.12) can be developed as:

$$SOC^{\min} \leq SOC_0 - Z \times \sum_{i=0}^{j-1} P_{5(j)} \leq SOC^{\max} \text{ or} \tag{4.46}$$

$$SOC^{\min} \leq SOC_0 - Z \times \sum_{i=1}^{j} P_{5(j)} \leq SOC^{\max} \tag{4.47}$$

- Dealing with the maximum inequality:

$$SOC_0 - Z \times \sum_{i=1}^{j} P_{5(j)} \leq SOC^{\max} \tag{4.48}$$

$$\text{For } j = 1 \rightarrow SOC_0 - Z \times x_9 \leq SOC^{\max} \rightarrow -Z \times x_9 \leq SOC^{\max} - SOC_0 \tag{4.49}$$

$$j = 2 \rightarrow SOC_0 - Z \times (x_9 + x_{10}) \leq SOC^{\max} \rightarrow -Z \times (x_9 + x_{10}) \leq SOC^{\max} - SOC_0 \tag{4.50}$$

- Dealing with the minimum inequality:

$$SOC^{\min} \leq SOC_0 - Z \times \sum_{i=1}^{j} P_{5(j)} \tag{4.51}$$

$$\text{For } j = 1 \rightarrow SOC^{\min} \leq SOC_0 - Z \times x_9 \rightarrow Z \times x_9 \leq SOC_0 - SOC^{\min} \tag{4.52}$$

$$j = 2 \rightarrow SOC^{\min} \leq SOC_0 - Z \times (x_9 + x_{10}) \rightarrow Z \times (x_9 + x_{10}) \leq SOC_0 - SOC^{\min} \tag{4.53}$$

Now grouping all the linear inequalities together:

$$-Z \times x_9 \leq SOC^{\max} - SOC_0 \tag{4.54}$$

$$-Z \times (x_9 + x_{10}) \leq SOC^{\max} - SOC_0 \tag{4.55}$$

$$Z \times x_9 \leq SOC_0 - SOC^{\min} \tag{4.56}$$

$$Z \times (x_9 + x_{10}) \leq SOC_0 - SOC^{\min} \tag{4.57}$$

Taking the coefficient of the equations, the system can be rewritten in a matrix form as:

$$\begin{pmatrix} 0 & 0 & 0 & 0 & 0 & 0 & 0 & 0 & -Z & 0 \\ 0 & 0 & 0 & 0 & 0 & 0 & 0 & 0 & -Z & -Z \\ 0 & 0 & 0 & 0 & 0 & 0 & 0 & 0 & Z & 0 \\ 0 & 0 & 0 & 0 & 0 & 0 & 0 & 0 & Z & Z \end{pmatrix} \begin{pmatrix} x_1 \\ . \\ . \\ . \\ x_{10} \end{pmatrix} \leq \begin{pmatrix} SOC^{\max} - SOC_0 \\ SOC^{\max} - SOC_0 \\ SOC_0 - SOC^{\min} \\ SOC_0 - SOC^{\min} \end{pmatrix} \tag{4.58}$$

Using the canonical formulation of the linear inequality constraints in fmincon, this can be finally expressed as:

$$A_1 = [zeros(N,N), zeros(N,N), zeros(N,N), zeros(N,N), -Z * tril(ones(N,N))] \tag{4.59}$$

$$A_2 = [zeros(N,N), zeros(N,N), zeros(N,N), zeros(N,N), Z * tril(ones(N,N))] \tag{4.60}$$

$$A = [A_1; A_2] \tag{4.61}$$

$$b_1 = (SOC\_\max - SOC_0) * ones(N,1) \tag{4.62}$$

$$b_1 = (SOC_0 - SOC\_\min) * ones(N,1) \tag{4.63}$$

$$b = [b_1, b_2] \tag{4.64}$$

4.6. Final Model

The final model is a complete MATLAB code via which the resources and load data can be changed by the user. The daily load, the DG capacity, HKT, PV, WT resource profiles, the battery capacity and SOC limits, can be inserted manually depending on the case study. After running the simulation, the developed model (solver and algorithm) will return the optimized hybrid system's daily operation cost and the hybrid system's optimal scheduling.

4.7. Summary

In this Chapter the mathematical model for the hybrid system's optimal operation control was presented. The problem's objective function as well as optimization constraints were derived. Fmincon solver with Interior-Point Algorithm has been proposed as an optimization solver and the reason for this choice have been stated. Finally, the derived objective function and constraints have been defined in the syntax required by fmincon solver for simulation purposes.

Chapter V: Simulation results and discussion

5.1. Introduction

In this Chapter the optimal operation control model of the hybrid energy system is simulated using fmincon interior-point in MATLAB. The objective of the present simulation is to demonstrate how to minimize the daily operation cost of the hybrid system working under variable renewable resources as well as variable load, using the developed model. Several load profiles and data resources are used and a sensibility analysis is made regarding the daily operation cost savings for each simulated hybrid system working under different conditions.

5.2. Data description

In this section the data used in the simulation are described. Two case studies are conducted on two different sites from which the environmental data, load energy profile and system component sizes are acquired and used as input to the developed model.

5.2.1. Case 1: Rural household

A 24 hours detailed load data is obtained from a typical household situated in the KwaZulu Natal province at 30.6 degrees latitude south and 29.4 degrees longitude east. The hybrid system is designed in such a way to provide electricity for low consumption electrical appliances such as lights, TV, radio, laptop, fridge, kettle, cell phone chargers, iron, toaster, etc. When scrutinizing this load profile, one can notice a general pattern arising from the daily activities of the users, which changes depending on different seasons of the year.

The daily water velocity, solar irradiance and wind speed taken on an hourly basis from the selected site, are shown in Table 5.1. It has to be noted that the lowest water velocity

record occurs in September. Therefore the considered hydrokinetic is sized in such a way to give a rated power of 1 kW at 1.4 m/s water velocity. Thus, it is assumed that the produced HKT power remains constant for water velocities above 1.5 m/s.

Table 5.1: Household case

Time	Summer				Winter			
(h)	Global Solar (kW/m^2)	Wind speed (m/s)	Water speed (m/s)	Load (kW)	Global Solar (kW/m^2)	Wind speed (m/s)	Water speed (m/s)	Load (kW)
00:00	0.000	0.821	1.41	0.3	0.000	2.505	1.41	0.3
01:00	0.000	1.665	1.41	0.2	0.000	2.440	1.41	0.2
02:00	0.000	0.998	1.41	0.1	0.000	1.332	1.41	0.1
03:00	0.000	0.956	1.41	0.0	0.000	2.540	1.41	0.0
04:00	0.000	2.549	1.41	0.3	0.000	2.430	1.41	0.3
05:00	0.000	2.558	1.41	0.0	0.000	2.190	1.41	0.0
06:00	0.000	2.775	1.41	2.4	0.000	2.385	1.41	3.0
07:00	0.002	3.754	1.41	0.6	0.000	1.072	1.41	0.7
08:00	0.141	2.948	1.41	4.3	0.145	1.431	1.41	8.0
09:00	0.417	2.828	1.41	5.6	0.244	0.876	1.41	5.6
10:00	0.687	2.870	1.41	3.2	0.306	1.907	1.41	2.6
11:00	0.940	2.522	1.41	1.6	0.512	1.894	1.41	3.0
12:00	1.062	1.766	1.41	0.3	0.611	2.096	1.41	0.5
13:00	1.061	2.576	1.41	2.0	0.614	2.123	1.41	3.4
14:00	0.978	2.017	1.41	0.4	0.568	2.133	1.41	0.7
15:00	0.846	2.282	1.41	0.8	0.428	3.038	1.41	1.3
16:00	0.679	3.116	1.41	3.9	0.460	2.521	1.41	1.4
17:00	0.464	2.626	1.41	1.8	0.266	2.227	1.41	1.5
18:00	0.208	3.427	1.41	1.7	0.000	1.819	1.41	3.8
19:00	0.043	2.972	1.41	1.9	0.000	2.825	1.41	4.6

20:00	0.000	2.543	1.41	2.2	0.000	3.571	1.41	5.9
21:00	0.000	2.336	1.41	0.9	0.000	2.070	1.41	2.1
22:00	0.000	1.863	1.41	0.7	0.000	2.537	1.41	0.8
23:00	0.000	1.231	1.41	0.3	0.000	1.523	1.41	0.3

5.2.2. Case 2: Base transceiver station

The base transceiver station selected for this study is situated in the Western Cape region at 32.8 degrees latitude south and 17.9 degrees longitude east. The energy needed by the BTS communication equipment and the cooling system used to remove heat from the cabin are given by Kusakana and Vermaak (2013b). The load profile resulting from the daily power demand of the radio, power conversion, antenna, transmission, security lights and cooling equipments at the base station site, is given in Table 5.2. It is noticeable from this table that except for the auxiliary equipments such as air-conditioning which is running during the day for only 6 hours (11:00h-17:00h), and the security lights for 11 hours throughout the night (19:00h-6:00h), the rest of the BTS communication equipment is running for 24 hours non-stop. However during winter, the air-conditioning is running for only 2 hours (13:00h-15:00h) and the security lights for 13 hours (18:00h-7:00h).

The BTS site is situated at almost 1500 km from the selected rural household's site; therefore the two sites are in different climatic regions. The monthly average water velocity, solar irradiance and wind speed available on the BST site are given in Table B2 (appendix B). As for case one, the hydrokinetic system designed to supply the BTS load must be able to operate during the month with low hydro resources.

Table 5.2: BTS case

Time (h)	Summer				Winter			
	Global Solar (kW/m^2)	Wind speed (m/s)	Water speed (m/s)	Load (kW)	Global Solar (kW/m^2)	Wind speed (m/s)	Water speed (m/s)	Load (kW)
00:00	0.000	1.844	1.41	1.8	0.000	0.871	1.41	1.8
01:00	0.000	3.040	1.41	1.8	0.000	0.381	1.41	1.8
02:00	0.000	3.459	1.41	1.8	0.000	0.947	1.41	1.8
03:00	0.000	2.998	1.41	1.8	0.000	1.425	1.41	1.8
04:00	0.000	2.342	1.41	1.8	0.000	1.575	1.41	1.8
05:00	0.000	1.146	1.41	1.8	0.000	1.463	1.41	1.8
06:00	0.000	0.840	1.41	1.6	0.000	0.932	1.41	1.8
07:00	0.001	1.118	1.41	1.6	0.000	1.560	1.41	1.6
08:00	0.110	1.719	1.41	1.6	0.054	1.337	1.41	1.6
09:00	0.291	2.918	1.41	1.6	0.178	1.761	1.41	1.6
10:00	0.694	3.242	1.41	1.6	0.184	2.611	1.41	1.6
11:00	0.882	2.492	1.41	1.6	0.212	3.542	1.41	1.6
12:00	1.013	3.585	1.41	4.0	0.364	3.956	1.41	1.6
13:00	1.086	3.327	1.41	4.0	0.742	4.698	1.41	4.0
14:00	0.963	4.743	1.41	4.0	0.460	4.898	1.41	4.0
15:00	0.709	4.263	1.41	4.0	0.253	4.089	1.41	1.6
16:00	0.654	4.253	1.41	4.0	0.192	5.544	1.41	1.6
17:00	0.440	3.865	1.41	4.0	0.039	4.404	1.41	1.6
18:00	0.261	3.766	1.41	4.0	0.000	4.547	1.41	1.8
19:00	0.027	3.267	1.41	1.8	0.000	4.711	1.41	1.8
20:00	0.000	3.418	1.41	1.8	0.000	3.881	1.41	1.8
21:00	0.000	2.576	1.41	1.8	0.000	4.610	1.41	1.8
22:00	0.000	1.897	1.41	1.8	0.000	2.537	1.41	1.8
23:00	0.000	0.732	1.41	1.8	0.000	2.370	1.41	1.8

5.2.3. Component size and simulation model parameters

As stated in the work delimitation (Chapter I, section 1.6) the focus of the current study is principally on the optimal energy management of the hybrid system; therefore the optimal sizing of the system's components has been done using the Hybrid Optimization Model for Electric Renewable (HOMER) and the results have been used as input to our model. As a result, the optimal combination of HKT (3kW) / PV (1kW) / WT (1kW) / DG (1kW) /13 batteries has been considered for simulation of the rural household and the optimal combination of HKT (2kW) / PV (1kW) / WT (1kW) / DG (1kW) /7 batteries has been considered for simulation purposes of the BTS load (Kusakana, 2014).

The battery as well as the DG parameters used in the simulation is shown in Table 5.3. The case in which the DG alone is supplying the load is also considered for purposes of comparison.

Table 5.3: Simulation parameters

Item	Figure
Sampling time	30min
Battery maximum SOC	95%
Battery minimum SOC	40%
Battery charging efficiency	85%
Battery discharging efficiency	100%
Diesel fuel price	1.4$/l
a	0.247
b	0.1
c	0.4200

5.3. Rural household simulation results and discussion

Two scenarios are considered in which the hybrid system is operating in different climatic conditions to supply the load. These scenarios are simulated to investigate how the climatic changes of loads and resources can influence the optimal operation of the hybrid system.

5.3.1. 24 hours load supplied in winter

- Load supplied by the hybrid system

Figures 5.1 to 5.4 show how the load demand "P_L" as well as the maximum and optimum output power flows from the HKT, PV and WT during the selected day in winter. It can be seen that the HKT system constitutes the major contribution of the power supplied by the renewable systems, and therefore has a primary role in the DG cost minimization and the battery charging process. Figure 5.5 shows the power balance between the load demand and the renewable resources; the DG output power, the battery power flow as well as the battery SOC during the 24 hours period are displayed in Figures 5.6 to 5.8 respectively.

The following observations on the hybrid system operation can be made after analysing these Figures:

From Figure 5.1, it can be noticed that during the night and early morning the load demand is low; therefore it is successfully met mainly by the HKT. The WT and PV systems are not able to generate during these periods because of the lack of wind and solar resources. The power balance "P_{BAL}" (on Figure 5.5) represents the difference between the sums of the optimum renewable outputs power minus the instantaneous load demand. If P_{BAL} is positive, the surplus of generated power can be used to charge the battery. If P_{BAL} is negative, the shortage of energy can be counteracted by using the battery "P_B" first within its operating limits; if more energy is needed while the renewable sources and battery cannot totally satisfy the load, the DG "P_{DG}" is switched to offset the deficit.

During the day when the solar and wind resources are available, the load demand is met by the HKT, PV, WT and battery bank.

The morning peak load demand occurs between 7:00h and 9:00h, therefore the HKT, PV and the battery are used at their maximum output to supply the load; the DG also switches on only to balance the energy needed and then switches off as soon as there is enough power from the other power sources. The DG operating time and output power depend on the load demand, battery SOC and the amount of power from the renewable sources within the studied sampling interval. It can be seen that the DG is not used to charge the battery but only to supply the deficit of power from the other sources to load.

After the morning peak, the SOC of the battery is at its minimum operation limit (40%); therefore the renewable outputs produce more power than the load requirement. This surplus is used to charge the battery bank to its maximum SOC (95%) which is reached at the end of the afternoon, as shown in Figure 5.6, where the negative part of the battery power flow "P_B" represents the charging process.

In the evening, the load demand gradually increases from 17:00h and reaches a peak between 19:00h, and 20:00h then finally decreases at 21:00h. Therefore from 17:00h to 18:00h, the HKT and PV are used at their maximum outputs in conjunction with a small contribution of the DG and the battery. After 18:00h the PV system can no longer provide energy while the load demand is increasing, therefore the contribution of the battery is maximal and the DG output power also increases to balance the energy needed by the load.

A poor WT output is noticeable in the afternoon and in the evening. This power is also used to supply the load and contributes to the battery charging power requirement.

The hybrid system's optimal power flow in winter for the N sampling interval is shown in appendix A, Table A1.

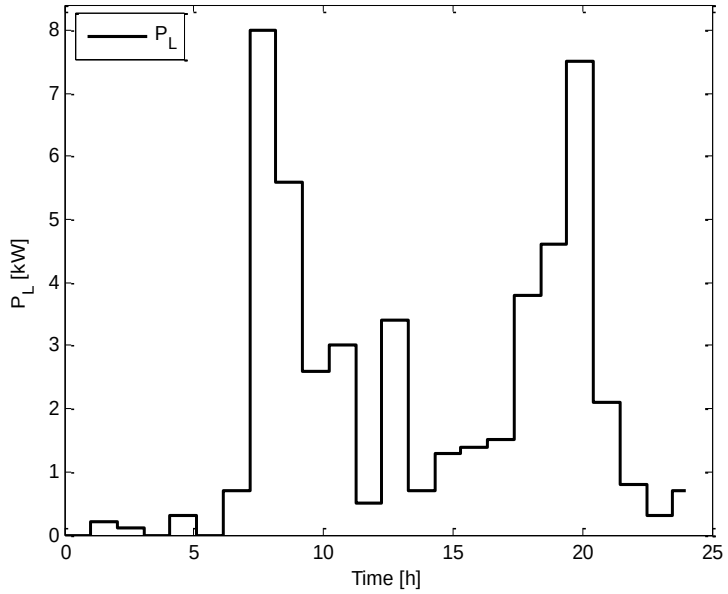

Figure 5.1: Daily load profile in winter

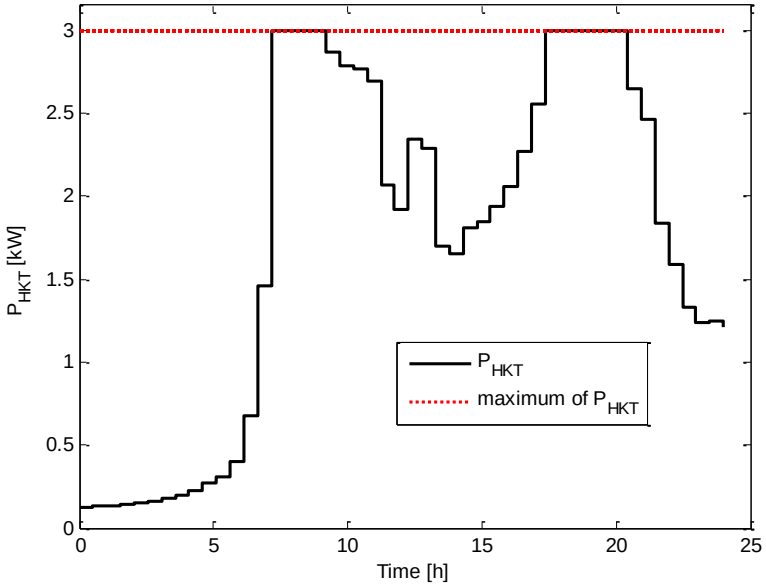

Figure 5.2: Hydrokinetic output power in winter

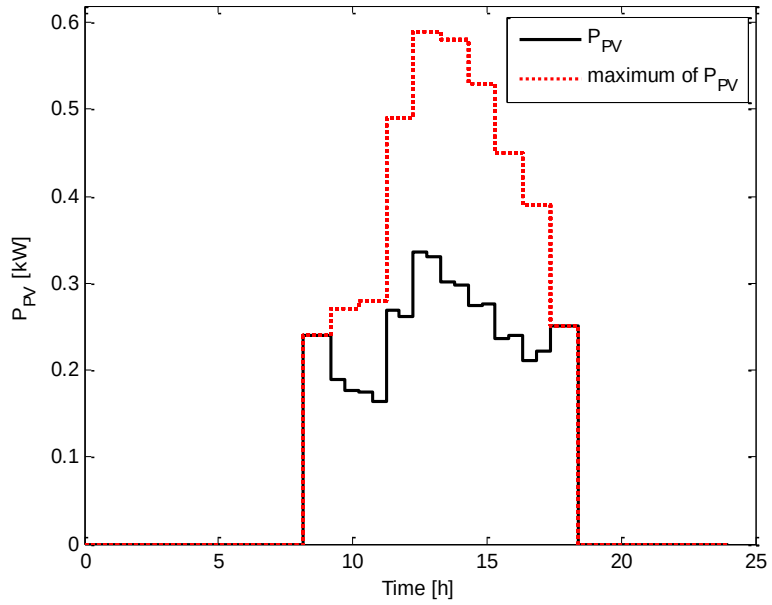

Figure 5.3: PV output power in winter

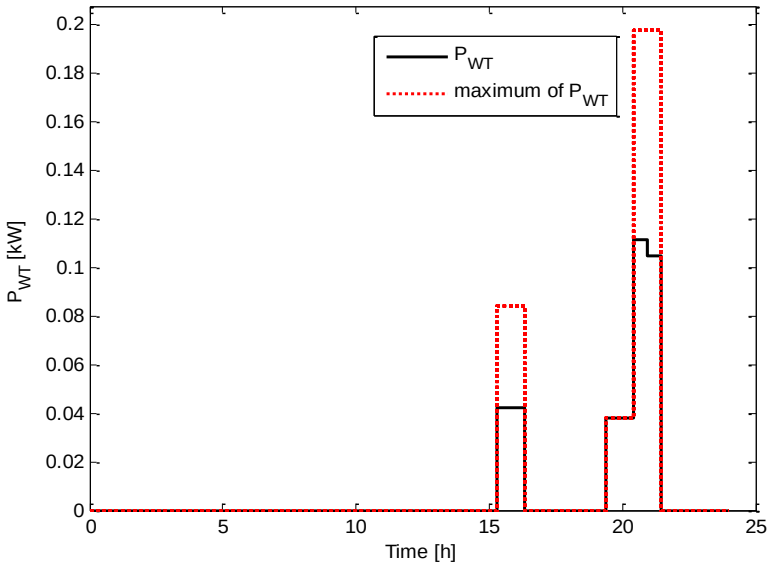

Figure 5.4: Wind output power in winter

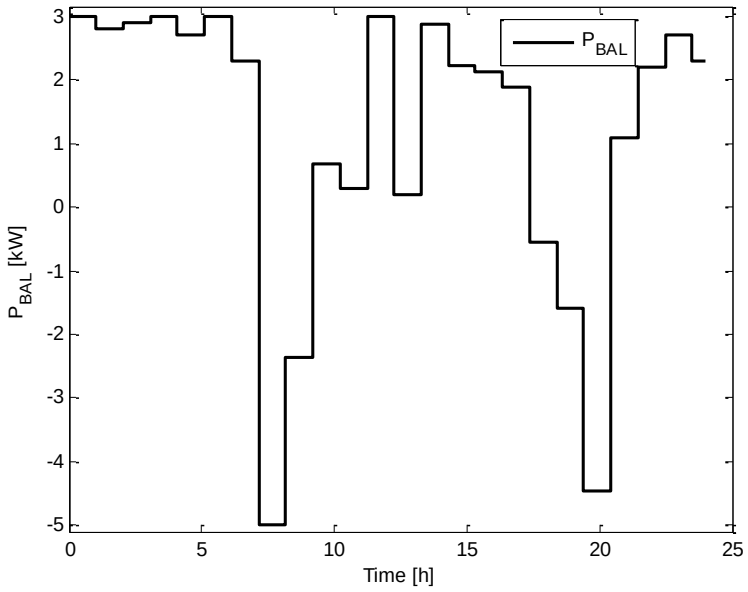

Figure 5.5: Power balance between the renewable sources and the load in winter

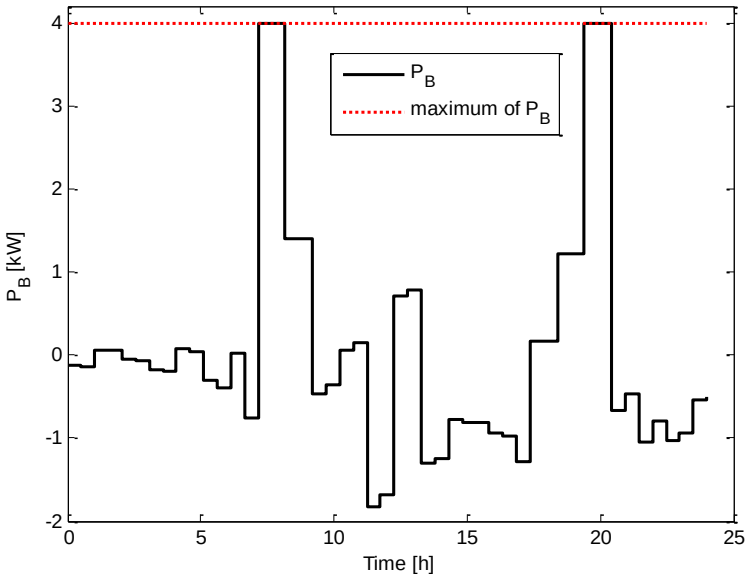

Figure 5.6: Battery output power in winter

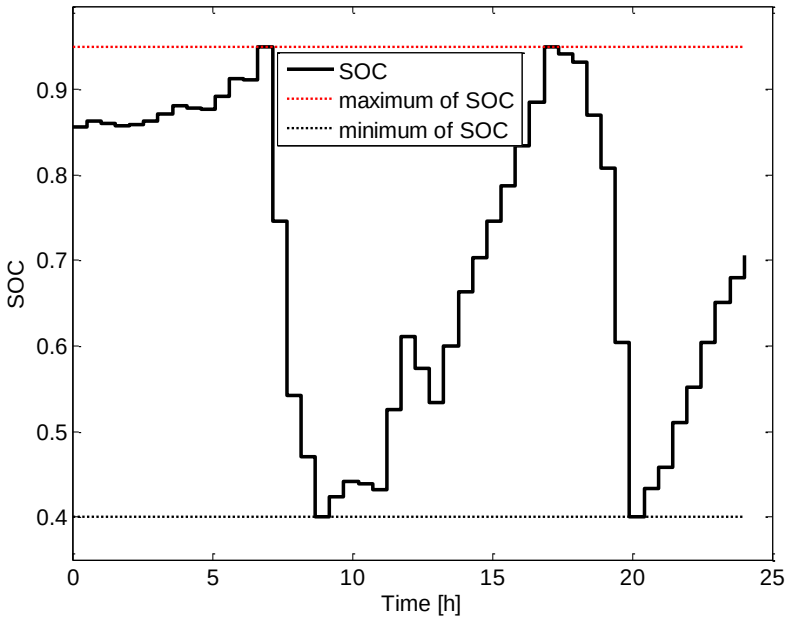

Figure 5.7: Battery dynamic state of charge in winter

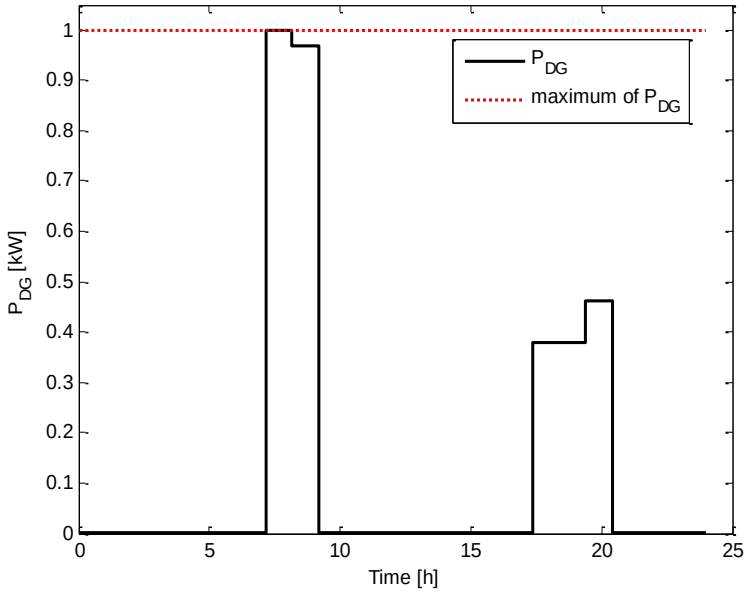

Figure 5.8: DG optimal scheduling and output power in winter

- Winter load supplied by the DG only

Figure 5.9 illustrates the case in which the DG is used as the only supply option. Therefore the DG used here has to be sized in such a way to be able to supply the peak load. This case is analysed to determine how much fuel can be spent while using the DG alone instead of the DG in the developed hybrid system optimal operation control model.

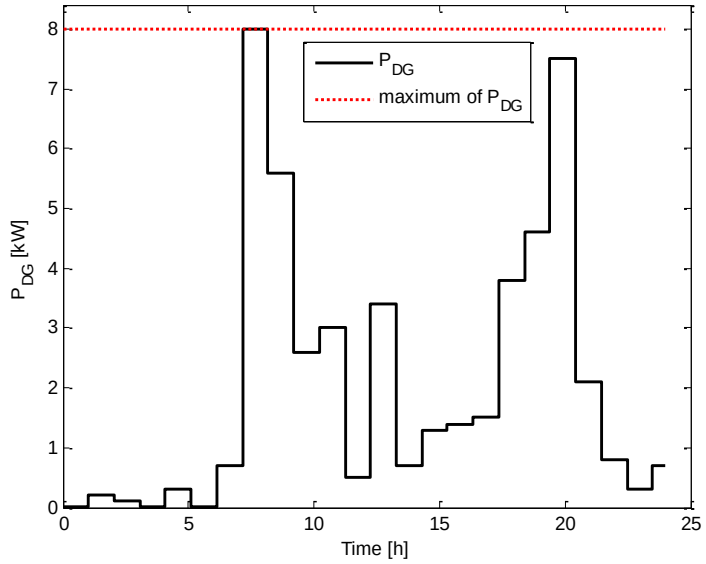

Figure 5.9: DG "only" optimal scheduling and output power in winter

5.3.2. 24 hours load supplied in summer

- Load supplied by the hybrid system

The developed model can also be used to analyse the difference in power flow during summer and winter due to different climatic conditions and load requirements which have significant effects on the diesel dispatch strategy and fuel consumption.

Using the data from Table 5.1, it can be noticed that the load demand is lower and the renewable resources are higher for the selected summer day than for the winter day. The simulation results reveal that the DG supplies more power in winter and stays off in

summer. This is due to higher PV and WT outputs, higher SOC of the battery as well as lower load demand in summer than in winter. This conclusion has been drawn by comparing the power flow results for the winter and summer cases available from Table 5.1 and Table 5.2 respectively.

5.3.3. Daily operation cost summary of the rural household case.

The actual daily fuel expense can be found by multiplying the diesel price ($/L) by the amount of fuel used (L/day). It has to be highlighted that this daily fuel expense is highly dependent on the size and type of DG (fuel cost curve and fitting parameters from the manufacturer) used in the simulation. Table 5.4 shows how much fuel can be saved by using the hybrid system instead of the selected DG during a winter or a summer day. These results demonstrate that it is very important to take into account the variations of the load and renewable energy resources relative seasons when calculating the system's daily operation cost.

Table 5.4: Daily fuel cost savings

	Winter		Summer	
	Consumption (L)	Cost ($)	Consumption (L)	Cost ($)
DG only	122L	171.03$	40.5L	56.7$
Hybrid system	1.84L	2.58$	0L	0$
Savings	120.16L	168.45$	40.5L	56.7$

5.4. BTS simulation results and discussion

As for the household case, two scenarios are also considered for the BTS case. It has to be noted that the load demand of the BTS decreases in winter while the one for the rural household increases in winter.

5.4.1. 24 hours load supplied in winter

- Load supplied by the hybrid system

While analysing the daily operation of the hybrid system supplying the BTS load in winter, the following observations can be made:

From Figure 5.10, it can be noticed that the BTS load profile is generally flat all through the night the night and during the day, except when the air-conditioning system is switched on leading to a two hour peak demand (from 13:00h to 15:00h). Therefore demand is successfully met mainly by the hydrokinetic system and the battery system. A soon as the WT and PV systems produce energy, the surplus from the renewable components is used to recharge the battery.

During the peak demand, all the renewable sources as well as the battery system are operating at their maximum limit to supply the load. The DG also switches on only to balance the energy needed and then switches off as soon as there is enough power from the other power sources. After the peak, the SOC of the battery is at its minimum operation limit (40%); therefore the renewable outputs produce more power than the load requirement, and this surplus is used to recharge the battery bank as shown in Figure 5.15 and 5.16.

In the evening, the load demand increases because the security lights are turned on. The hydrokinetic system operating in conjunction with the battery and other available renewable sources produce enough energy through the night and the use of the DG is avoided (Figure 5.17).

The hybrid system's optimal power flow in winter for the N sampling interval is shown in appendix A, Table A3.

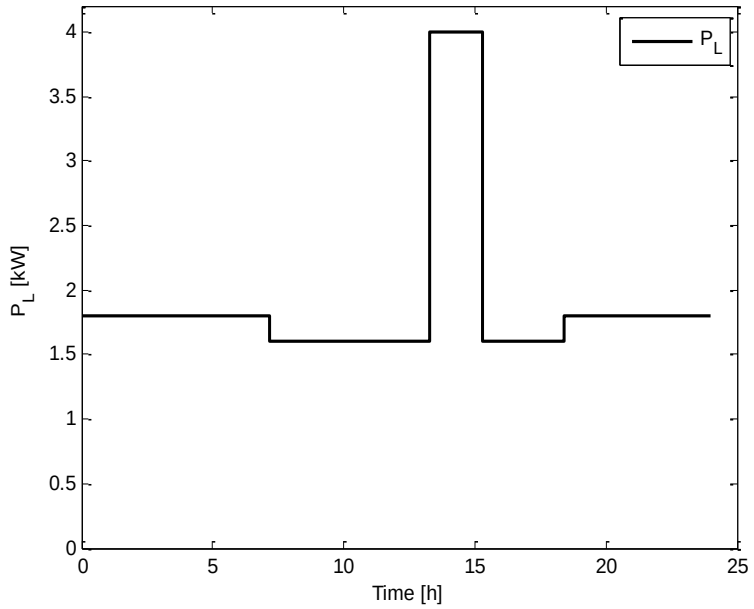

Figure 5.10: BTS daily load profile in winter

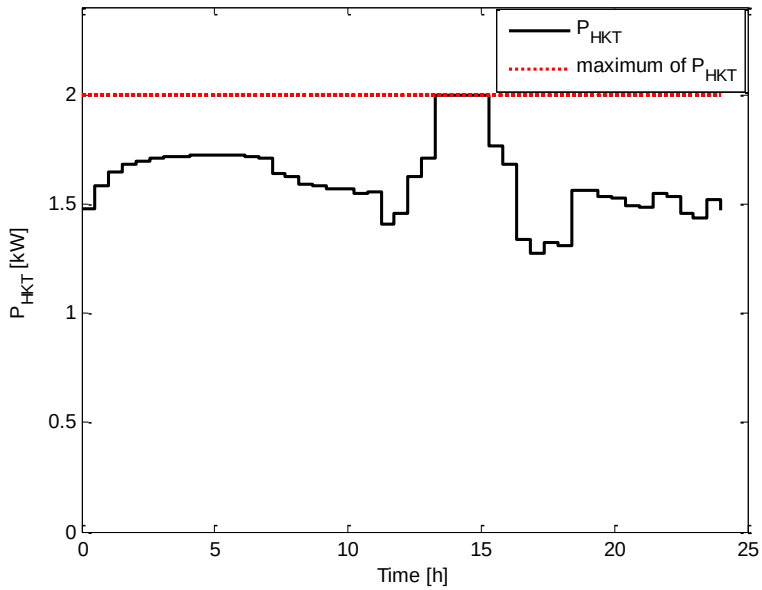

Figure 5.11: Hydrokinetic output power in winter

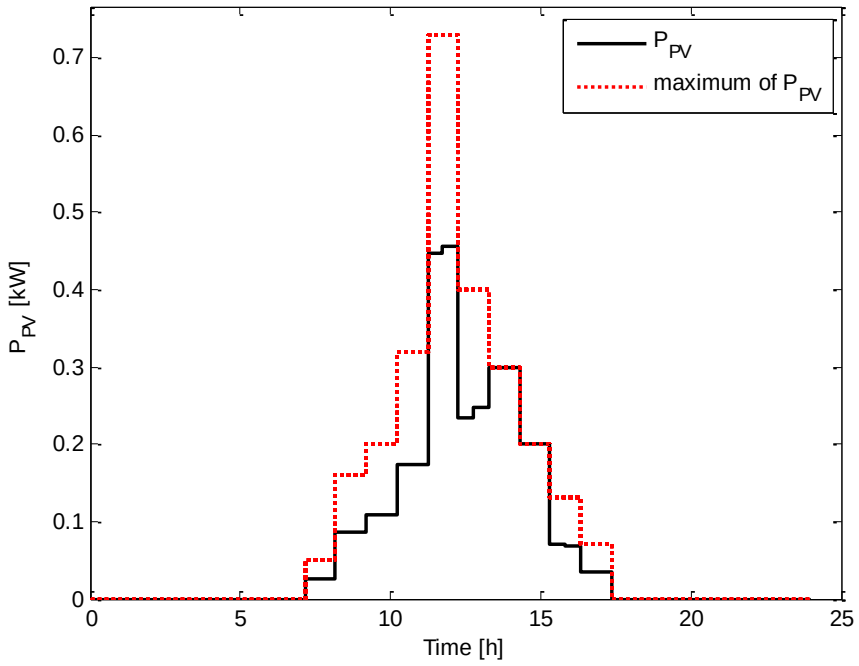

Figure 5.12: PV output power in winter

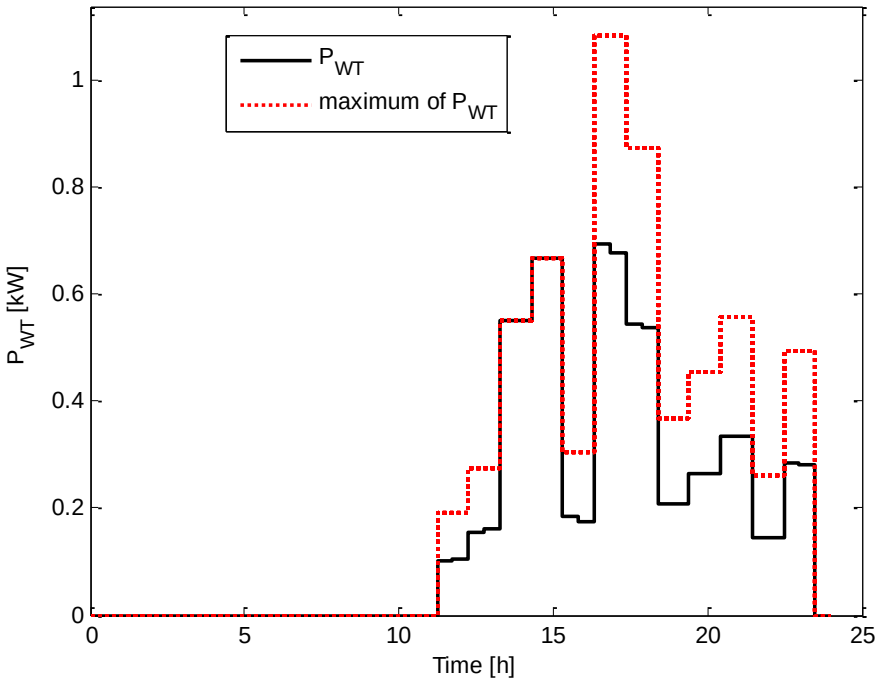

Figure 5.13: WT output power in winter

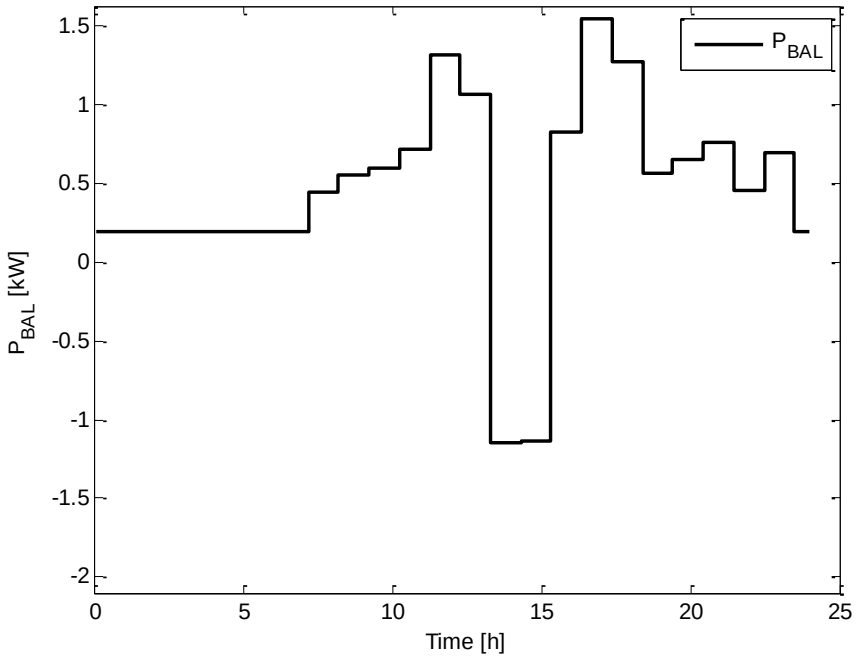

Figure 5.14: Power balance between the renewable sources and the load in winter

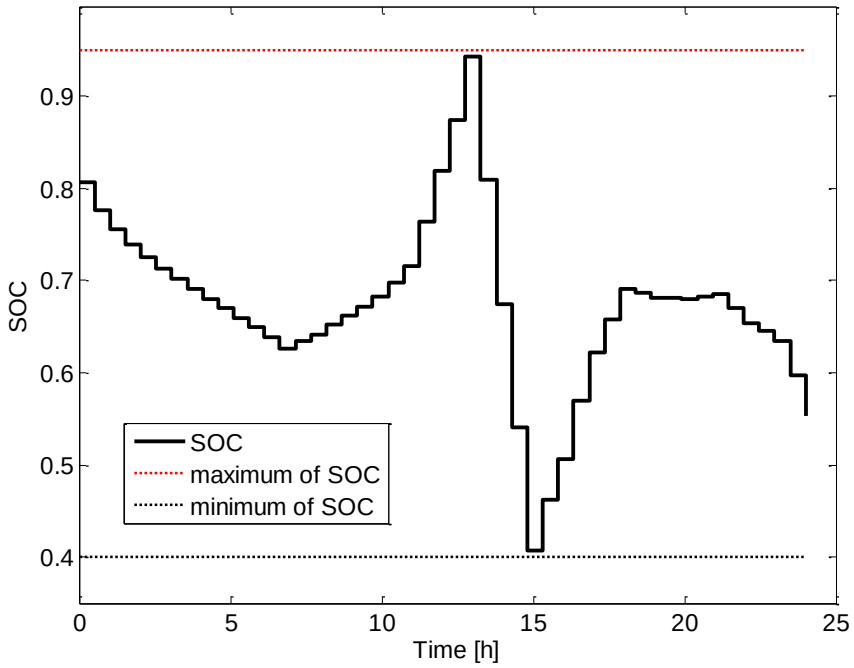

Figure 5.15: Battery dynamic SOC

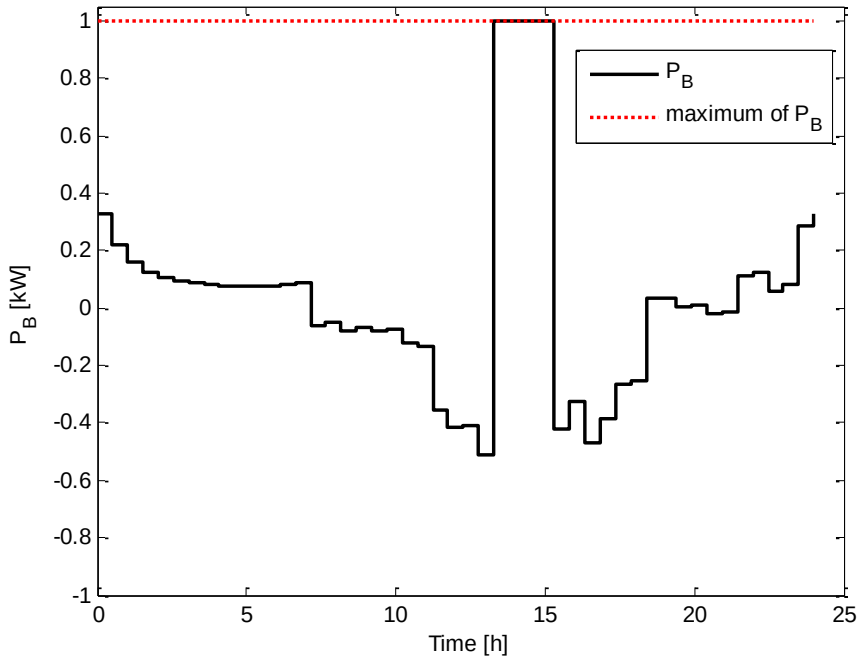

Figure 5.16: Battery output power in winter

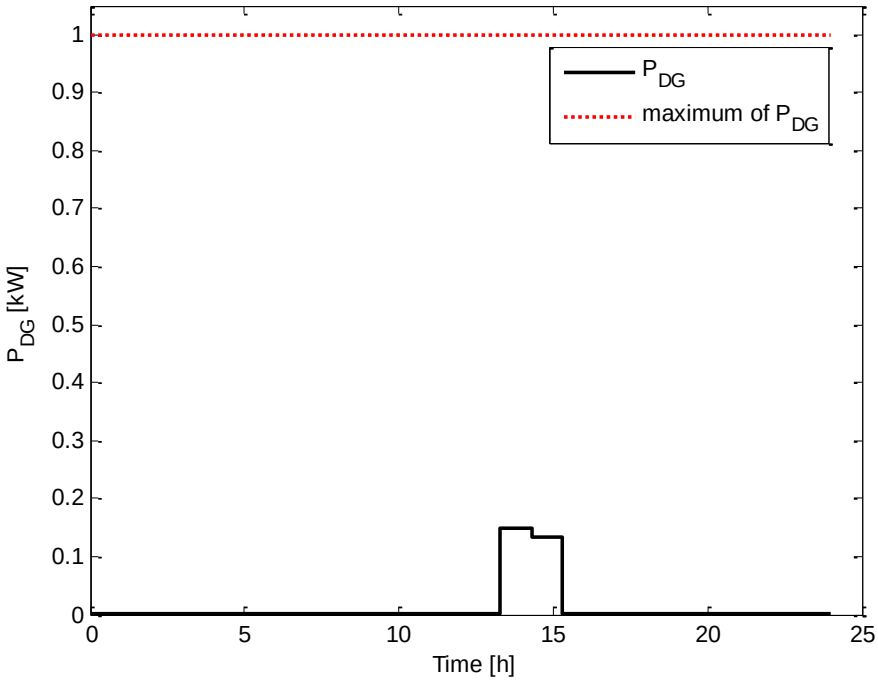

Figure 5.17: DG output power in winter

- Winter load supplied by the DG only

Figure 5.18 illustrates the case where the DG is used as the only supply option. Therefore the DG used here has to be sized in such a way to be able to supply the peak load. It can be noticed that the DG power output profile is the same profile with the load one.

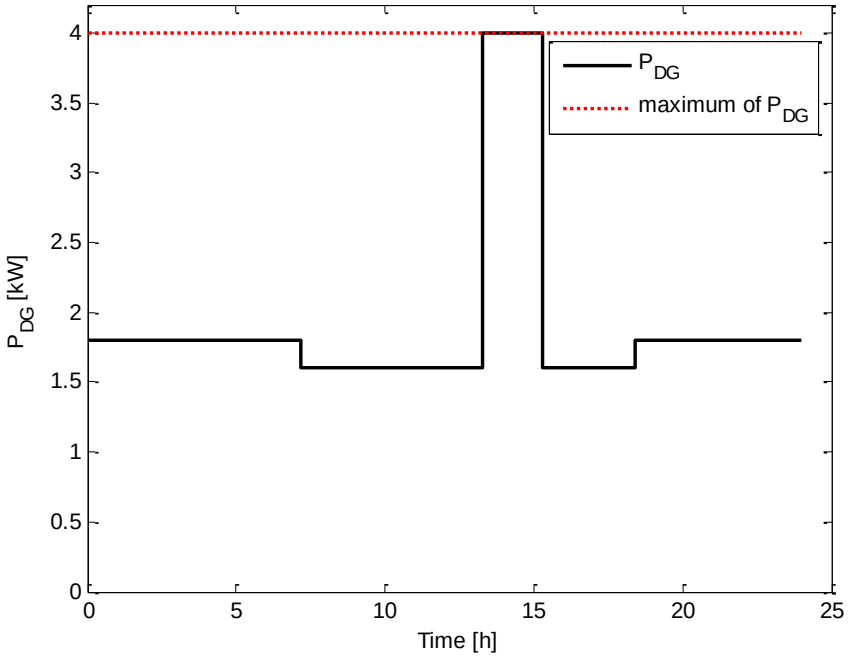

Figure 5.18: DG "only" optimal scheduling and output power in winter

5.4.2. 24 hours load supplied in summer

- Load supplied by the hybrid system

The BTS load demand during the summer day is higher compared to the winter day. Therefore the developed model is used to simulate and compare the daily operation cost between the winter and the summer days. The simulation results reveal that the DG supplies more power in summer than in winter, and this is due to the fact that the air-conditioning system is used for a longer time, resulting in a higher daily load demand in summer than in

winter. This conclusion has been drawn by comparing the power flow results for the winter and summer cases available from Table A3 and Table A4 respectively (Appendix A).

5.4.3. Daily operation costs summary in the BTS load case.

Table 5.5 shows how much fuel can be saved by using the hybrid system instead of the selected DG during a winter or a summer day. As in the household case, the results obtained here demonstrate the importance of considering the non-linearity of the renewable resources as well as that of the load when operating the hybrid system in order to minimize the daily operation costs. It can be seen that unlike the household case, the BTS uses more fuel in summer than in winter, mainly because the load demand is higher in summer that in winter.

Table 5.5: Daily fuel cost savings

	Winter		Summer	
	Consumption (L)	Cost ($)	Consumption (L)	Cost ($)
DG only	57L	80$	92.38L	129.33$
Hybrid system	0.08L	0.1$	2.85L	4$
Savings	56.92L	79.9$	89.53L	125.33$

5.5. Analysis of different DGs and battery control settings

In this section, the developed model is used to simulate the impact of different DGs and the battery operating limits of the hybrid system operation cost.

5.5.1. Influence of DG fuel consumption curve.

For the same kW rating, different DGs from different manufacturers present different fuel consumption curves. Table 5.6 is a sample of three different DGs with their respective

fuel consumption curve parameters. The simulation here is conducted to analyse the impact on the daily operation cost of different types of DG used in the hybrid system's configuration. The household case supplied in winter is used for illustration purposes.

Table 5.6: Fuel consumed using different DGs

DG Type (Manufacturer)	a ($L/h.kW^2$)	b (L/h.kW)	c (L/h)	Fuel used (L)	Cost ($)
USR (EV10i)	0.246	0.0815	0.4333	1.73L	2.42$
Cummins power	0.0074	0.2333	0.4200	1.52L	2.13$
Power Rush	0.247	0.1	0.4200	1.84L	2.58$

5.5.2. Influence of the battery operation limits

The battery operating limits set by the user can have a significant impact on the hybrid system's daily operation cost. Here a sensitivity analysis will be done on the battery SOC upper and lower limits to see how it affect the daily operation cost. Data from the hybrid system supplying the rural household in winter are used here for illustration purposes. The simulation results summarized in Table 5.7 reveal that a battery having high depth of discharge can considerably reduce the running time as well as the fuel consumed by the DG. However, for certain types of battery, a high depth of discharge may result in the reduction of the battery life which leads to premature replacement of the battery. Therefore a compromise between the high depth of discharge and the battery operating life needs to be found; this is beyond the scope of the current study.

Table 5.7: Impact of the SOC limits on the operating cost

Limits (SOC_{max}, SOC_{min})	Fuel consumed (L)	Fuel cost ($)
(95%, 40%)	1.83L	2.56$
(95%, 38%)	1.51L	2.14$
(95%, 36%)	1.21L	1.69$
(97%, 40%)	1.50L	2.10$
(97%, 38%)	1.21L	2.14$
(97%, 36%)	0.99L	1.39$
(99%, 40%)	1.20L	1.68$
(99%, 38%)	0.94L	1.32$
(99%, 36%)	0.70L	0.98$

5.6. Summary

In this Chapter the hybrid system's optimal operation control model has been simulated using fmincon interior-point in MATLAB. Using realistic and actual data, the developed model has been successfully used to analyse the complex interaction between the daily non-linear load, the non-linear renewable resources as well as the battery dynamic and their impact of the hybrid system's daily operation cost.

The developed optimal operation control model has also been used to:

- Analyse the minimized operation costs achieved by using different manufacturers' DG in the configuration of the proposed hybrid system.
- Analyse the impact of the battery operation limits or battery control settings on the hybrid system's operation cost.
- Demonstrate the importance of considering the seasonal load and renewable energy resources' variations when calculating the hybrid system's daily operation cost.
- Highlight the important role of the hydrokinetic module in the hybrid system's cost minimization.

The model developed, as well as the solver and algorithm used in this work, have low computational requirements for achieving results within a reasonable time, therefore this can be seen as a faster and more accurate optimization tool.

Chapter VI: Conclusions

6.1. Final conclusions

This Chapter draws conclusions on the simulation and optimal operation control of a hybrid energy system consisting of a hydrokinetic module, photovoltaic module, wind module, a battery bank and diesel generator.

The interaction between the varying load and weather conditions is a major concern in the hybrid system's operation; this has a significant impact on the operation cost. This was the context on which this research was based, aiming to develop a tool to minimize the daily operation costs of standalone hybrid systems.

As a preparation for the optimal operation control, the different components of the hybrid system have been described in Chapter III. The emphasis was on component design, their standalone operation principle and issues, as well as on their operation in a hybrid system configuration.

In Chapter IV the mathematical model for the hybrid system's optimal operation control was presented. This model aims to minimize the use of a diesel generator while maximizing the use of the available renewable energy sources. The problem's objective function as well as operation constraints were derived. Fmincon solver with Interior-Point algorithm has been proposed as optimization solver, and the reasons for this choice have been stated.

As mentioned in the introduction, this work considers the non-linearity of the renewable resources, load demand as well as diesel fuel consumption resulting in uniform daily operational costs. Therefore in Chapter V, the hourly water velocity, solar irradiation, wind speed, load demand, as well as the diesel generator fuel consumption curve parameter data have been used as input data for simulation purposes. The simulation results obtained show that by using the proposed non-linear hybrid system optimal operation model, more accurate operation costs can be obtained in comparison to linear fuel consumption models such as the one used in HOMER software.

The discrepancies in daily operation cost achieved highlight the potential of the proposed optimization model to reduce fuel consumptions for the hybrid system as opposed to the diesel only scenario. These results also demonstrate that it is very important to take into account the seasonal variations affecting the load and renewable energy resources when calculating the system's daily operation cost. The developed optimal operation control model has also been used to:

- Analyse the minimized operation costs achieved by using different manufacturers' GD in the configuration of the proposed hybrid system.
- Analyse the impact of the battery operation limits or battery control settings on the hybrid systems operation cost.
- Demonstrate the importance of considering seasonal load and renewable energy resource variations when calculating the hybrid system's daily operation cost.
- Highlight the important role of the hydrokinetic module in the hybrid system's cost minimization.

6.2. Suggestions for further research

This thesis has been presented as part of an ongoing research project at the Central University of Technology, studying different aspects of hybrid renewable systems. This thesis is not the conclusion of the work, it is just a step along the road, and several questions remain in relation to hybrid systems optimal operation control.

This thesis has focused on a general hybrid system layout comprising a micro hydrokinetic, wind, solar, battery and diesel generator, and a number of other system configurations would merit further study.

The model developed in this thesis is based on the hybrid system optimal operation control. Further models combining the hybrid system long-term optimal operation control to the optimal sizing should be developed to determine the system's life cycle cost.

The load and renewable resources data used for simulation in this work have been collected on an hourly basis. It would be interesting to acquire data on a minute basis to

conduct further analysis with the aim of evaluating the performance of the developed model in terms of simulation time and results accuracy.

A key limitation of the investigations conducted in this thesis is that the hybrid system is considered in isolation. For further study, the optimal operation control of grid-connected renewable hybrid systems with storage system and DG back-up should be investigated.

References

ARDAKANI F.J., RIAHY G. & ABEDI M. 2010. Design of an optimum hybrid renewable energy system considering reliability indices. In 18th Iranian Conference on Electrical Engineering (ICEE), 842-847, Iran.

ARDAKANI F.J., RIAHY G. & ABEDI M. 2010. Optimal sizing of a grid-connected hybrid system for north-west of Iran-case study. In 9th International Conference on Environment and Electrical Engineering (EEEIC), 29-32, Prague, Czech Republic.

ASHARI M. & NAYAR C.V. 1999. An optimum dispatch strategy using set points for a photovoltaic (PV)–diesel–battery hybrid power system. Solar Energy, 66(1):1-9.

ASHOK S. 2007. Optimised model for community-based hybrid energy system. Renewable Energy, 32:1155-1164.

BAJPAI P. & DASH V. 2012. Hybrid renewable energy systems for power generation in stand-alone applications: A review. Renewable and Sustainable Energy Reviews, 16: 2926-2939.

BAKARE G.A., KROST G., VENAYAGAMOORTHY G.K. & ALIYU U.O. 2007. Differential Evolution Approach for Reactive Power Optimization of Nigerian Grid System. IEEE Power Engineering Society General Meeting. 1-6, Florida, USA.

BANOS R., MANZANO-AGUGLIARO F., MONTOYA F.G., GIL C., ALCAYDE A. & GOMEZ J. 2011. Optimization methods applied to renewable and sustainable energy: A review. Renewable and Sustainable Energy Reviews, 15:1753–1766.

BARLEY C. D., WINN C. B., FLOWERS L. & GREEN H. J. 1995. Optimal control of remote hybrid power systems Part I: Simplified model. Annual conference and exhibition on wind power, 26-30 Washington, DC (United States).

BASHIR M. & SADEH J. 2012. Optimal Sizing of Hybrid Wind/Photovoltaic/Battery Considering the Uncertainty of Wind and Photovoltaic Power Using Monte Carlo. In the 11th International Conference on Environment and Electrical Engineering (EEEIC), 1081-1086. Venice, Italy.

BASHIR M. & SADEH J. Size Optimization of New Hybrid Standalone Renewable Energy System Considering a Reliability Index. In the 11th International Conference on Environment and Electrical Engineering (EEEIC), 989-994. Venice, Italy.

BERNAL-AGUSTIN J. L. & DUFO-LOPEZ R. 2009. Simulation and optimization of stand-alone hybrid renewable energy systems. Renewable and Sustainable Energy Reviews, 13:2111-2118.

BOROWY B.S. & SALAMEH Z.M. 1996. Methodology for optimally sizing the combination of a battery bank and PV array in a wind/PV hybrid system. IEEE Transaction on Energy Conversion, 11(2):367–73.

CHEN F., DUIC N., ALVES L.M. & CARVALHO M.G. 2007. Renewislands – Renewable energy solutions for islands. Renewable and Sustainable Energy Reviews, 11(8):1888-902.

CLARK R.H. 2007. Elements of tidal-electric engineering. Wiley-IEEE Press.

CONNOLLY D., LUND H., MATHIESEN B.V. & LEAHY M. 2010. A review of computer tools for analysing the integration of renewable energy into various energy systems. Applied Energy, 87:1059-82.

DAGDOUGUI H., MINCIARDI R., OUAMMI A., ROBBA M. & SACILE R. 2010. A Dynamic Decision Model for the Real-Time Control of Hybrid Renewable Energy Production Systems. IEEE Systems Journal, 4(3):323-333.

DAGDOUGUI H., MINCIARDIA R., OUAMMI A., ROBBAA M. & SACILEA R. 2010. Modelling and control of a hybrid renewable energy system to supply demand of a green-building. In iEMSs International Congress on Environmental Modelling and Software Modelling for Environment's Sake, Fifth Biennial Meeting, 1-8. Ottawa, Ontario, Canada.

DEHGHAN S., KIANI B., KAZEMI A. &PARIZAD A. 2009. Optimal Sizing of a Hybrid Wind/PV Plant Considering Reliability Indices. World Academy of Science, Engineering and Technology, 56:527-535.

DESHMUKH M.K. & DESHMUKH S.S. 2008. Modelling of hybrid renewable energy systems. Renewable and Sustainable Energy Reviews, 12:235-249.

DIAF S., DIAF D., BELHAMEL M., HADDADI M. & LOUCHE A. 2006. Analyse technico économique d'un système hybride (photovoltaïque/éolien) autonome pour le site

d'Adrar. Revue des Energies Renouvelables. 9(3):127-134.

DIAF S., DIAF D., BELHAMEL M., HADDADI M. & LOUCHE A. 2007. A methodology for optimal sizing of autonomous hybrid PV/wind system. Energy Policy, 35:5708-5718.

DUFFIE J.A. & BECKAM W.A. 2006. Solar Engineering of Thermal Processes" JOHN WILEY & SONS, INC.

DUFO-LOPEZ R. & BERNAL-AGUSTIN J. L. 2005. Design and control strategies of PV-Diesel systems using genetic algorithms. Solar Energy, 79:33-46.

DUFO-LOPEZ R. & BERNAL-AGUSTIN J. L. 2006. Design of isolated hybrid systems minimizing costs and pollutant emissions" Renewable Energy 31 (2006) 2227–2244.

DUFO-LOPEZ R. & BERNAL-AGUSTIN J. L. 2008. Influence of mathematical models in design of PV-Diesel systems. Energy Conversion and Management, 49:820-831.

DUFO-LOPEZ R. & BERNAL-AGUSTIN J. L. 2009. Multi-objective design and control of hybrid systems minimizing costs and unmet load. Electric Power Systems Research, 79:170-180.

DUFO-LOPEZ R. & BERNAL-AGUSTIN J. L., Rivas-Ascaso D.M. 2006. Design of isolated hybrid systems minimizing costs and pollutant emissions. Renewable Energy 31:2227-2244.

DUFO-LOPEZ R. & BERNAL-AGUSTIN J.L. 2008 .Multi-objective design of PV– wind– diesel– hydrogen– battery systems. Renewable Energy 33:2559-2572.

DURSUN E. & KILIC O. 2012. Comparative evaluation of different power management strategies of a standalone PV/Wind/PEMFC hybrid power system. Electrical Power and Energy Systems, 34:81-89.

ELIZONDO J., MARTINEZ J. & PROBST O. 2009. Experimental study of a small wind turbine for low- and medium-wind regimes. International Journal of Energy Research, 33:309-26.

ENGELBRECHT A.P. 2007. Computational Intelligence: An Introduction (Second ed.). Chichester, England: John Wiley & Sons, Ltd.

ENGIN M. 2013. Sizing and simulation of PV-wind hybrid power system. International

Journal of Photoenergy.10.

ERDINC O. & UZUNOGLU M. 2012. Optimum design of hybrid renewable energy systems: Overview of different approaches. Renewable and Sustainable Energy Reviews, 16: 1412-1425.

FERNÁNDEZ I.J., CALVILLO C.F., SÁNCHEZ-MIRALLES A. & BOAL J. 2013. Capacity fade and aging models for electric batteries and optimal charging strategy for electric vehicles. Energy, 60:35-43.

FRAENKEL P. 2000. Marine currents - a promising large clean energy resource. IMechE Seminar Publication Power Generation by Renewables, 221-233. Bury St Edmunds, UK.

FULZELE J.B. & DUTT S. 2012. Optimium Planning of Hybrid Renewable Energy System Using HOMER. International Journal of Electrical and Computer Engineering (IJECE), 2(1):68-74.

GHEDAMSI K. & AOUZELLAG D. 2010. Improvement of the performances for wind energy conversions systems. International Journal of Electrical Power & Energy Systems, 32:936-45.

GHOSH G.C., EMONTS B. & STOLEN D. 2003. Comparison of hydrogen storage with diesel generator system in a PV-WEC hybrid system. Solar Energy, 75:187-98.

GIANNAKOUDIS G., PAPADOPOULOS A. I., SEFERLIS P. & VOUTETAKIS S. 2010. Optimum design and operation under uncertainty of power systems using renewable energy sources and hydrogen storage. International journal of hydrogen energy, 35:872-891.

GOEDECKEB M., THERDTHIANWONG S. & GHEEWALA S.H. 2007. Life cycle cost analysis of alternative vehicles and fuels in Thailand. Energy Policy, 35(6):3236-46.

GÜNEY M.S. & KAYGUSUZ K. 2010. Hydrokinetic energy conversion systems: A technology status review. Renewable and Sustainable Energy Reviews, 14(9):2996-3004.

GUPTA A., SAINI R.P. & SHARMA M.P. 2008a. Computerized Modelling of Hybrid Energy System-Part II: Combined Dispatch Strategies and Solution Algorithm. In 5th International Conference on Electrical and Computer Engineering (ICECE), 13-18. Dhaka, Bangladesh.

GUPTA A., SAINI R.P. & SHARMA M.P. 2008b. Computerized Modelling of Hybrid

Energy System - Part I: Problem Formulation and Model Development. In 5th International Conference on Electrical and Computer Engineering (ICECE), 20-22, Dhaka, Bangladesh.

HAKIMI S. M., MOGHADDAS-TAFRESHI S. M. & HASSANZADEHFARD H. 2011. Optimal sizing of reliable hybrid renewable energy system considered various load types. Journal of renewable and sustainable energy 3(6) 062701.

HASSANZADEHFARD H., MOGHADDAS-TAFRESH S.M. & HAKIMI S.M. 2011. Optimal Sizing of an Islanded Micro-grid for an area in north-west Iran Using Particle Swarm Optimization Based on Reliability Concept. World Renewable Energy Congress, 2969-2976. Linkoping, Sweden.

HEPBASLI A. 2008. A key review on exergetic analysis and assessment of renewable energy resources for a sustainable future. Renewable and Sustainable Energy Reviews, 12(3):593-661.

HU K. & WANG B. 2012. Comparison of several types of methods for solving constrained function optimization problems. IEEE Symposium on Robotics and Applications (ISRA). 821-824. Kuala Lumpur, Malaysia.

HU Y. & SOLANA P. 2013. Optimization of a hybrid diesel-wind generation plant with operational options. Renewable Energy, 51:364-372.

IBRAHIM H., LEFEBVRE J., METHOT J. F. & DESCHENES J. S. 2011. Numerical Modeling Wind-Diesel Hybrid System: Overview of the Requirements, Models and Software Tools. In IEEE Electrical Power and Energy Conference. 23-28. Winnipeg, Canada.

JALILZADEH S., KORD H. & ROHANI A. 2010. Optimization and Techno-Economic Analysis of Autonomous Photovoltaic/Fuel Cell Energy System. ECTI Transactions on Electrical Engineering, Electronics, and Communications, 8(1):118-125.

JANSEN B., ROOS C. & TERLAKY T. 1993. Interior point methodology for linear programming: duality, sensitivity analysis and computational aspects, Optimisation in Planning and Operation of Electric Power Systems. Physica-Verlag, Heidelberg.

JENNINGS S. 1996. Development and Application of a Computerized Design Tool for Remote Area Power Supply Systems, PhD Thesis at Murdoch University, Department of Electrical Engineering.

KAVIANI A.K., RIAHY G.H. & KOUHSARI S.H.M. 2008. Optimal design of a reliable hydrogen-based stand-alone wind/PV generation system. In Proceeding of 11th international conference on optimization of electrical and electronic equipment (OPTIM'08), Brasov, Romania.

KAVIANI A.K., RIAHY G.H. & KOUHSARI S.H.M. 2009. Optimal design of a reliable hydrogen-based stand-alone wind/PV generating system, considering component outages. Renewable Energy, 34:2380–2390.

KHABURI D.A. & NAZEMPOUR A. 2012. Design and simulation of a PWM rectifier connected to a PM generator of micro turbine unit. Scientia Iranica D, 19(3):820-828.

KIRTHIGA M.V. & DANIEL S.A. 2010. Optimal Sizing of Hybrid Generators for Autonomous Operation of a Micro-grid. In the IEEE 26th Convention of Electrical and Electronics Engineers, 864-868, Israel.

KRIEGER E.M., CANNARELLA J. & ARNOLD C.B. 2013. A comparison of lead-acid and lithium-based battery behavior and capacity fade in off-grid renewable charging applications. Energy, 60:492-500.

KUSAKANA K. & VERMAAK H.J. 2011. Hybrid Photovoltaic-Wind system as power solution for network operators in the D.R.Congo. IEEE International Conference on Clean Electrical Power (ICCEP), 703-708, Ischia, Italy.

KUSAKANA K. & VERMAAK H.J. 2012 .Feasibility Study of Hydrokinetic Power for Energy Access in Rural South Africa. In Proceedings of the IASTED Asian Conference, Power and Energy Systems, 433-438, Phuket, Thailand.

KUSAKANA K. & VERMAAK H.J. 2013. A survey of Particle Swarm Optimization Applications for Sizing Hybrid Renewable Power Systems. Advanced Science Letters, 19(8):2463-2467.

KUSAKANA K. & VERMAAK H.J. 2013a. Hybrid diesel generator-battery systems for off-grid rural applications. IEEE International Conference on Industrial Technology (ICIT 2013), 839-844, Cape Town, South Africa.

KUSAKANA K. & VERMAAK H.J. 2013b. Hybrid renewable power systems for mobile telephony base station in developing countries. Renewable Energy, 51:419-425.

KUSAKANA K. & VERMAAK H.J. 2013c. Hydrokinetic power generation for rural electricity supply: Case of South Africa. Renewable Energy, 55:467-473.

KUSAKANA K., MUNDA J.L., & JIMOH A.A. 2009. A survey of technologies increasing the viability of micro-hydropower for remote communities. In IEEE Africon 2009, Nairobi Kenya.

KUSAKANA K., VERMAAK H.J. & NUMBI B.P. 2012. Optimal sizing of a hybrid renewable energy plant using linear programming. In IEEE PES Conference and Exposition (PowerAfrica). 1-5. Johannesburg, South Africa.

KUSAKANA. K. 2014. Techno-economic analysis of off-grid hydrokinetic-based hybrid energy systems for onshore/remote area in South Africa. Energy 68: 947-957.

LYDIA M., KUMAR S.S., SELVAKUMAR A.I. & KUMAR G.E.P. A comprehensive review on wind turbine power curve modeling techniques. Renewable and Sustainable Energy Reviews, 30:452-460.

MAHMOUD M. M. & IBRIK I. H. 2006. Techno-economic feasibility of energy supply of remote villages in Palestine by PV-systems, diesel generators and electric grid. Renewable and Sustainable Energy Reviews, 10:128-138.

MANCHESTER S.C. & SWAN L.G. 2013. Off-grid mobile phone charging: An experimental study. Energy for Sustainable Development, 17:564-571.

MANIACI D.C. & LI. Y. 2011. Investigating the influence of the added mass effect to marine hydrokinetic horizontal-axis turbines using a general dynamic wake wind turbine code. Oceans' 11conference, 1-7, Hawaii, USA.

MOHD A., ORTJOHANN E., MORTON D. & OMARI O. 2010. Review of control techniques for inverters parallel operation. Electric Power Systems Research. 80:1477–1487

MURALIKRISHNA M. & LAKSHMINARAYANA V. 2008. Hybrid (solar and wind) energy systems for rural electrification. ARPN Journal of Engineering and Applied Sciences, 3(5) 50-58.

NAFEH A. 2009. Fuzzy Logic Operation Control for PV-Diesel-Battery Hybrid Energy System. The Open Renewable Energy Journal, 2:70-78.

NEHRIR M. H., WANG C., STRUNZ K., AKI H., RAMAKUMAR R., BING J., MIAO

Z., & SALAMEH Z. 2011. A Review of Hybrid Renewable/Alternative Energy Systems for Electric Power Generation: Configurations, Control, and Applications. IEEE transactions on sustainable energy, 2(4): 392-403.

NEMA P., NEMA R.K. & RANGNEKAR S. 2009. A current and future state of art development of hybrid energy system using wind and PV-solar: A review. Renewable and Sustainable Energy Reviews, 13:2096-2103.

NUMBI B. P., JUMA D. W., MUNDA J. L. & JIMOH A. A. 2011. Constraint handling approach in optimal reactive power dispatch when using unconstrained standard Particle Swarm Optimization. In 20th Southern African Universities' Power Engineering Conference (SAUPEC). Cape Town.

NUMBI B.P. 2012. Optimization of reactive power flow in a wind farm-connected electric power system. M.Tech. Dissertation, Department of Electrical Engineering, Tshwane University of Technology, South Africa.

PAISH O. 2002. Small hydropower: Technology and current status. Renewable and Sustainable Energy Reviews, 6(6):537-56.

RAO S. S. 2009. Engineering Optimization: Theory and Practice (Fourth ed.): John Wiley & Sons, Inc.

RASHTCHI V., KORD K. & ROHANI A. 2009. Application of GA and PSO in Optimal Design of a Hybrid Photovoltaic/Fuel Cell Energy System. In 24th International Power System Conference (PSC). Tehran, Iran.

RAZAK J. A., NOPIAH Z. M., SOPIAN K. & ALI Y. 2007. Genetic algorithms for optimization of hybrid renewable energy system. In Regional Conference on Engineering Mathematics, Mechanics, Manufacturing & Architecture (EM3ARC). 186-193. Malaysia.

RAZAK J.A., SOPIAN K., ALI Y., ALGHOUL M.A., ZAHARIM A. & AHMAD I. 2009. Optimization of PV-Wind-Hydro-Diesel Hybrid System by Minimizing Excess Capacity. European Journal of Scientific Research, 25(4):663-671.

RAZAK J.A., SOPIAN K., ALI Y., ALGHOUL M.A., ZAHARIM A. & AHMAD I. 2008. Optimization of Renewable Energy Hybrid System. In 8th WSEAS International Conference on POWER SYSTEMS. 271-276, Santander, Cantabria, Spain.

RAZAK N.A, OTHMAN M.M. & MUSIRIN I. 2010. Optimal Sizing and Operational Strategy of Hybrid Renewable Energy System Using HOMER. In the 4th International Power Engineering and Optimization Conference (PEOCO), 495-501, Shah Alam, Selangor, Malaysia.

RIBEIRO L.A.S., SAAVEDRA O.R., LIMA S.L. & MATOS J.G. 2011. Isolated Micro-Grids with Renewable Hybrid Generation: The Case of Lençóis Island. IEEE Transactions on Sustainable Energy, 2(1): 1-11.

RODRÍGUEZ J.,LEZANA P. KOURO S & WEINSTEIN A. 2011. Single-phase Controlled Rectifiers. Power Electronics Handbook (Third Edition). 183-204.

SÁNCHEZ V., RAMIREZ J. M. & ARRIAGA G. 2010. Optimal sizing of a hybrid renewable system. In IEEE International Conference on Industrial Technology (ICIT), 949 - 954, Vi a del Mar.

SANDIA NATIONAL LABORATORIES. 1995. Standalone Photovoltaic Systems: A Handbook of Recommended Design Practices. Albuquerque.

SATAR O.H.A., EID S.M.A, SAAD E.M. & DARWISH R.R. 2012. Adaptive and Reliable Control Algorithm for Hybrid System Architecture. IJCSI International Journal of Computer Science Issues, 9(1):465-474.

SCHALLENBERG-RODRIGUEZ J. 2013. A methodological review to estimate techno-economical wind energy production. Renewable and Sustainable Energy Reviews, 21:272-287.

SCHMITT W. 2002. Modeling and simulation of photovoltaic hybrid energy systems optimization of sizing and control. In Proceedings of the 29th IEEE photovoltaic specialists conference, 1656-1659. New Orleans, Louisiana, USA.

SECHILARIU M., WANG B. C. & LOCMENT F. 2014. Supervision control for optimal energy cost management in DC microgrid: Design and simulation. Electrical Power and Energy Systems. 58:140-149.

SEELING-HOCHMUTH G. 1998. Optimization of Hybrid Energy Systems Sizing and Control, Dr. Ing. Dissertation, University of Kassel.

SEELING-HOCHMUTH G.C. 1997. A combined optimization concept for the design and

operation strategy of hybrid-PV energy systems. Solar Energy, 61(2):77-87.

SINGH G.K. 2013. Solar power generation by PV (Photovoltaic) technology: A review. Energy, 53:1-13.

SKOPLAKI E. & PALYVOS J.A. 2009. On the temperature dependence of photovoltaic module electrical performance. A review of efficiency/power correlations. Solar Energy, 83:614-24.

SOPIAN K., ZAHARIM A., ALI Y., NOPIAH Z.M., RAZAK J.A. & MUHAMMAD N.S. 2008. Optimal Operational Strategy for Hybrid Renewable Energy System Using Genetic Algorithms. WSEAS Transactions on Mathematics, 7(4):130-140.

SOUISSI A., HASNAOUI O. & SALLAMI ANIS. 2010. Optimal Sizing of a Hybrid System of Renewable Energy for a Reliable Load Supply without Interruption. European Journal of Scientific Research, 45(4):620-629.

SUPRIYA C.S. & SIDDARTHAN M. 2011. Optimization and sizing of a grid-connected hybrid PV-Wind Energy System. International Journal of Engineering Science and Technology (IJEST), 3(5):4296-4323.

TAZVINGA H., XIA X. & ZHANG J. 2013. Minimum cost solution of photovoltaic–diesel–battery hybrid power systems for remote consumers. Solar Energy, 96: 292-299.

TINA G, GAGLIANO S & RAITI S. 2006. Hybrid solar/wind power system probabilistic modeling for long-term performance assessment. Solar Energy, 80(5):578-88.

TIRYONO R., REHBOCK V. & LAWRENCE W. B. 2003. Optimal control of hybrid power systems. Dynamics of Continuous, Discrete and Impulsive Systems Series B: Applications & Algorithm, 10:429-439.

TONG W. 2010. Wind Power Generation and Wind Turbine Design. WIT Press.

VERMAAK H.J., KUSAKANA K. & KOKO S.P. 2014. Status of micro-hydrokinetic river technology in rural applications: A review of literature. Renewable and Sustainable Energy Reviews, 29:625-633.

WANG L. & SINGH C. 2007. Compromise between Cost and Reliability in Optimum Design of an Autonomous Hybrid Power System Using Mixed-Integer PSO Algorithm. In International Conference on Clean Electrical Power (ICCEP). 682-689, Capri, Italy.

WANG L. & SINGH C. 2007. PSO-Based Multi-Criteria Optimum Design of A Grid-Connected Hybrid Power System with Multiple Renewable Sources of Energy. IEEE Swarm Intelligence Symposium (SIS). 250-257, Honolulu, Hawaii.

WANG L. 2008. Integration of Renewable Energy Sources: Reliability-constrained Power System Planning and Operations Using Computational Intelligence. PhD dissertation, Office of Graduate Studies of Texas A&M University.

WANG X., WANG J. & WANG H. 2014. Improvement of the efficiency and power output of solar cells using nanoparticles and annealing. Solar Energy. 101:100–104.

WOON S. F., REHBOCK V. & SETIAWAN A.A. 2008. Modeling A PV-Diesel-Battery Power System: An Optimal Control Approach. World Congress on Engineering and Computer Science (WCECS). San Francisco, USA.

XIANZHANG W., HAIFENG X., DELI W. & TAOSONG L. 2013. Optimum Balanced and Integrated Power System. In proceedings of the 35th International Telecommunications Energy Conference 'Smart Power and Efficiency' (INTELEC), 1-6, Hamburg, Germany.

YANG H., ZHOU W., LU L. & FANG Z. 2008. Optimal sizing method for stand-alone hybrid solar–wind system with LPSP technology by using genetic algorithm. Solar Energy, 82:354-367.

YANG H.X., LU L. & ZHOU W. 2007. A novel optimization sizing model for hybrid solar–wind power generation system. Solar energy, 81(1):76-84.

YU W., HE H. & ZHANG N. 2009. Optimal Reactive Power Dispatch Using Particle Swarms Optimization Algorithm Based Pareto Optimal Set. Springer-Verlag Berlin Heidelberg.152-161.

ZHANG, H. 2011. Optimal sizing and operation of pumping systems to achieve energy efficiency and load shifting, Master's Dissertation, Department of Electrical, Electronic and Computer Engineering, University of Pretoria.

ZHIGANG L. & LIYE M. 2008. Power system reactive power optimization based on direct neural dynamic programming. 3rd International Conference on Intelligent System and Knowledge Engineering (ISKE). 862-866, Xiamen, China.

ZHOU W., LOU C., LI Z., LU L. & YANG H. 2010. Current status of research on

optimum sizing of stand-alone hybrid solar–wind power generation systems. Applied Energy, 87:380-389.

ZHOU W., LOU C., LI Z., LU L. & YANG H. 2010. Current status of research on optimum sizing of stand-alone hybrid solar–wind power generation systems. Applied Energy 87:380-389.

ZHU, J. 2009. "Optimization of Power System Operation". Hoboken, New Jersey: John Wiley & Sons, Inc.

Appendixes

Appendix A: Selected optimal operation control program (using fmincon)

A1: Main code

```
% Simulation data
% Sampling time in minute
deltaT=30;
hours=24;
N=hours*60/deltaT;
soc_max=0.95;
Soc_min=0.40;
soc0=0.85;
% Hydrokinetic output power
PHKT_max=3*ones(N,1);  % only one because it is constant during the day
% PV output power
PPV_max=[0*ones(1,N/24),0*ones(1,N/24),0*ones(1,N/24),0*ones(1,N/24),0*ones(1,N/24),0*ones(1,N/24),0.12*ones(1,N/24),0.25*ones(1,N/24),0.52*ones(1,N/24),0.76*ones(1,N/24),0.98*ones(1,N/24),1.08*ones(1,N/24),1.07*ones(1,N/24),0.99*ones(1,N/24),0.86*ones(1,N/24),0.72*ones(1,N/24),0.52*ones(1,N/24),0.25*ones(1,N/24),0.16*ones(1,N/24),0*ones(1,N/24),0*ones(1,N/24),0*ones(1,N/24),0*ones(1,N/24),0*ones(1,N/24)]';
% Wind turbine output power
PWT_max=[0*ones(1,N/24), 0*ones(1,N/24), 0*ones(1,N/24), 0*ones(1,N/24),
0*ones(1,N/24), 0*ones(1,N/24), 0.03*ones(1,N/24), 0.24*ones(1,N/24),
0.06*ones(1,N/24), 0.04*ones(1,N/24), 0.05*ones(1,N/24), 0*ones(1,N/24),
```

```
0*ones(1,N/24), 0*ones(1,N/24), 0*ones(1,N/24), 0*ones(1,N/24), 0.1*ones(1,N/24),
0*ones(1,N/24), 0.17*ones(1,N/24), 0.07*ones(1,N/24), 0*ones(1,N/24), 0*ones(1,N/24),
0*ones(1,N/24), 0*ones(1,N/24)]';
% Load demand
PL=[0.3*ones(1,N/24), 0.1*ones(1,N/24), 0.2*ones(1,N/24), 0.1*ones(1,N/24), 0
*ones(1,N/24), 0.3*ones(1,N/24), 0*ones(1,N/24), 2.4*ones(1,N/24), 0.6*ones(1,N/24),
4.3*ones(1,N/24), 5.6*ones(1,N/24), 3.2 *ones(1,N/24), 1.6*ones(1,N/24),
0.3*ones(1,N/24), 2*ones(1,N/24), 0.4*ones(1,N/24), 0.8*ones(1,N/24), 3.9*ones(1,N/24),
1.8*ones(1,N/24), 1.7*ones(1,N/24), 1.9*ones(1,N/24), 2.2*ones(1,N/24), 0.9
*ones(1,N/24), 0.7 *ones(1,N/24)]';
% Power balance between the renewable source and the load
PBAL=PHKT_max+PPV_max+PWT_max-PL;
% DG output power
PDG_max =1;
% Battery maximum output power
PB_max=5;
Eff=0.85;
En=500;
K=(deltaT*Eff)/En;
A1=[zeros(N,N),zeros(N,N),zeros(N,N),zeros(N,N),-K*tril(ones(N,N))];
A2=[zeros(N,N),zeros(N,N),zeros(N,N),zeros(N,N),K*tril(ones(N,N))];
A=[A1;A2];
b1=(soc_max-soc0)*ones(N,1);
b2=(soc0-Soc_min)*ones(N,1);
b=[b1;b2];
Aeq =[eye(N,N),eye(N,N),eye(N,N),eye(N,N),eye(N,N)];
beq=PL(1:N);
lb=[zeros(N,1),zeros(N,1),zeros(N,1),zeros(N,1),-PB_max*ones(N,1)];
```

```
ub=[PHKT_max(1:N),PPV_max(1:N),PWT_max(1:N),PDG_max*ones(N,1),PB_max*ones
(N,1)];
x0=ub;
options=optimset('Algorithm','interior-point');
 optnew=optimset(options,'MaxFunEvals',90000,'Tolx',1e-8);
% Syntax
[x,fuel] = fmincon(@fun_optimization,x0,A,b,Aeq,beq,lb,ub,[],optnew);
%exctract different variable vectors
P_HKT=x(1:N);
P_PV=x(N+1:2*N);
P_WT=x(2*N+1:3*N);
P_DG=x(3*N+1:4*N);
P_B=x(4*N+1:5*N);
%state of battery extraction
for i=1:N
 soc(i)=soc0-K*P_B(i);
 soc0=soc(i);
end
soc1=soc(1:N);
%plots
%load profile
figure (1)
stairs(linspace(0,hours,N),PL(1:N),'k','linewidth',1.5)
ylabel('P_L [kW]')
axis([0 hours+1 0 1.05*max(PL)]);
xlabel('Time [h]')
legend('P_L')
% hydrokinetic
figure (2)
```

```
stairs(linspace(0,hours,N),P_HKT(1:N),'k','linewidth',1.5)
hold on
stairs(linspace(0,hours,N),PHKT_max*ones(1,N),':r','linewidth',1.5)
ylabel('P_H_K_T [kW]')
xlabel('Time [h]')
legend('P_H_K_T','maximum of P_H_K_T')
axis([0 hours+1 0 1.05*max(PHKT_max)]);
% PV
figure (3)
stairs(linspace(0,hours,N),P_PV(1:N),'k','linewidth',1.5)
hold on
stairs(linspace(0,hours,N),PPV_max*ones(1,N),':r','linewidth',1.5)
ylabel('P_P_V [kW]')
axis([0 hours+1 0 1.05*max(PPV_max)]);
xlabel('Time [h]')
legend('P_P_V','maximum of P_P_V')
% Wind
figure (4)
stairs(linspace(0,hours,N),P_WT(1:N),'k','linewidth',1.5)
hold on
stairs(linspace(0,hours,N),PWT_max*ones(1,N),':r','linewidth',1.5)
ylabel('P_W_T [kW]')
axis([0 hours+1 0 1.05*max(PWT_max)]);
xlabel('Time [h]')
legend('P_W_T','maximum of P_W_T')
% Battery
figure (5)
stairs(linspace(0,hours,N),P_B(1:N),'k','linewidth',1.5)
hold on
```

```
stairs(linspace(0,hours,N),PB_max*ones(1,N),':r','linewidth',1.5)
ylabel('P_B [kW]')
axis([0 hours+1 -2 1.05*max(PB_max)]);
xlabel('Time [h]')
legend('P_B','maximum of P_B')
%SOC
figure (6)
stairs(linspace(0,hours,N),soc1(1:N),'k','linewidth',1.5)
hold on
stairs(linspace(0,hours,N),soc_max*ones(1,N),':r','linewidth',1.5)
hold on
stairs(linspace(0,hours,N),Soc_min*ones(1,N),':k','linewidth',1.5)
ylabel('SOC')
axis([0 hours+1 0.35 1.05*max(soc_max)]);
xlabel('Time [h]')
legend('SOC','maximum of SOC', 'minimum of SOC')
% DG
figure (7)
stairs(linspace(0,hours,N),P_DG(1:N),'k','linewidth',1.5)
hold on
stairs(linspace(0,hours,N),PDG_max*ones(1,N),':r','linewidth',1.5)
ylabel('P_D_G [kW]')
xlabel('Time [h]')
axis([0 hours+1 0 1.05*max(PDG_max)]);
legend('P_D_G','maximum of P_D_G')
% Balance
figure (8)
stairs(linspace(0,hours,N),PBAL(1:N),'k','linewidth',1.5)
ylabel('P_B_A_L [kW]')
```

```
xlabel('Time [h]');
axis([0 hours+1 -5.1 1.05*max(PBAL(1:N))]);
legend('P_B_A_L')
```

A2: Objective function

```
function f = fun_optimization(x)
deltaT=30; %sampling time in minute
hours=24;
N=hours*60/deltaT;
fc=14;
a=0.0074;
b=0.233;
c=0.4200;
f= sum(a*(x(3*N+1:4*N).^2)+b*x(3*N+1:4*N)+c);
end
```

Appendix B: Supplementary simulation results: Optimal power flow.

Table B1: Winter power flow: Household case

N	P_HKT	P_PV	P_WT	P_DG	P_B	PL
1	0.1288	0	0	0.0003	-0.1292	0
2	0.1324	0	0	0.0003	-0.1328	0
3	0.1345	0	0	0.0003	0.0651	0.2000
4	0.1413	0	0	0.0003	0.0584	0.2000
5	0.1507	0	0	0.0003	-0.0510	0.1000
6	0.1609	0	0	0.0003	-0.0613	0.1000
7	0.1751	0	0	0.0003	-0.1754	0
8	0.1937	0	0	0.0003	-0.1941	0
9	0.2271	0	0	0.0003	0.0725	0.3000
10	0.2690	0	0	0.0003	0.0307	0.3000
11	0.3090	0	0	0.0003	-0.3094	0
12	0.3985	0	0	0.0003	-0.3989	0
13	0.6789	0	0	0.0004	0.0207	0.7000
14	1.4559	0	0	0.0003	-0.7562	0.7000
15	3.0000	0	0	1.0000	4.0000	8.0000
16	3.0000	0	0	1.0000	4.0000	8.0000
17	2.9999	0.2399	0	0.9680	1.3921	5.6000
18	2.9999	0.2399	0	0.9680	1.3921	5.6000
19	2.8729	0.1872	0	0.0004	-0.4604	2.6000
20	2.7869	0.1738	0	0.0004	-0.3611	2.6000
21	2.7638	0.1756	0	0.0003	0.0602	3.0000
22	2.6908	0.1666	0	0.0003	0.1423	3.0000
23	2.0673	0.2653	0	0.0003	-1.8329	0.5000
24	1.9171	0.2584	0	0.0003	-1.6758	0.5000

25	2.3446	0.3382	0	0.0003	0.7168	3.4000
26	2.2895	0.3324	0	0.0003	0.7778	3.4000
27	1.7019	0.2946	0	0.0003	-1.2969	0.7000
28	1.6535	0.2916	0	0.0003	-1.2455	0.7000
29	1.8105	0.2704	0	0.0003	-0.7813	1.3000
30	1.8461	0.2717	0	0.0004	-0.8182	1.3000
31	1.9406	0.2328	0.0423	0.0004	-0.8161	1.4000
32	2.0542	0.2370	0.0425	0.0004	-0.9340	1.4000
33	2.2694	0.2108	0	0.0003	-0.9805	1.5000
34	2.5524	0.2258	0	0.0004	-1.2785	1.5000
35	2.9999	0.2499	0	0.3783	0.1720	3.8000
36	2.9999	0.2499	0	0.3781	0.1721	3.8000
37	2.9999	0	0	0.3796	1.2205	4.6000
38	2.9999	0	0	0.3790	1.2212	4.6000
39	2.9999	0	0.0379	0.4631	3.9992	7.5000
40	2.9999	0	0.0379	0.4631	3.9992	7.5000
41	2.6496	0	0.1115	0.0003	-0.6615	2.1000
42	2.4659	0	0.1050	0.0003	-0.4712	2.1000
43	1.8400	0	0	0.0003	-1.0404	0.8000
44	1.5918	0	0	0.0004	-0.7921	0.8000
45	1.3286	0	0	0.0003	-1.0290	0.3000
46	1.2393	0	0	0.0004	-0.9397	0.3000
47	1.2447	0	0	0.0003	-0.5451	0.7000
48	1.2129	0	0	0.0003	-0.5133	0.7000

Table B2: Summer power flow: Household case

N	P_HKT	P_PV	P_WT	P_DG	P_B	PL
1	0.1529	0	0	0.0000	0.1471	0.3000
2	0.1326	0	0	0.0000	0.1674	0.3000
3	0.1480	0	0	0.0000	-0.0480	0.1000
4	0.1425	0	0	0.0000	-0.0425	0.1000
5	0.1438	0	0	0.0000	0.0562	0.2000
6	0.1578	0	0	0.0000	0.0422	0.2000
7	0.1725	0	0	0.0000	-0.0725	0.1000
8	0.1911	0	0	0.0000	-0.0911	0.1000
9	0.2105	0	0	0.0000	-0.2105	0
10	0.2392	0	0	0.0000	-0.2392	0
11	0.2943	0	0	0.0000	0.0057	0.3000
12	0.3341	0	0	0.0000	-0.0341	0.3000
13	0.3720	0.0543	0.0149	0.0000	-0.4412	0
14	0.4519	0.0554	0.0150	0.0000	-0.5224	0
15	0.9172	0.1170	0.1133	0.0000	1.2526	2.4000
16	1.1930	0.1198	0.1158	0.0000	0.9715	2.4000
17	1.0040	0.2545	0.0294	0.0000	-0.6879	0.6000
18	1.2344	0.2620	0.0293	0.0000	-0.9258	0.6000
19	2.4066	0.4741	0.0199	0.0000	1.3993	4.3000
20	2.5267	0.4894	0.0199	0.0000	1.2640	4.3000
21	2.5758	0.6869	0.0263	0.0000	2.3111	5.6000
22	2.5696	0.6837	0.0262	0.0000	2.3205	5.6000
23	2.2950	0.7096	0	0.0000	0.1953	3.2000
24	2.1662	0.6771	0	0.0000	0.3566	3.2000
25	1.5934	0.6029	0	0.0000	-0.5963	1.6000
26	1.4503	0.5693	0	0.0000	-0.4196	1.6000
27	1.1468	0.4568	0	0.0000	-1.3037	0.3000

28	1.1003	0.4444	0	0.0000	-1.2447	0.3000
29	1.3840	0.4131	0	0.0000	0.2029	2.0000
30	1.3799	0.4112	0	0.0000	0.2089	2.0000
31	1.0947	0.3203	0	0.0000	-1.0150	0.4000
32	1.1113	0.3220	0	0.0000	-1.0333	0.4000
33	1.2343	0.2388	0.0492	0.0000	-0.7223	0.8000
34	1.3290	0.2431	0.0493	0.0000	-0.8214	0.8000
35	2.1477	0.1284	0	0.0000	1.6238	3.9000
36	2.1887	0.1288	0	0.0000	1.5825	3.9000
37	1.7355	0.0799	0.0847	0.0000	-0.1001	1.8000
38	1.7250	0.0797	0.0846	0.0000	-0.0893	1.8000
39	1.7217	0	0.0357	0.0000	-0.0574	1.7000
40	1.7101	0	0.0357	0.0000	-0.0458	1.7000
41	1.7539	0	0	0.0000	0.1461	1.9000
42	1.7303	0	0	0.0000	0.1697	1.9000
43	1.7690	0	0	0.0000	0.4310	2.2000
44	1.7108	0	0	0.0000	0.4892	2.2000
45	1.3671	0	0	0.0000	-0.4671	0.9000
46	1.3160	0	0	0.0000	-0.4160	0.9000
47	1.2654	0	0	0.0000	-0.5655	0.7000
48	1.2496	0	0	0.0000	-0.5496	0.7000

Table B3: Winter power flow: BTS case

N	P_HKT	P_PV	P_WT	P_DG	P_B	PL
1	1.4738	0	0	0.0000	0.3262	1.8000
2	1.5810	0	0	0.0000	0.2190	1.8000
3	1.6431	0	0	0.0000	0.1569	1.8000
4	1.6776	0	0	0.0000	0.1224	1.8000
5	1.6969	0	0	0.0000	0.1031	1.8000
6	1.7080	0	0	0.0000	0.0920	1.8000
7	1.7148	0	0	0.0000	0.0852	1.8000
8	1.7190	0	0	0.0000	0.0810	1.8000
9	1.7216	0	0	0.0000	0.0784	1.8000
10	1.7229	0	0	0.0000	0.0771	1.8000
11	1.7230	0	0	0.0000	0.0770	1.8000
12	1.7215	0	0	0.0000	0.0785	1.8000
13	1.7179	0	0	0.0000	0.0821	1.8000
14	1.7110	0	0	0.0000	0.0890	1.8000
15	1.6399	0.0250	0	0.0000	-0.0649	1.6000
16	1.6257	0.0249	0	0.0000	-0.0507	1.6000
17	1.5915	0.0872	0	0.0000	-0.0788	1.6000
18	1.5828	0.0872	0	0.0000	-0.0700	1.6000
19	1.5695	0.1086	0	0.0000	-0.0781	1.6000
20	1.5681	0.1085	0	0.0000	-0.0766	1.6000
21	1.5455	0.1742	0	0.0000	-0.1197	1.6000
22	1.5564	0.1747	0	0.0000	-0.1311	1.6000
23	1.4060	0.4477	0.1027	0.0000	-0.3565	1.6000
24	1.4561	0.4553	0.1031	0.0000	-0.4146	1.6000
25	1.6244	0.2334	0.1531	0.0000	-0.4109	1.6000
26	1.7057	0.2477	0.1599	0.0000	-0.5133	1.6000
27	2.0000	0.3000	0.5500	0.1500	1.0000	4.0000

28	2.0000	0.3000	0.5500	0.1500	1.0000	4.0000
29	2.0000	0.2000	0.6670	0.1330	1.0000	4.0000
30	2.0000	0.2000	0.6670	0.1330	1.0000	4.0000
31	1.7621	0.0712	0.1857	0.0000	-0.4190	1.6000
32	1.6807	0.0691	0.1759	0.0000	-0.3257	1.6000
33	1.3387	0.0354	0.6936	0.0000	-0.4677	1.6000
34	1.2741	0.0353	0.6781	0.0000	-0.3875	1.6000
35	1.3243	0	0.5439	0.0000	-0.2682	1.6000
36	1.3122	0	0.5386	0.0000	-0.2508	1.6000
37	1.5583	0	0.2070	0.0000	0.0347	1.8000
38	1.5586	0	0.2075	0.0000	0.0339	1.8000
39	1.5318	0	0.2645	0.0000	0.0037	1.8000
40	1.5251	0	0.2641	0.0000	0.0108	1.8000
41	1.4882	0	0.3343	0.0000	-0.0225	1.8000
42	1.4817	0	0.3327	0.0000	-0.0145	1.8000
43	1.5474	0	0.1431	0.0000	0.1095	1.8000
44	1.5338	0	0.1435	0.0000	0.1228	1.8000
45	1.4589	0	0.2844	0.0000	0.0567	1.8000
46	1.4352	0	0.2812	0.0000	0.0836	1.8000
47	1.5171	0	0	0.0000	0.2829	1.8000
48	1.4732	0	0	0.0000	0.3268	1.8000

Table B4: Summer power flow: BTS case

N	P_HKT	P_PV	P_WT	P_DG	P_B	PL
1	1.4688	0	0	0.0000	0.3312	1.8000
2	1.5766	0	0	0.0000	0.2234	1.8000
3	1.6183	0	0.0435	0.0000	0.1383	1.8000
4	1.6493	0	0.0437	0.0000	0.1070	1.8000
5	1.6559	0	0.0964	0.0000	0.0477	1.8000
6	1.6694	0	0.0969	0.0000	0.0337	1.8000
7	1.6899	0	0.0384	0.0000	0.0717	1.8000
8	1.6961	0	0.0385	0.0000	0.0655	1.8000
9	1.7050	0	0	0.0000	0.0950	1.8000
10	1.7048	0	0	0.0000	0.0952	1.8000
11	1.7009	0	0	0.0000	0.0991	1.8000
12	1.6925	0	0	0.0000	0.1075	1.8000
13	1.6369	0	0	0.0000	-0.0369	1.6000
14	1.6185	0	0	0.0000	-0.0185	1.6000
15	1.5749	0.0853	0	0.0000	-0.0601	1.6000
16	1.5594	0.0850	0	0.0000	-0.0444	1.6000
17	1.5155	0.1765	0	0.0000	-0.0920	1.6000
18	1.5130	0.1762	0	0.0000	-0.0892	1.6000
19	1.3901	0.4559	0.0293	0.0000	-0.2753	1.6000
20	1.4320	0.4632	0.0294	0.0000	-0.3245	1.6000
21	1.4412	0.5700	0.0665	0.0000	-0.4777	1.6000
22	1.5518	0.6049	0.0675	0.0000	-0.6241	1.6000
23	2.0000	1.0300	0	0.7279	0.2421	4.0000
24	2.0000	1.0300	0	0.7279	0.2421	4.0000
25	2.0000	1.0900	0.2010	0.7279	-0.0189	4.0000
26	2.0000	1.0900	0.2010	0.7279	-0.0189	4.0000
27	2.0000	0.9700	0.1460	0.7279	0.1561	4.0000

28	2.0000	0.9700	0.1460	0.7279	0.1561	4.0000
29	2.0000	0.7100	0.5780	0.7279	-0.0159	4.0000
30	2.0000	0.7100	0.5780	0.7279	-0.0159	4.0000
31	2.0000	0.6900	0.3390	0.7279	0.2431	4.0000
32	2.0000	0.6900	0.3390	0.7279	0.2431	4.0000
33	2.0000	0.4900	0.3370	0.7279	0.4451	4.0000
34	2.0000	0.4900	0.3370	0.7279	0.4451	4.0000
35	2.0000	0.3500	0.2480	0.7279	0.6741	4.0000
36	2.0000	0.3500	0.2480	0.7279	0.6741	4.0000
37	1.9132	0.0222	0.1802	0.0000	-0.3156	1.8000
38	1.8862	0.0216	0.1666	0.0000	-0.2744	1.8000
39	1.8657	0	0.0805	0.0000	-0.1463	1.8000
40	1.8447	0	0.0790	0.0000	-0.1237	1.8000
41	1.8266	0	0.1005	0.0000	-0.1271	1.8000
42	1.8102	0	0.0986	0.0000	-0.1088	1.8000
43	1.7990	0	0	0.0000	0.0010	1.8000
44	1.7798	0	0	0.0000	0.0202	1.8000
45	1.7556	0	0	0.0000	0.0444	1.8000
46	1.7222	0	0	0.0000	0.0778	1.8000
47	1.6697	0	0	0.0000	0.1303	1.8000
48	1.5776	0	0	0.0000	0.2224	1.8000

Appendix C: Household supplementary simulation results (summer)

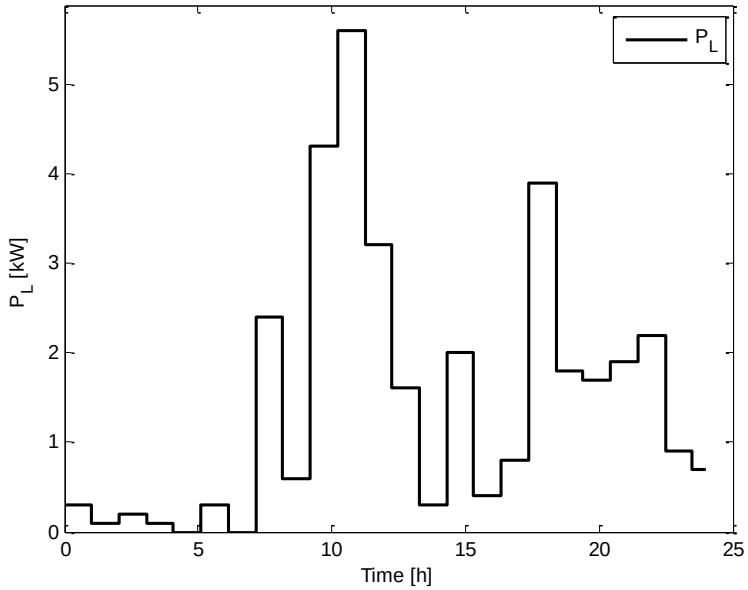

Figure C1: Daily load profile in summer

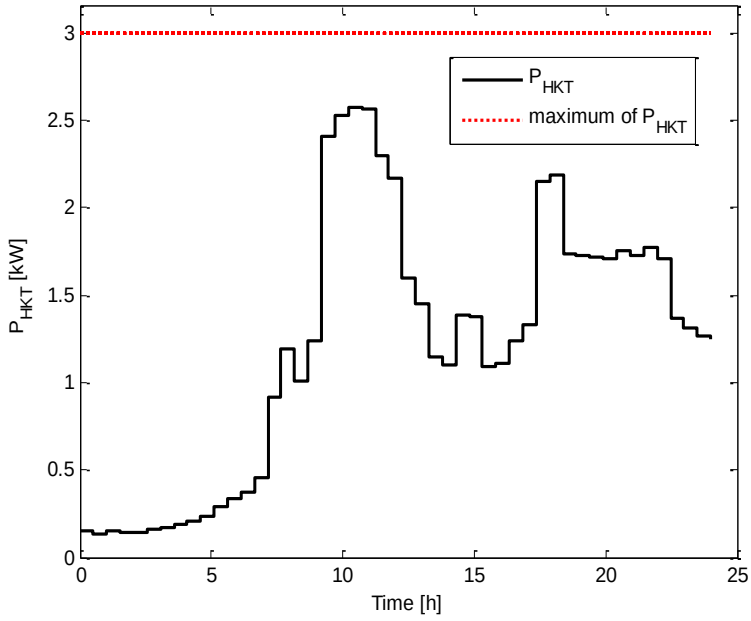

Figure C2: Hydrokinetic output power in summer

O

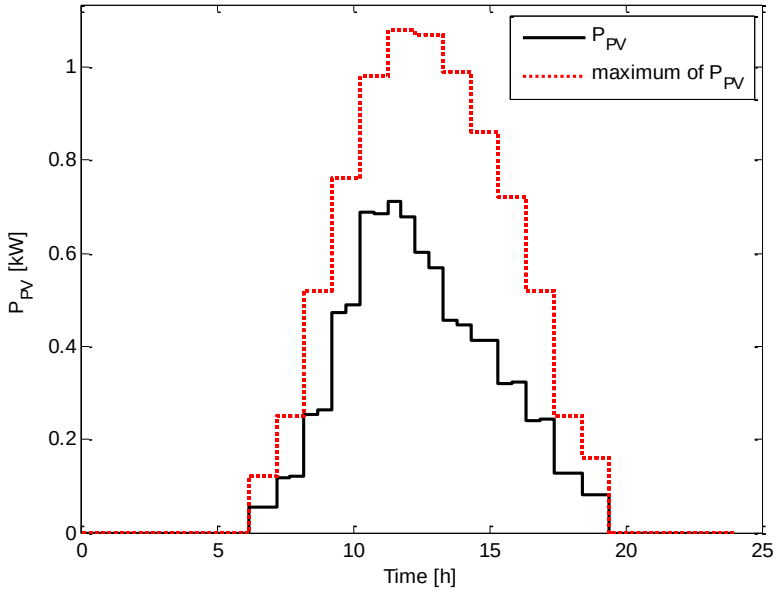

Figure C3: PV output power in summer

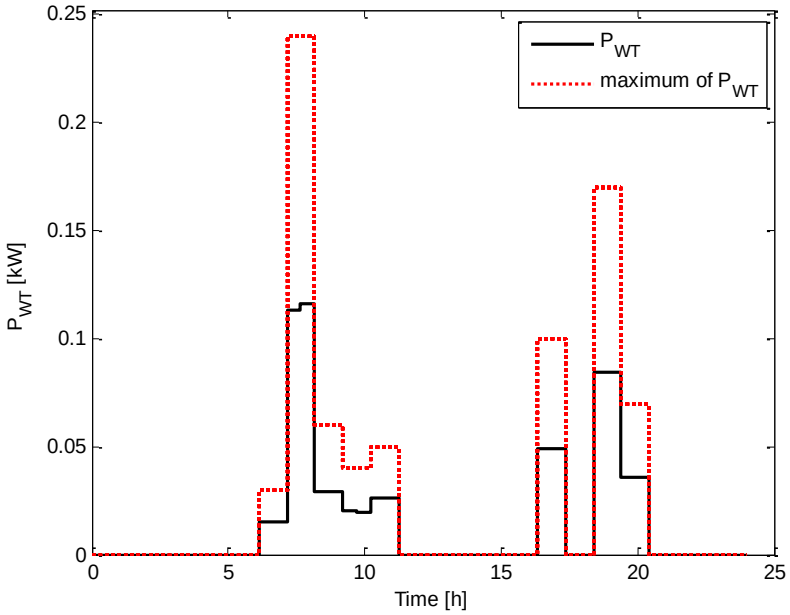

Figure C4: WT output power in summer

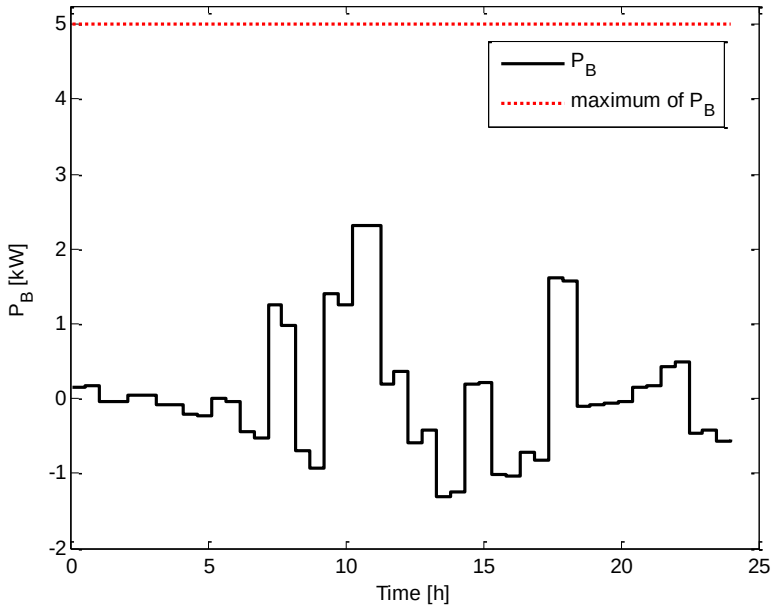

Figure C5: Battery output power in summer

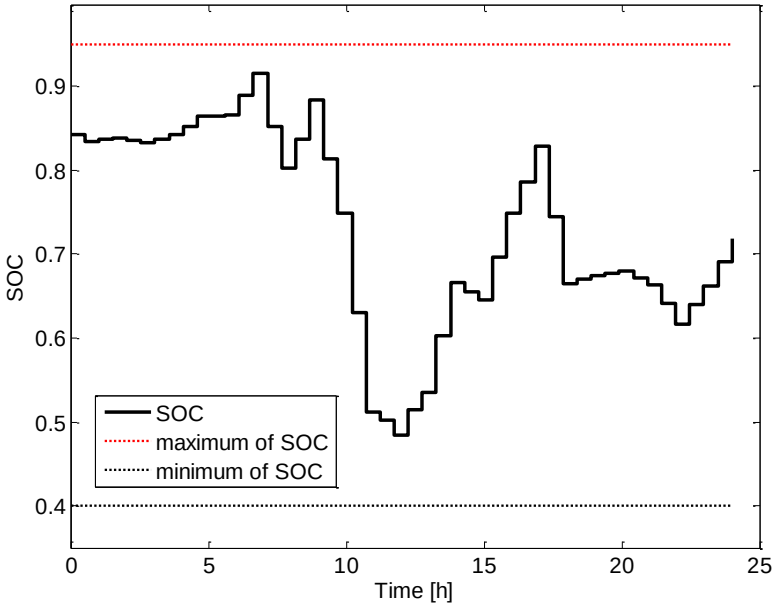

Figure C6: Battery dynamic state of charge in summer

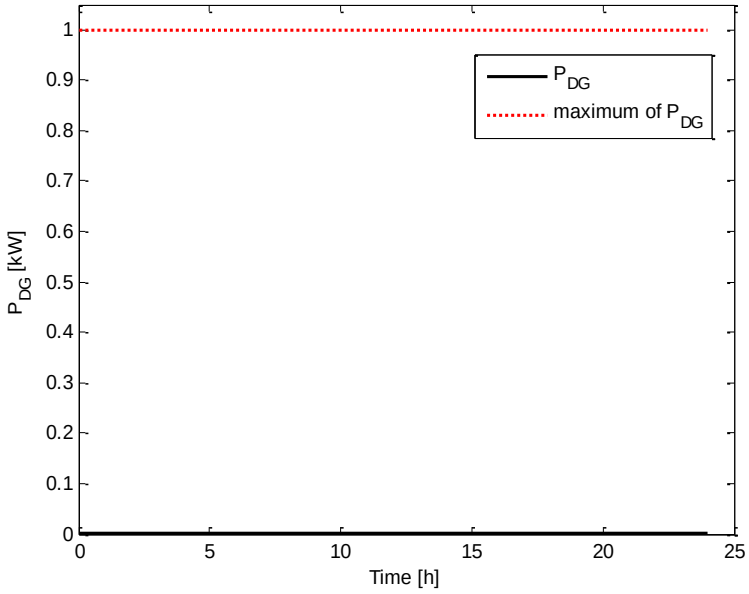

Figure C7: DG output power in summer

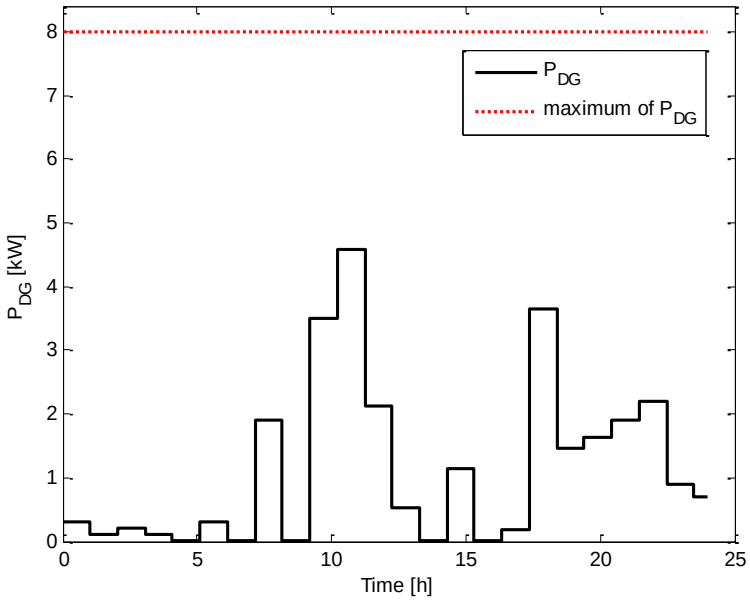

Figure C8: DG "alone" optimal scheduling and output power in summer

Appendix D: BTS supplementary simulation results (summer)

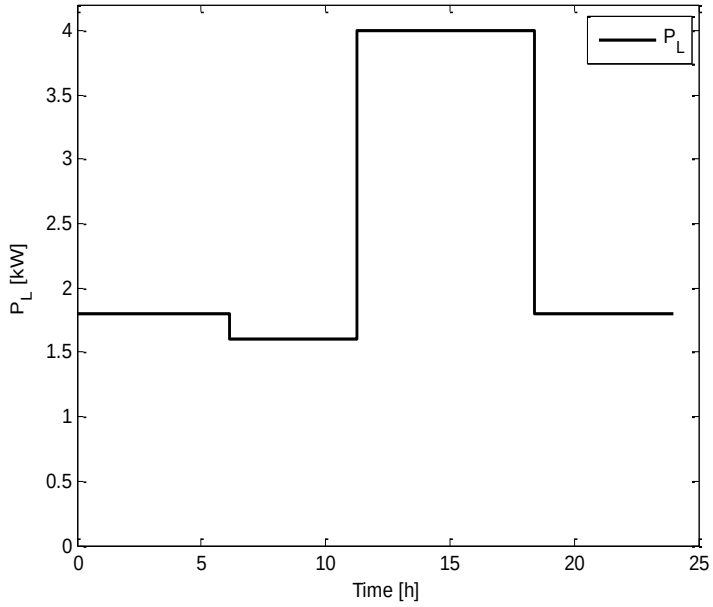

Figure D1: Daily load profile in summer

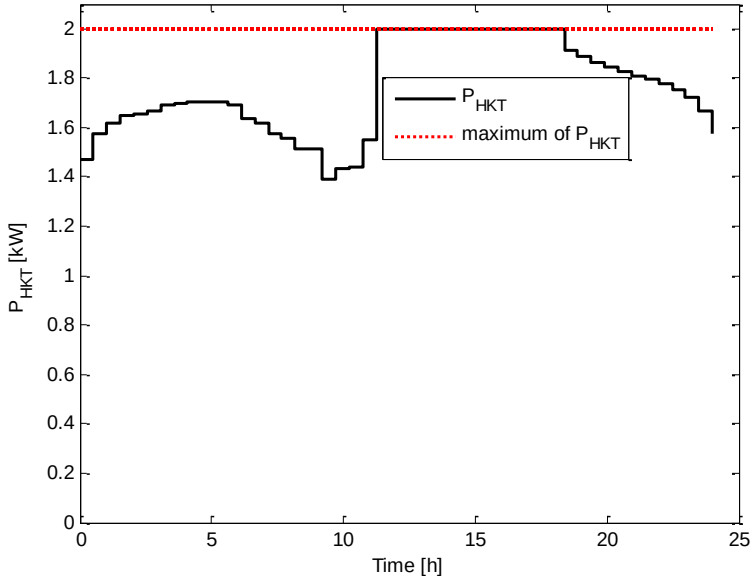

Figure D2: Hydrokinetic output power in summer

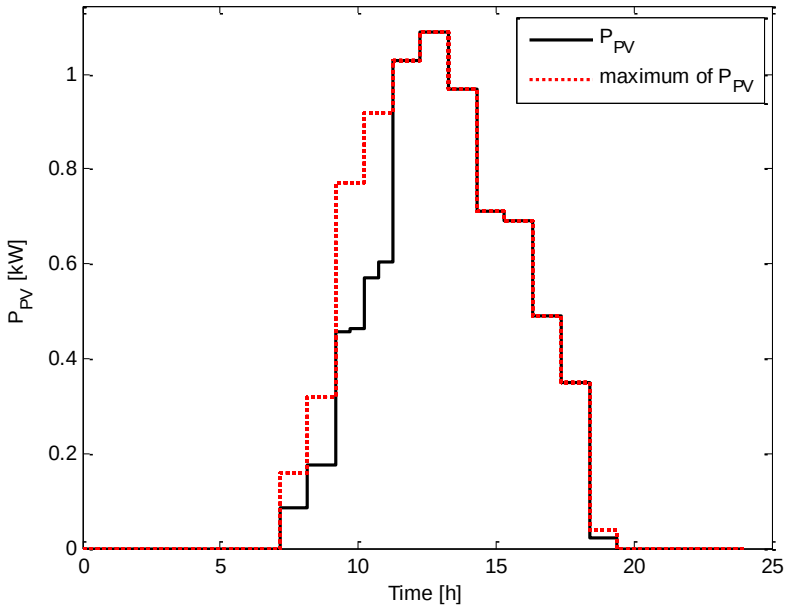

Figure D3: PV output power in summer

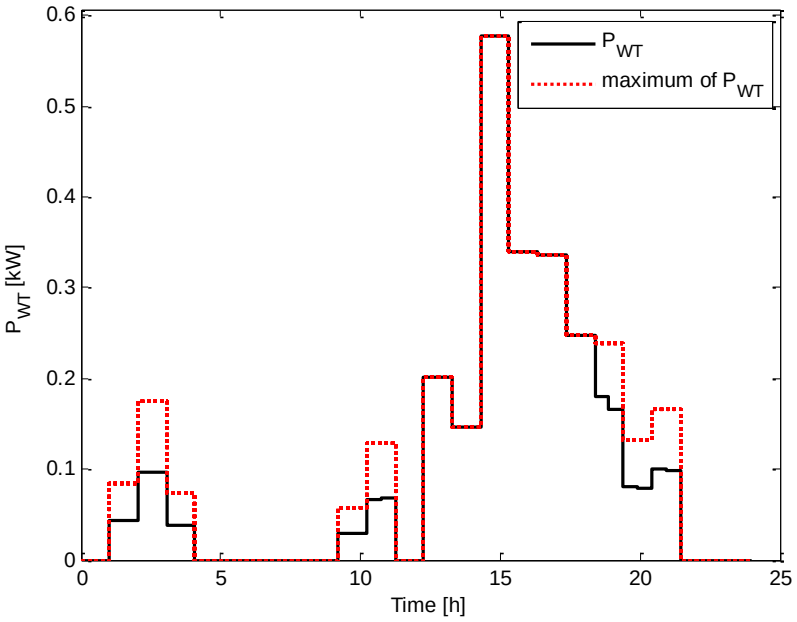

Figure D4: WT output power in summer

T

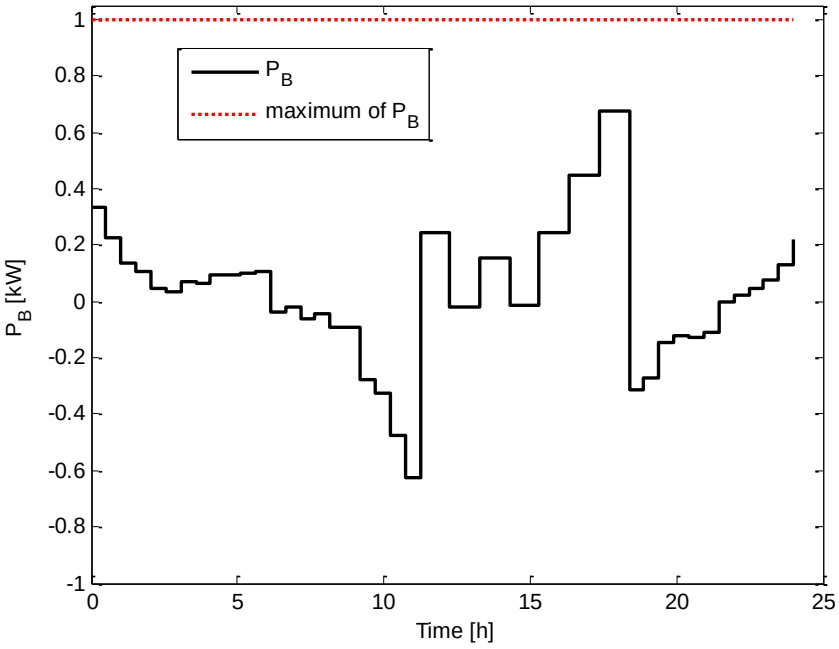

Figure D5: Battery output power in summer

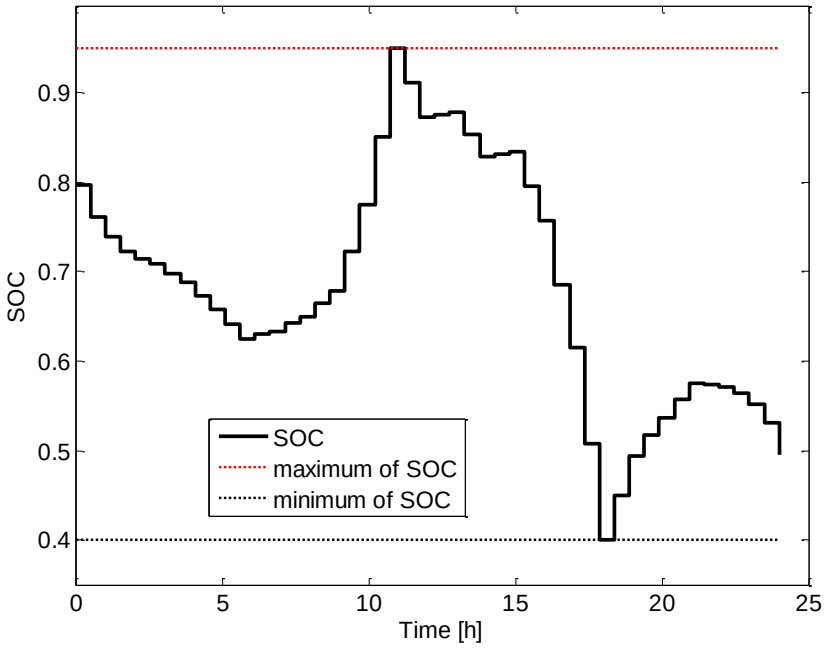

Figure D6: Battery dynamic state of charge in summer

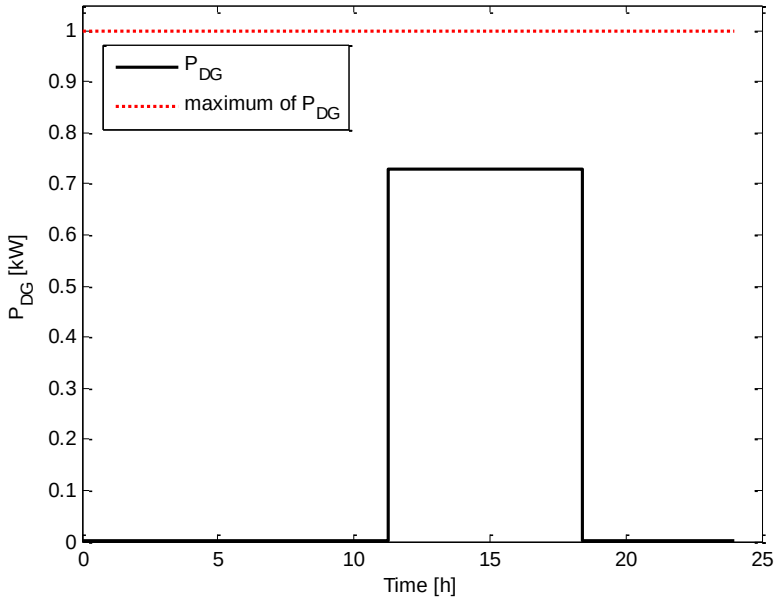

Figure D7: DG output power in summer

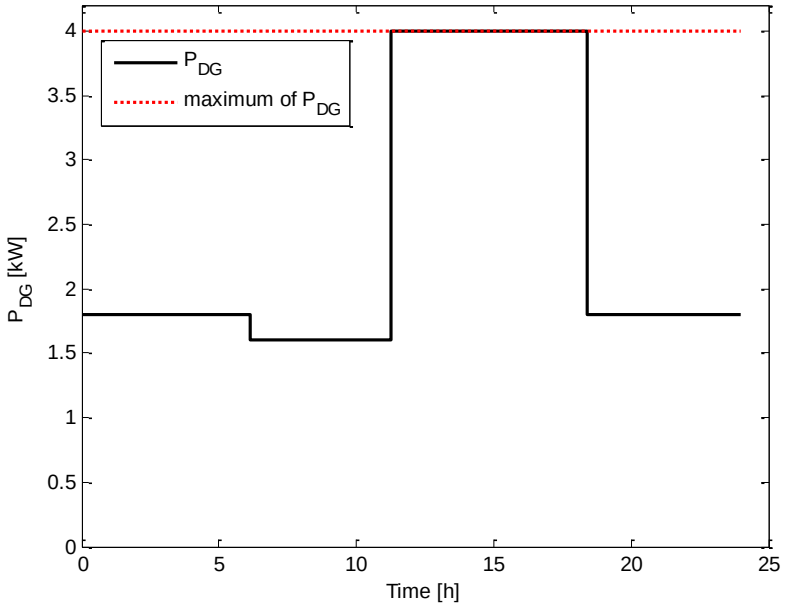

Figure D8: DG "alone" optimal scheduling and output power in summer

Appendix E: Generic Logical architecture of the integrated hardware-software hybrid system

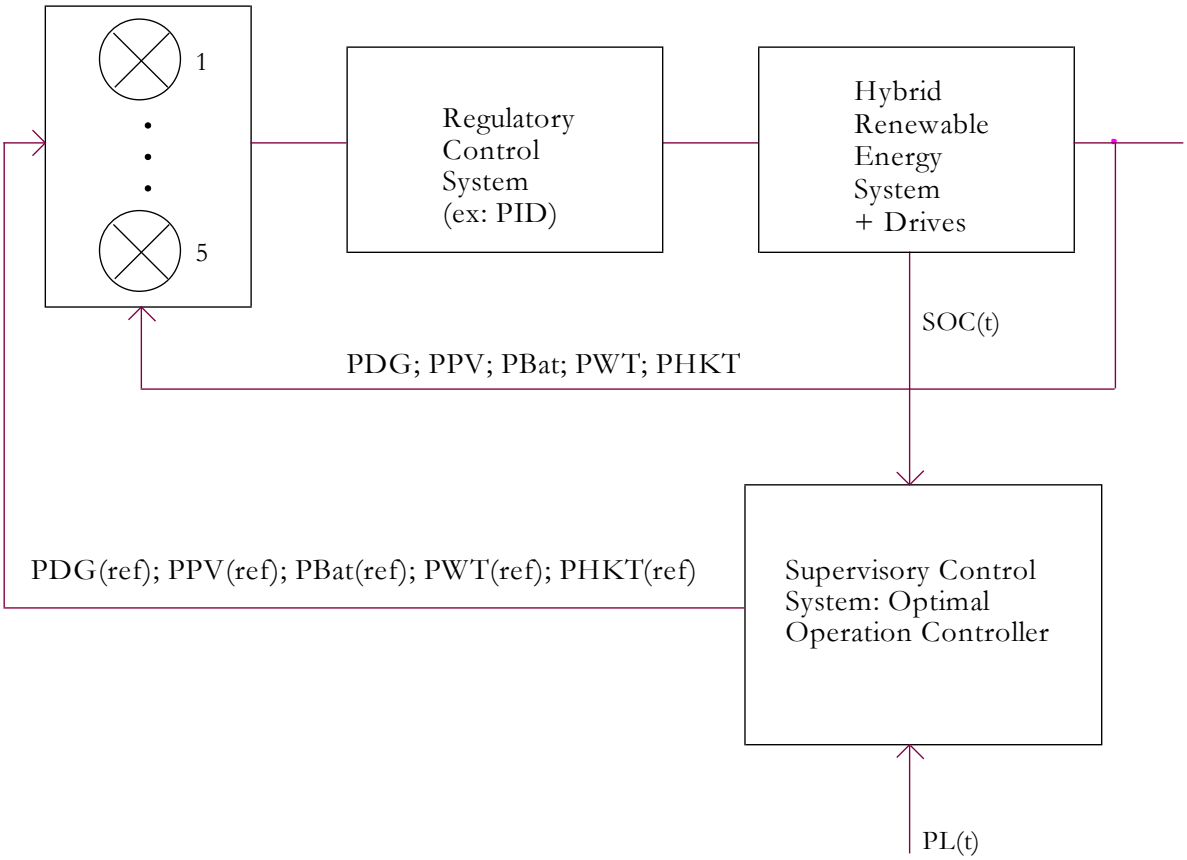

Figure E1: Logical architecture of the integrated hardware-software hybrid system